State of Illinois
Rod. R. Blagojevich, Governor
Illinois Department of Natural Resources
Illinois State Geological Survey

The Late-Glacial and Early Holocene Geology, Paleoecology, and Paleohydrology of the Brewster Creek Site, a Proposed Wetland Restoration Site, Pratt's Wayne Woods Forest Preserve, and James "Pate" Philip State Park, Bartlett, Illinois

B. Brandon Curry, Eric C. Grimm, Jennifer E. Slate,
Barbara C.S. Hansen, and Michael E. Konen

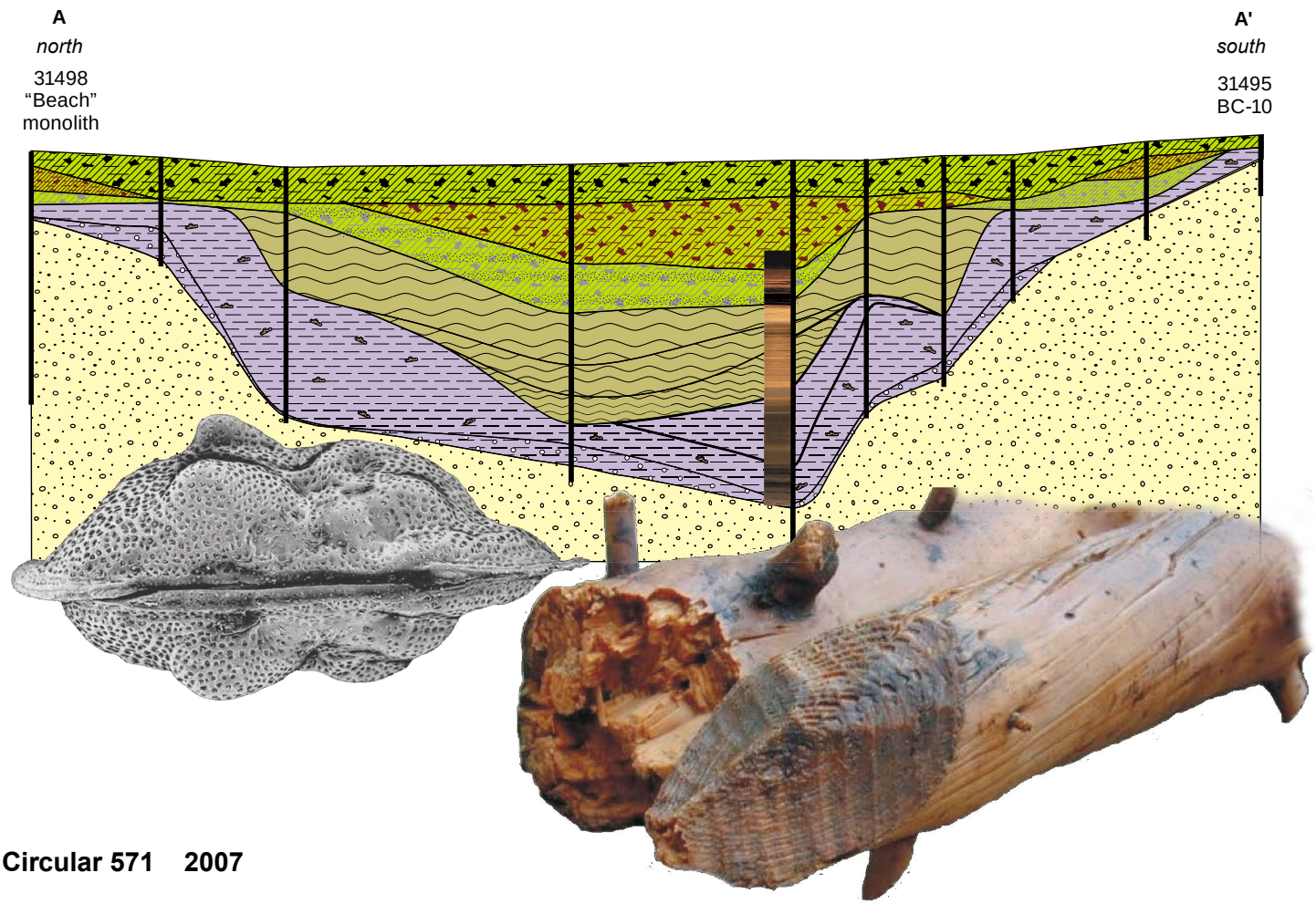

Circular 571 2007

Illinois Department of Natural Resources
ISGS Illinois State Geological Survey

Disclaimer

Front Cover: *Collage of report figures, including a carapace of* Limnocythere verrucosa *(lower left), a beaver-gnawed tree branch (lower right), and a geologic cross section of the Brewster Creek site.*

Released by the authority of the State of Illinois 1/08

The Late-Glacial and Early Holocene Geology, Paleoecology, and Paleohydrology of the Brewster Creek Site, a Proposed Wetland Restoration Site, Pratt's Wayne Woods Forest Preserve, and James "Pate" Philip State Park, Bartlett, Illinois

B. Brandon Curry
Illinois State Geological Survey

Eric C. Grimm
Illinois State Museum, Research and Collections Center,
1011 East Ash Street, Springfield, IL 62703

Jennifer E. Slate
Department of Biology, Northeastern University,
Chicago, IL 60625

Barbara C.S. Hansen
Limnological Research Center, University of Minnesota,
220 Pillsbury Hall, 310 Pillsbury Drive Southeast, Minneapolis, MN 55455

Michael E. Konen
Department of Geography, Northern Illinois University,
212 Davis Hall, De Kalb, IL 60115

Circular 571 2007

Illinois Department of Natural Resources
ILLINOIS STATE GEOLOGICAL SURVEY
William W. Shilts, Chief
615 E. Peabody Drive
Champaign, Illinois 61820-6964
217-333-4747
www.isgs.uiuc.edu

Contents

Figures

Abstract

The Brewster Creek site is a wetland that archives fossils and sediment deposited during the last transition from late-glacial to interglacial conditions dating from 13,870 to 9,185 radiocarbon years before present (^{14}C yr BP). An 8-m-long core was sampled from near the deepest part of a kettle basin. Significant changes in lithology correspond with the major events interpreted from Greenland ice cores. The tripartite succession of (1) 2.6 m of redeposited loess (smectite-rich silt), (2) 2.5 m of illite-rich marl, and (3) 3.5 m of peat corresponds, with some complications, to (1) the final stages of the last glaciation (the Oldest Dryas), (2) the Bølling-Allerød-Younger Dryas, and (3) the early Holocene. Twelve radiocarbon ages show that the sediment accumulation rate was nonlinear and slowest at the base of the major lithologic units. Additional cores of the basin show that the zones of slow sediment accumulation grade shoreward to unconformities that are in places marked by deposits of fine sand.

The pollen record at Brewster Creek differs from that at other sites in the region, indicating significant local variation in vegetation growing under the same climatic regime. Dominant plant types during the Older Dryas include spruce, fir, and black ash. Later other species became important, including pine, birch, oak, and elm. In general, the responses in spruce and black ash pollen observed in other records during the Younger Dryas, such as at Nelson Lake (Geneva, Kane County, Illinois) and Crystal Lake (McHenry County, Illinois), are muted at Brewster Creek. Spruce pollen persists until about 9,300 ^{14}C yr BP at Brewster Creek but is nearly absent by the end of the Younger Dryas (10,000 ^{14}C yr BP) at the other sites.

Ostracode evidence indicates that the paleohydrology of Brewster Creek initially was a lake with water enriched in sulfate and bicarbonate ions. At 12,500 ^{14}C yr BP (the onset of the Bølling chronozone), the lake became depleted in sulfate ion and remained that way for the remainder of the record. From about 12,500 to 11,600 ^{14}C yr BP, the sediment accumulation rate decreased significantly as the dominant sediment changed from silt to marl. The lithology changed over from marl to peat at about 10,500 ^{14}C yr BP. Fossils contained in the marl indicate that the lake bottom was within the photic zone, promoting the growth of aquatic plants and algae, notably charophytes and epiphytic diatoms. Lake levels likely dropped during this time as indicated by an abundance of illite, a mineral that was reworked from the local glacial sediment. Shallow hydrologic conditions persisted throughout the Younger Dryas and Early Holocene, and an upward increasing abundance of the ostracode *Limnocythere verrucosa* indicates the presence of an encroaching, groundwater-fed wetland.

Introduction

Climate change is in the forefront of the public's awareness and interest in natural sciences (e.g., *An Inconvenient Truth* 2007), and so climate change is a topic that many Quaternary scientists embrace as a means to relate their work to the public. Our aim in this investigation is to inform the public about how the postglacial environment in northeastern Illinois developed based on fossil and sediment records in lake and wetland deposits at the Pratt's Wayne Woods Forest Preserve near Bartlett, Illinois, and how this knowledge helps increase the understanding of climate and environmental change during the transition from the last glacial period to the current interglacial period.

The Brewster Creek site is located in Section 6, T40N, R9E on the West Chicago 7.5-minute Quadrangle, in DuPage County, Illinois (fig. 1). The site was discovered during summer 2002, when test pits were excavated for the Forest Preserve District of DuPage County under a temporary impact permit in the wetland in an area proposed for wetland restoration. The exposed successions included about 0.5 to 2.5 m of peat over more than about 2.5 m of shell-rich marl. One test pit revealed a branch of a boreal tree, located about 0.24 m below uniform peat in the upper marl unit; the branch yielded a radiocarbon age of 10,860 ± 70 ^{14}C yr before present (BP) (fig. 2). In addition, numerous rooted larch stumps with intact bark were found in the basal peat in these excavations. One sample yielded a radiocarbon age of 9,150 ± 70 ^{14}C yr BP (fig. 3). The age of these fossils piqued the interest of scientists from the Illinois State Geological Survey (ISGS) and Illinois State Museum (ISM) who had just completed a collaborative paleoenvironmental study at Nelson Lake near Batavia, Illinois (Curry et al. 2002). There the scientists had discovered significant response to climate changes that occurred during the last glacial-interglacial transition (Grimm and Maher 2002, Curry et al. 2004). The problem was, however, that the Nelson Lake site sediment that contained the record was less than 1 m thick and deeply buried. The marl at Brewster Creek was presumed to contain material of the same age, and it was about three times thicker, ostensibly allowing scientists to obtain better resolution of climate change events than at Nelson Lake. The ISGS and ISM then contracted with the Forest Preserve District of DuPage County to study the paleoecology and development of the wetland at the Brewster Creek site and to provide material suitable for a display at the James "Pate" Philip State Park Visitor Center.

The scientific purpose for this multidisciplinary investigation was to determine the timing and kinds of changes in paleovegetation and paleohydrology at Brewster Creek from about 16,500 calibrated years (cal yr) BP to about 10,300 cal yr BP, the age of the youngest fossiliferous material preserved at the site. The parameters include pollen, diatoms, ostracodes, and the physical characteristics of the sediment. Of key scientific interest is the part of the record that shows changes during the transition from the last glaciation to modern interglacial conditions, that

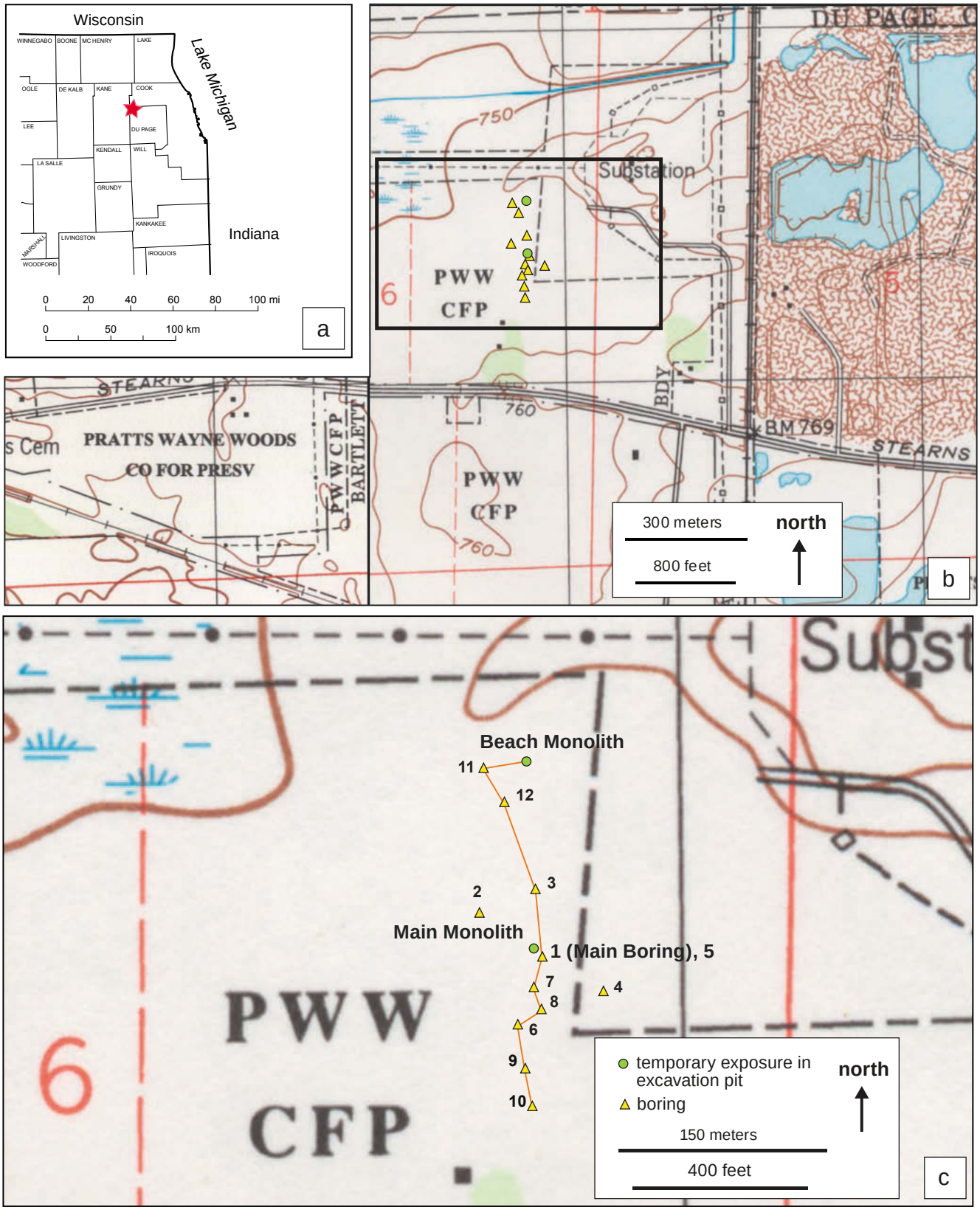

Figure 1 Location of Brewster Creek study area, DuPage County, on index map (a); from the West Chicago and Geneva 7.5-minute Quadrangle base maps (b, c), and on U.S. Geological Survey digital orthophoto quadrangle base maps (d, e). Line of cross section (fig. 14) is shown (c and e).

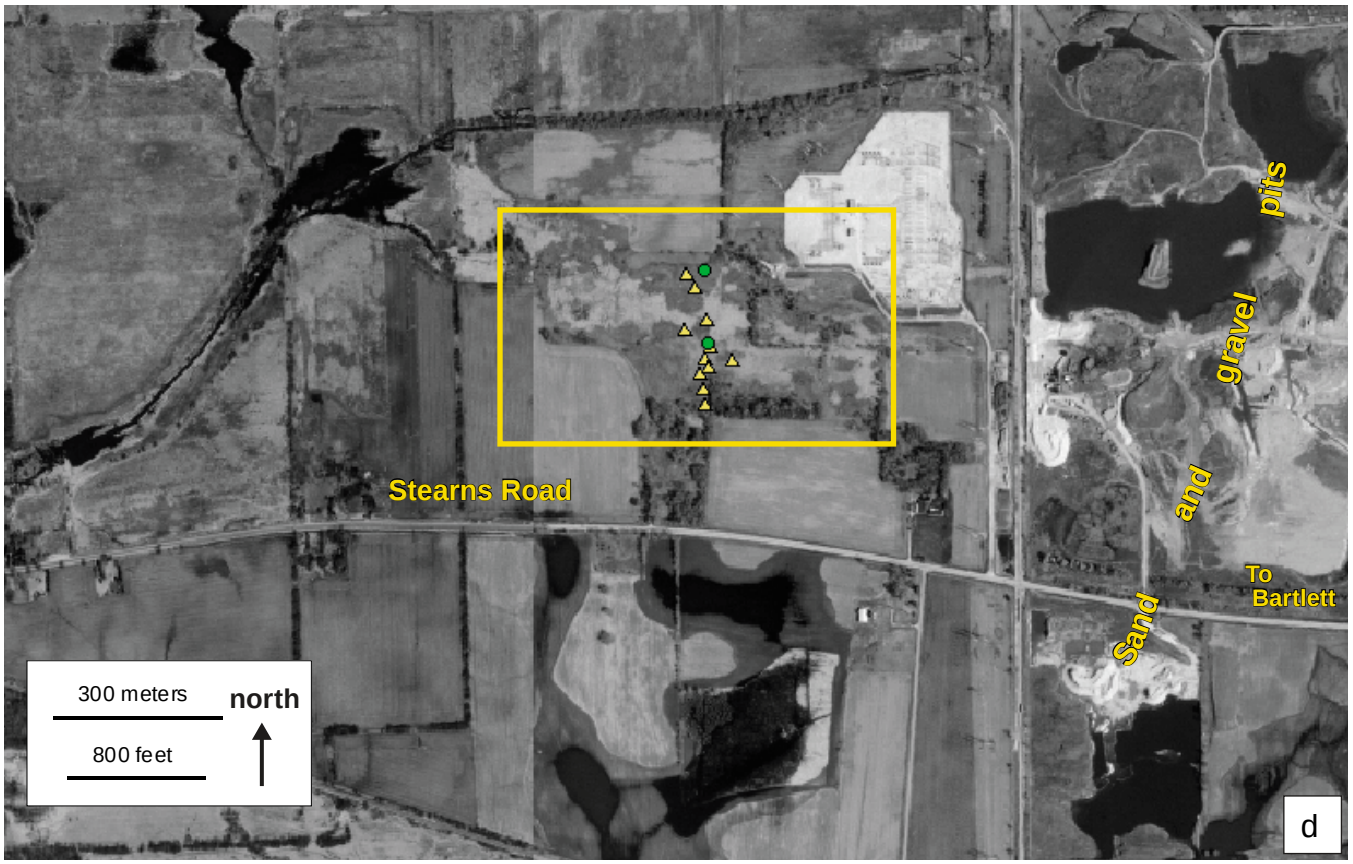
Stearns Road
Sand and gravel pits
To Bartlett
300 meters
800 feet
north
d

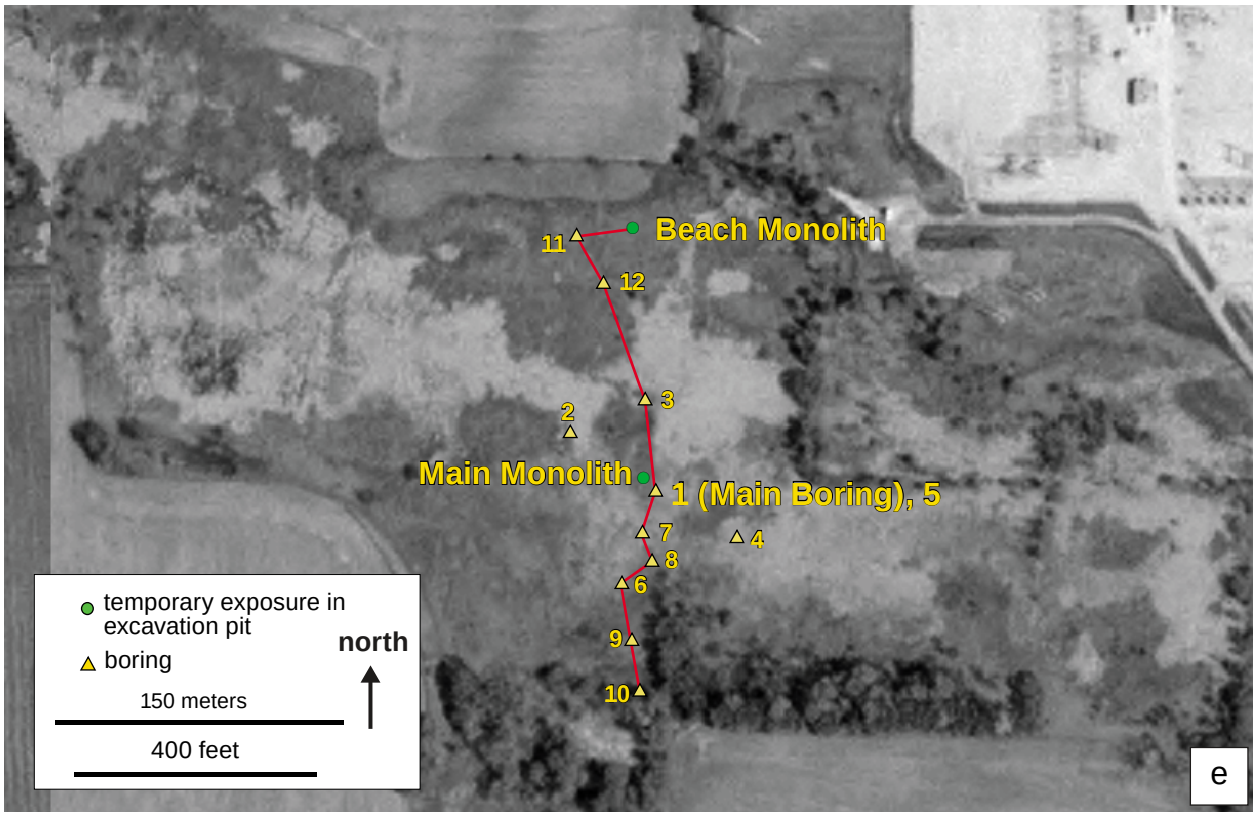
Beach Monolith
Main Monolith
1 (Main Boring), 5
2
3
4
6
7
8
9
10
11
12
temporary exposure in excavation pit
boring
150 meters
400 feet
north
e

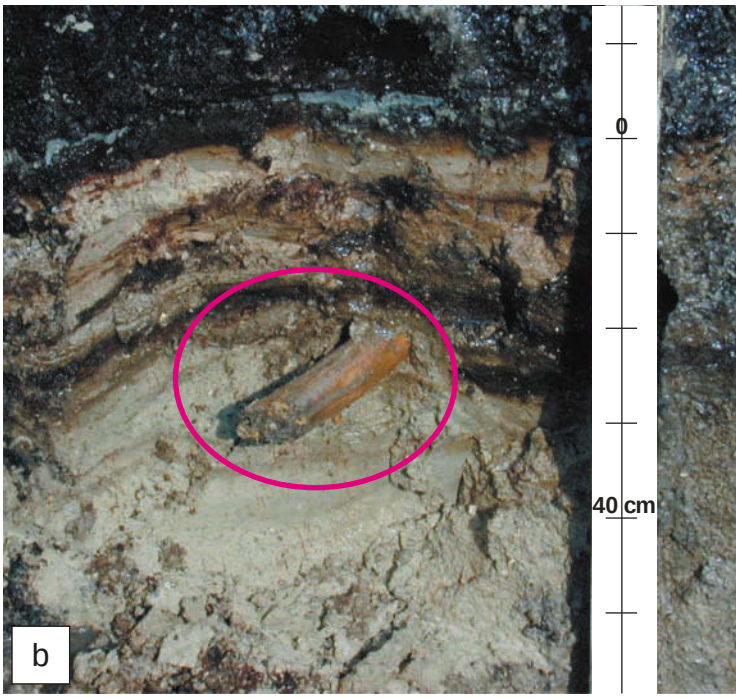

Figure 2 (a) A beaver-gnawed spruce *(Picea)* or fir *(Abies)* branch, dated as 10,860 ± 70 ^{14}C yr BP, from the Brewster Creek site; (b) wood fragment as it was discovered in the field and (c) in more detail.

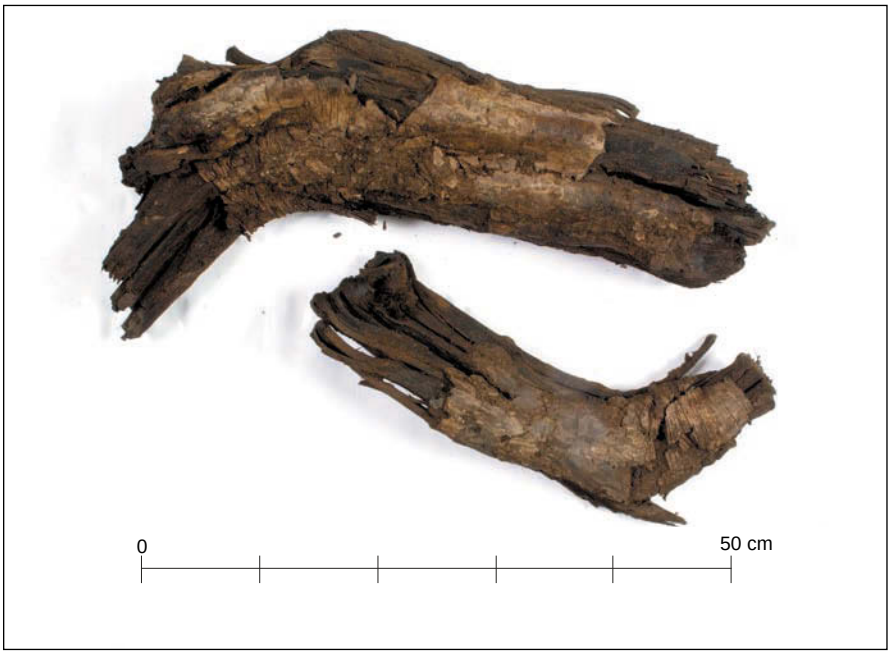

Figure 3 Two pieces of larch *(Larix)* from about 7 feet (2.13 m) below the ground surface in the upper peat unit at the Brewster Creek site. Larch wood fragments from a nearby horizon radiocarbon date at 9,150 ± 70 ^{14}C yr BP.

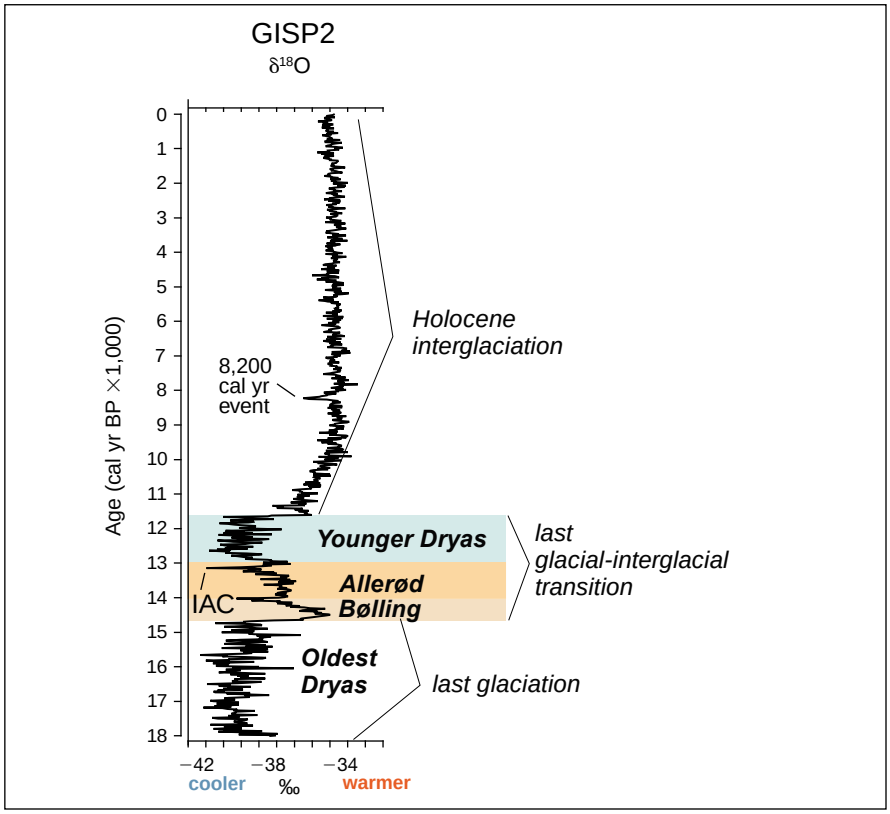

Figure 4 The oxygen isotope (δ^{18}O) record of the Greenland Ice Sheet Project 2 (GISP2) ice core (Stuiver et al. 1995). IAC, Inter-Allerød Cold Period; ‰, per mil.

is, the period between the final retreat of the glaciers from the Chicago region at the end of the Pleistocene to the onset of the Holocene interglaciation (fig. 4)(Curry et al. 1999, Killey 2007). Recent investigations of arctic ice cores, fossils in deep-sea sediment, and other proxies of global climate show that this transition from cold glacial to warm interglacial conditions was not smooth, but, instead, was characterized by several abrupt climatic reversals, including changes from coldest to warmest temperatures in 30 years or less (Alley et al. 1993; Taylor et al. 1993, 1997). These new discoveries show that there is much to learn about the global climate system (Alley 2000), especially the degree to which these changes in global climate affected local climate and environments in places, such as Illinois, in the continental interior.

There are several lines of evidence for abrupt climate change during the last glacial to interglacial transition interpreted from arctic ice cores. Evidence includes the measurement of ^{18}O (a stable oxygen isotope and a proxy for temperature), dust concentration, trace element composition of the dust, and the concentration of "greenhouse gases" such as carbon dioxide and methane in bubbles trapped in the ice. The ages of the changes are known by counting annual layers of accumulation in the ice, which is much like determining the age of a tree by counting its annual growth rings (Alley et al. 1993, Alley 2000). The variability of global temperature change recorded in the arctic ice-core records has been correlated to well-dated changes in vegetation and moraine margins in northwestern Europe. The first hint that the climate was warming occurred at about 14,670 cal yr BP during the onset of the Bølling interval (Mangerud et al. 1974, Yu and Wright 2001). Oxygen isotope data (δ^{18}O) from ice cores indicate that Greenland temperatures warmed during this period to nearly what they are today. The warming was uneven, and several names are given to the peaks and valleys in the record (fig. 4) such as the Inter-Allerød Cold Period. The Younger Dryas is the most notable part of the transition marking a

return in the North Atlantic region to cold, windy conditions similar to that of the preceding full glacial period (Yu and Wright 2001). This change was brought on by interruption of the heat transfer by ocean currents from the tropics to the North Atlantic Ocean. The interruption may have been caused by an inundation of cold, fresh water into the North Atlantic Ocean through catastrophic drainage of a large proglacial lake, Lake Agassiz, which covered much of southern Manitoba and Saskatchewan during the last deglaciation (Broecker et al. 1989, Cronin 1999). At the end of the Younger Dryas, climate abruptly reversed to the modern interglaciation at about 11,650 cal yr BP. Within the context of the global climate over the past 1.5 million years, the climate of the Holocene Epoch (11,650 cal yr BP to the present) has been relatively uneventful. The only evidence for a climatic perturbation in the ice-core records during the Holocene occurred at about 8,200 cal yr BP (fig. 4; Alley et al. 1997) when a short-lived cold, dry event occurred.

Radiocarbon Dating

Accurate and precise chronologies are key elements in paleoclimate studies spanning in age from the last glaciation to modern times. Three issues are important in this regard. First is the advance in radiocarbon dating technology that allows the dating of very small samples. Available commercially since the middle 1980s, accelerator mass spectrometers (AMS) determine radiocarbon ages on samples containing as little as 1 mg of carbon. Prior to this, a sample with a radiocarbon age of 10,000 cal yr BP required about 2 g of carbon for a reasonably accurate age determination. As an example, for AMS dating, a sample might include two or three needles of boreal trees, about 40 flecks of microscopic charcoal, four or five bulrush seeds, or one fingernail-sized wood fragment. A meaningful radiocarbon age using traditional techniques, such as benzene scintillation, would require the analysis of a wood fragment as large as a man's finger. Terrestrial plant fossils that large are rarely encountered in lake cores, but fossils that can be dated by AMS may be found in discrete layers less than 5 cm thick.

Second, although lake sediment typically contains abundant carbon, little of it may be representative of the actual age of the sediment. Radiocarbon ages may be dated too old if a significant proportion of the sediment contains carbon ultimately sourced from ancient bedrock. In the study area, the bedrock is hundreds of millions of years old (the practical limit of ^{14}C dating is about 45,000 years). The form of old carbon in most lake water in Illinois is as bicarbonate ions (HCO_3^-). Contamination by this source is often referred to as "the hard water effect." Much old bicarbonate may enter the lake or wetland as seepage or from springs. Rainwater, or shallow groundwater, contains carbon that has exchanged with or was formed from carbon dioxide in the atmosphere rather than from bedrock. Thus, most terrestrial plants and animals contain carbon that yields reliable radiocarbon ages; aquatic plants and aquatic animals contain carbon that may contain a significant proportion of carbon derived from ancient sources.

The third important issue affecting radiocarbon dating is age calibration. Calibration is necessary because radiocarbon ages are not the same as calendar ages. Many important proxy records of climate, such as ice-core records, are dated by non-chemical means. Therefore, calibration is necessary to correlate our local ^{14}C chronologies to global records. The calibration process is illustrated in figure 5. Figure 5a is the simpler calibration. All radiocarbon ages are subject to lab errors; hence, a radiocarbon "age" is not a discrete number, but a span of years during which the true event occurred. This range is indicated by the σ value. The probability is 68% that the "true" age falls within the timespan provided by adding and subtracting the σ value; if time span is doubled (2σ), the probability increases to 95% (fig. 5). The calibration curve is derived from careful analysis of paired ages (one determined by ^{14}C techniques and the other by counting annual bands or layers such as tree rings or corals) or from age determinations using more accurate dating methods, such as uranium series (Cronin 1999). Several calibration curves and online programs are available; we used the CALIB 5.02 program (Reimer et al. 2006).

Calibration is achieved by determining the points of intersection between σ values along a bell-shaped probability curve of the radiocarbon age (shown on the y-axis) with the calibration curve (fig. 5). In figure 5, vertical lines were drawn from the point at which the horizontal lines intersected the calibration curve. Note that, in figure 5b, the horizontal line intersects the calibration curve in two areas, resulting in two calibrated age ranges at the 1σ level. Also note that the mean calibrated age (the weighted mean of the shaded regions) is not the most likely age; there are actually two "most likely" ages related to the two bell-shaped areas on the calibrated age range. Also note that, although the calibrated age range at the 1σ confidence interval (68%) results in two age ranges, there is only one age range at the 2σ confidence interval (95%). The calibrations illustrate why it is important to minimize the error in the radiocarbon age by providing adequate material for analysis. It may be disconcerting to realize that a radiocarbon assay of a carefully cleaned and identified sample may yield a non-unique result. One remedy is to have as many ages as possible, but, at a cost of about $500 per sample, this option is expensive.

Regional Geology

During the last 2 million years or so (the Pleistocene Epoch), the southern margin of the Laurentide Ice Sheet waxed and waned about nine times across the midwestern United States (fig. 6)(Roy et al. 2004). For the Midwest region of North America, the last glaciation began about 55,000 years ago (Curry and Follmer 1992) when the southern margin of the Laurentide Ice Sheet reached the Mississippi River drainage basin (Dorale et al. 1998, Curry and Grimley 2006). The massive ice sheet took until about

29,000 cal yr BP to form Illinois' first Wisconsin-age moraines, the Burlington and Marengo Moraines in northwestern Kane County and western McHenry County (fig. 7) (Curry et al. 1999, Curry and Pavich 1996, Curry 2008). These arc-shaped landforms of glacial debris were deposited at glacier margins. From about 29,000 cal yr BP to 24,000 cal yr BP, ice from the west-flowing Huron-Erie lobe interacted with the Lake Michigan lobe, causing the latter to change its flow direction (fig. 6). Consequently, moraines of that age in Kane County

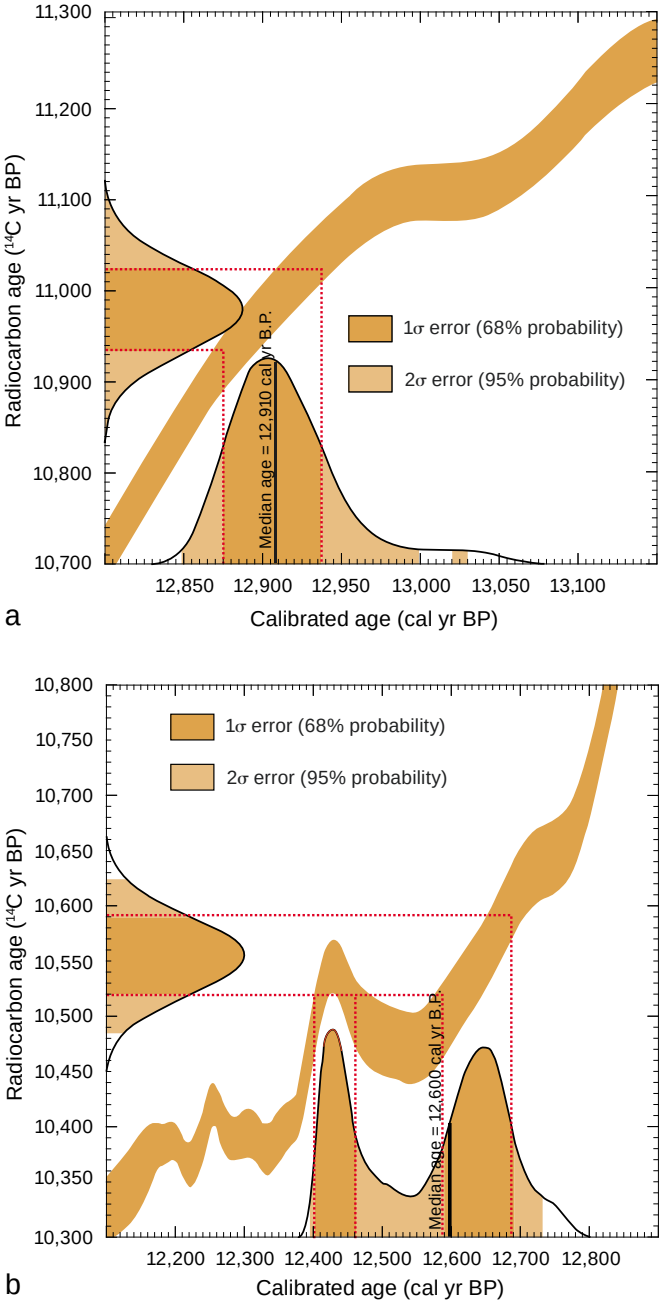

Figure 5 Graphic representation of the calibration of the radiocarbon ages (a) 10,980 ± 40 ^{14}C yr BP and (b) 10,555 ± 35 ^{14}C yr BP using the online program CALIB 5.02 (http://calib.qub.ac.uk/calib/calib.html).

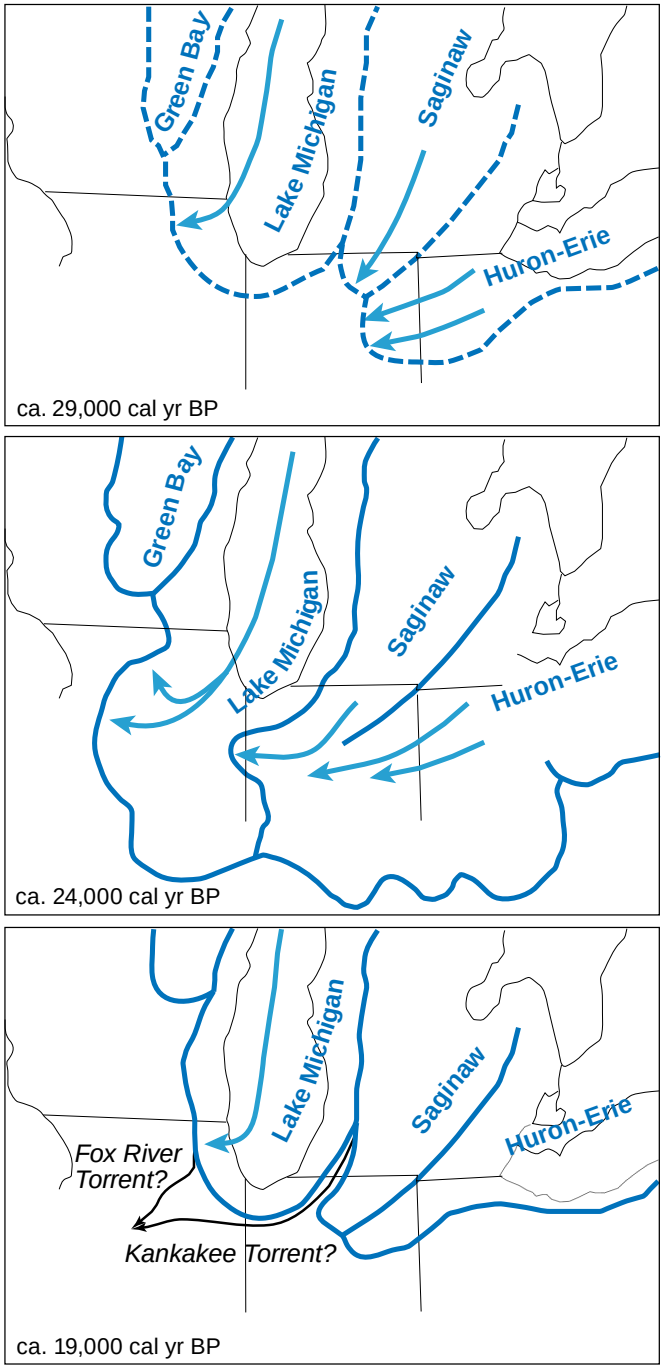

Figure 6 Major lobes of the south-central part of the Laurentide Ice Sheet at about 29,000, 24,000, and 19,000 cal yr BP showing how interaction with the Huron-Erie lobe impacted the flow direction of the Lake Michigan lobe. The approximate routes of the Fox River and Kankakee torrents are shown.

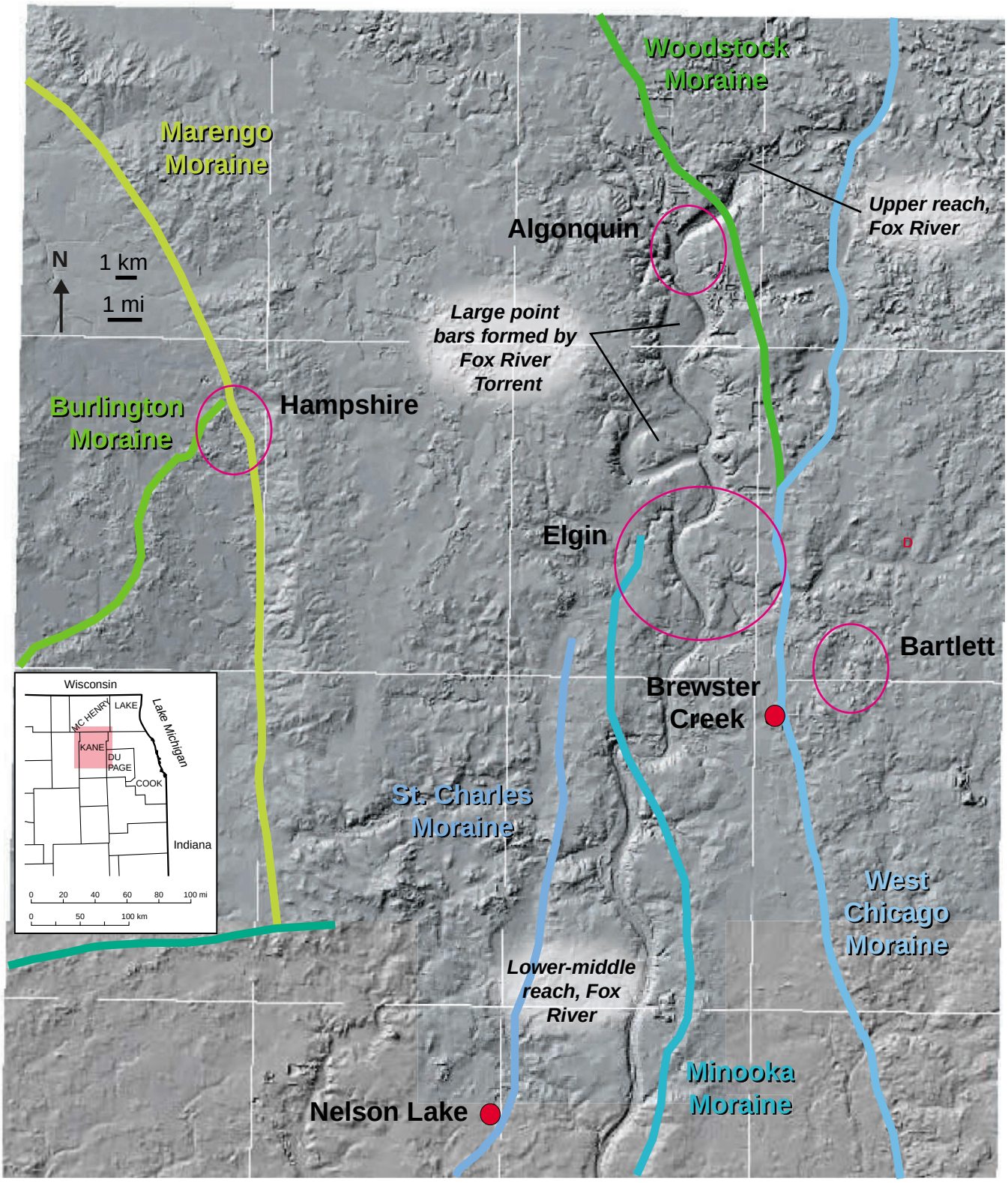

Figure 7 Location of moraines, significant landforms, and study sites. The white lines show the boundaries of the 7.5-minute U.S. Geological Survey topographic maps. Inset map shows the location of the study area in northeastern Illinois. Pink circles show the location of towns.

are oriented east to west (such as the Arlington Moraine, figs. 7 and 8) instead of north to south (Wickham et al. 1988, Curry and Yansa 2004). Later, as the Huron-Erie and Lake Michigan lobes began to retreat and no longer interacted, the recessional moraines reverted back to a north-south orientation, which in the study region parallels the nearest shoreline of Lake Michigan (figs. 6, 7, and 8). The morphology of the southern portion of the St. Charles Moraine (fig. 8) suggests that it formed while the Lake Michigan lobe continued to interact with the Huron-Erie lobe. The next-youngest moraine, the Minooka Moraine, shows no indication of interaction. The age of this shift in glacier behavior was about 21,100 cal yr BP (Curry et al. 1999). The West Chicago and related Woodstock Moraine (fig. 7) formed between about 18,800 to 18,030 cal yr BP (Curry and Yansa 2004), which roughly coincides with the age of large deglacial floods known as the Fox River and Kankakee torrents. The Lake Michigan lobe retreated from the southern part of present-day Lake Michigan at about 17,380 cal yr BP (Hansel and Johnson 1996).

The Brewster Creek site is in a wide and shallow depression (about 1 km wide and 8 m deep) formed in a glacial outwash plain that extends west from the West Chicago Moraine (fig. 7). Such depressions are known as kettles. The classic interpretation of their formation is that the depression formed as the ice that was encased in glacial debris melted. Other related processes may also have contributed to the form and size of the depression, including the discharge of large springs (groundwater) at the glacier margin. Kettles also may form from water flow around large objects, such as blocks of ice (Fay 2002). The rise of the West Chicago Moraine is evident when traveling east on Stearns Road toward Bartlett; Route 59 is located locally on the western margin of the moraine. The sand and gravel outwash, exposed in several pits along Stearns Road (fig. 1), was deposited by meltwater that flowed away from the glacier (fig. 9). The ice that melted to form the kettle at Brewster Creek likely was buried by the outwash or perhaps by deeper glacial debris.

The West Chicago Moraine east of Brewster Creek is a compound end moraine, which means that it is formed of sediment deposited during separate glacial advances. The first advance deposited a thick layer of sand and gravel outwash, known as the Beverly Tongue of Henry Formation (Hansel et al. 1985), and a thin, discontinuous layer of sandy diamicton, a sediment that includes particles ranging in size from clay to boulders. This diamicton has been named the Haeger Member of the Lemont Formation. The second advance deposited little if any outwash and a relatively thin layer of silty and clayey diamicton of the Wadsworth Formation (Johnson and Hansel 1989, Hansel and Johnson 1996). Several miles north of the site, the Woodstock Moraine emerges from beneath the West Chicago Moraine (fig. 7) and continues west across the Fox River just north of Algonquin diagonally across McHenry County. At the land surface, the Woodstock Moraine lacks the capping layer of Wadsworth diamicton and is formed wholly of the Haeger unit. North of the juncture of the moraines, the younger West Chicago Moraine is located east of the Fox River, primarily in Lake County.

Why is the Woodstock Moraine important to the story of the Brewster Creek site? Because the Brewster Creek site is located on the same outwash deposit associated with the Woodstock Moraine. The minimum age of the Woodstock Moraine (18,150 ± 140 cal yr BP) is estimated from radiocarbon ages of terrestrial plant fossils that accumulated in lake sediment deposited in kettles on the surface of the moraine (Curry 2005). The Woodstock Moraine is breached by a channel currently occupied by the Fox River north of Algonquin. In the reach between Algonquin and South Elgin, the Fox River valley contains terraces and abandoned channels that indicate the channel was formed by large floods (Curry 2005). One hypothesis is that a glacial lake overtopped the moraine resulting in one or more large floods known as the Fox River Torrent. The upper reach of the Fox River occupies the area once covered by this lake, of which the Chain-O-Lakes are remnants. Large landforms downstream of this moraine-breaching channel were likely formed by the Fox River Torrent. The age of the torrent is unknown, but it is older than 17,360 ± 150 cal yr BP, an age assayed from fine organic debris in alluvium that fills one of the abandoned channels (Curry 2007). The sand and gravel outwash plain in which the Brewster Creek site exists is about the same age as the approximately 18,100 cal yr BP Woodstock Moraine and somewhat older than the age of the Fox River Torrent. The difference between the age of the oldest dated organics in the Brewster Creek basin (16,530 ± 190 cal yr BP; table 1) and the age of the outwash plain (about 18,100 cal yr BP) is explained by the insulating properties of the sand and gravel that covered the ice and inhibited melting, which led to formation of the kettle basin (Curry and Yansa 2004).

Paleovegetation

During the late-glacial period, forest dominated by spruce covered the Midwest. In contrast to the modern boreal forest, the late-glacial forest did not contain pine *(Pinus)*, and birch *(Betula)* was a minor component. This forest contained a number of deciduous tree species that today occur south of the boreal forest; chief among them was black ash *(Fraxinus nigra)*. This general picture for the Midwest has been known for some time (Cushing 1965, Wright and Rauscher 1990); however, few late-glacial sites from Illinois have been investigated. In fact, the only sites with published pollen diagrams are Volo Bog in McHenry County and Chatsworth Bog in Livingston County (King 1981). The cores from these sites did not sample the entire post-glacial succession, however, and the radiocarbon ages (done on samples of bulk sediment) are unreliable. Consequently, little detail is known about late-glacial vegetation change in northern Illinois.

Before the advent of radiocarbon dating (Deevey 1951), early studies attempted to correlate changes in

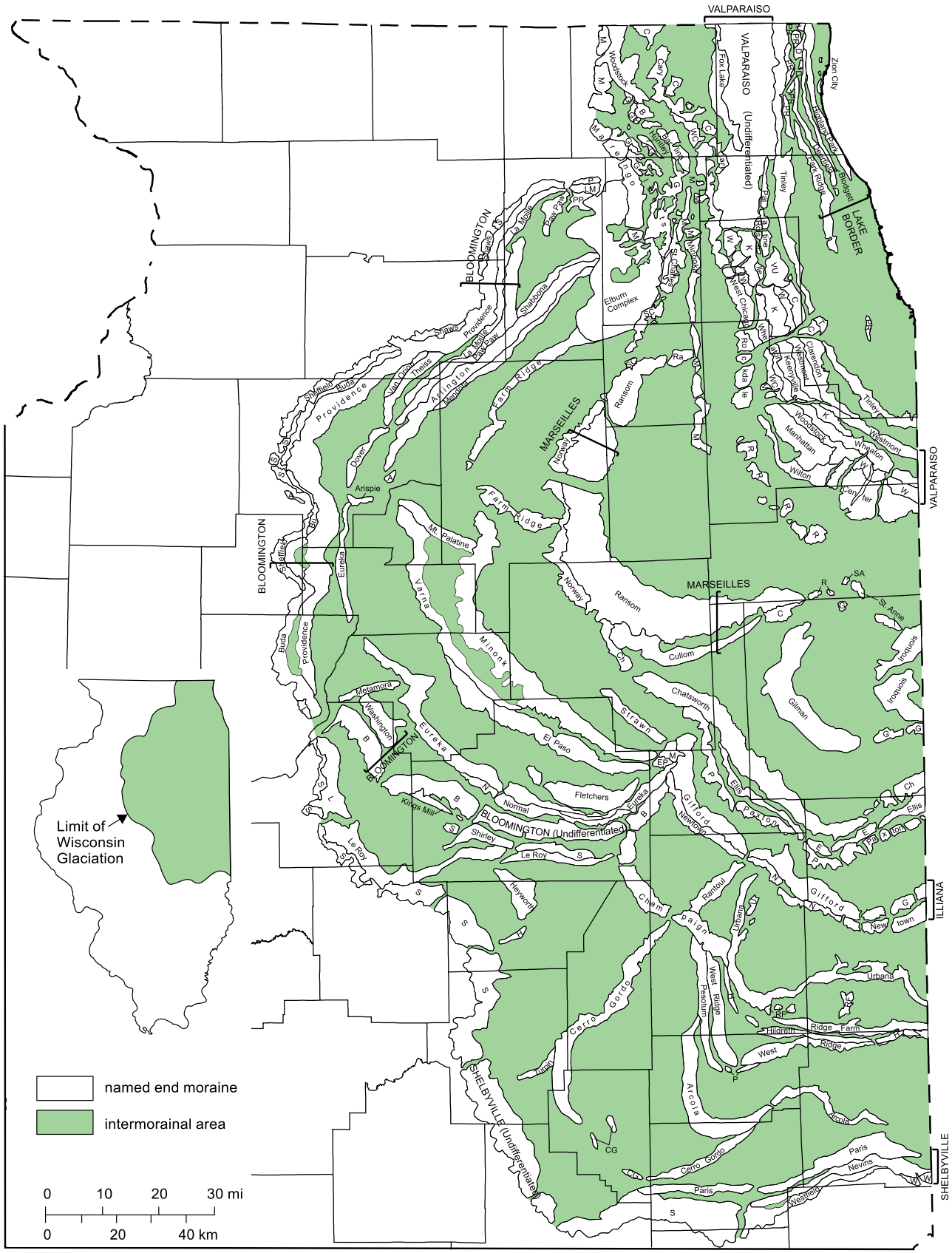

Figure 8 End moraines of the Wisconsin Glacial Episode.

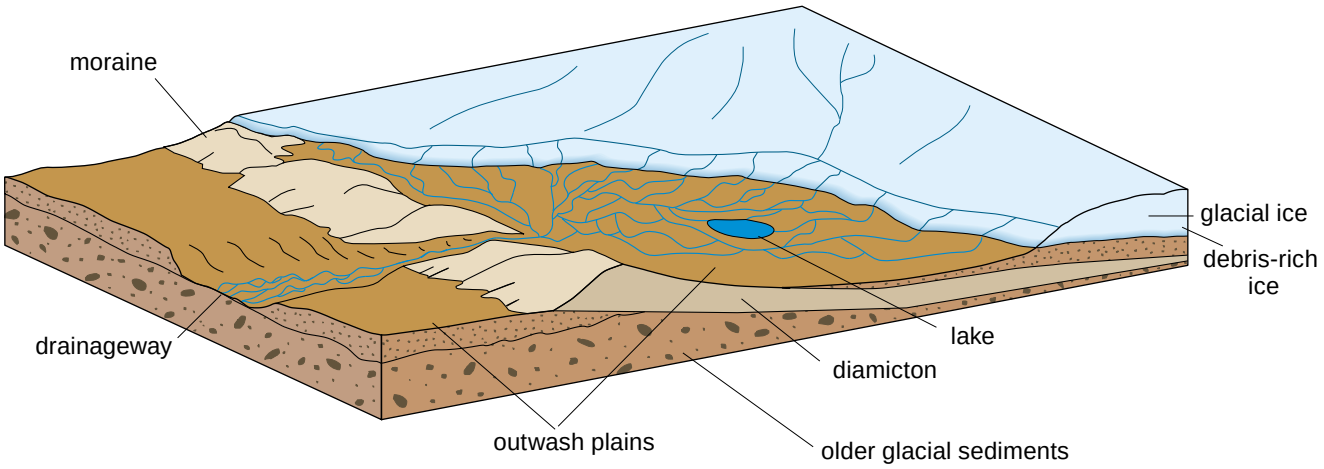

Figure 9 Conceptual model of landforms and sediment assemblages associated with the margin of a retreating continental glacier. In this depiction, the ice has melted back from its earlier position where it formed the moraine.

late-glacial vegetation in North America with the classic Bølling-Allerød-Younger Dryas sequence in northern Europe (Björck et al. 1998, 2002) and the North Atlantic (Southon 2002). Fluctuations in pollen assemblages are common in late-glacial sequences from the Midwest (Wright et al. 1963), but uncertain radiocarbon dating has hampered precise correlation (Grimm and Jacobson 2004). Analyses based on high stratigraphic resolution and AMS radiocarbon dating now unequivocally show close correlation with the North European sequence in New England and the Maritime Provinces of Canada (Mayle et al. 1993; Levesque et al. 1994, 1996; Mayle and Cwynar 1995a; 1995b; Cwynar and Levesque 1995; Doner 1996; Dorion 1997; Stea and Mott 1998; Borns et al. 2003). In southern Ontario, stable isotope ($\delta^{18}O$ and $\delta^{13}C$) studies of bulk carbonates from lake sediments show a striking correlation of the late-glacial climatic events with Europe and the North Atlantic. Not only is there evidence of the Bølling, Allerød, and Younger Dryas chronozones, but also of minor cold events, including the Intra-Bølling Cold Period, the Older Dryas, and the Intra-Allerød Cold Period (Yu and Eicher 1998, 2001; Yu 2000; Yu and Wright 2001).

In the Midwest, the details of the late-glacial vegetation have remained somewhat nebulous. An increase in spruce occurs near the top of the late-glacial spruce zone at many sites in the eastern Midwest (Rind et al. 1986, Shane and Anderson 1993), although the occurrence generally is not well dated (Grimm and Jacobson 2004). On the till plains of Ohio and Indiana, this recurrence of spruce appears to correlate with the Younger Dryas (Shane 1987), but dating and stratigraphic resolution are not sufficient to show events correlative with the Bølling-Allerød or with any of the briefer late-glacial events documented from northern Europe and the North Atlantic. Such events are documented farther east (Yu and Eicher 2001). In Minnesota, Amundson and Wright (1979) concluded that the date of the spruce decline was time-transgressive with no apparent late-glacial climatic reversals. However, Shuman et al. (2002) argued that climate changes at the beginning and the end of the Younger Dryas were synchronous but spatially variable. Those scientists featured Devil's Lake, Wisconsin (Maher 1982, Baker et al. 1992), which has a consistent series of bulk-sediment radiocarbon dates obtained by the conventional decay-count method. Although this method is susceptible to contamination by old ^{14}C-depleted carbon, until recently, the Devil's Lake ages had been viewed as reliable. This series of dates has no age reversals, and the lake is in a quartzite basin with little carbonate in the sediment. According to the chronology derived from these bulk-sediment dates, spruce declined and pine increased at the beginning of the Younger Dryas, and then pine decreased and oak and other deciduous trees increased at the termination of the Younger Dryas. Thus, Shuman et al. (2002) argued that, although climatic changes were synchronous with the Younger Dryas chronozone, the Younger Dryas was a warm event in southern Wisconsin. However, a new series of AMS radiocarbon dates from Devil's Lake shows that the earlier chronology is about 1,000 years too old. In fact, a recurrence of spruce corresponds with the Younger Dryas, and the increase in pine occurs at the end of the Younger Dryas rather than at the beginning, indicating a colder, not a warmer climate (Grimm and Maher 2002).

Although the general contention of Shuman et al. (2002) for synchronous Younger Dryas response but spatial variability in direction and magnitude might be correct (Grimm and Jacobson 2004), other regional data suggest that warmer climate during the Younger Dryas chronozone in Wisconsin is improbable. The increase in spruce to the southeast in Indiana and Ohio suggest cooler climate, as does the readvance of the Laurentide Ice Sheet to the Marquette Moraine in northern Wisconsin and

the Upper Peninsula of Michigan during the Younger Dryas (Drexler et al. 1983, Farrand and Drexler 1985, Lowell et al. 1999, Larson and Schaetzl 2001). These debates can only be resolved by the establishment of a more precise temporal framework based on AMS dates of appropriate material (e.g., terrestrial macrofossils).

The thick sediments comprising the Bølling, Allerød, and Younger Dryas chronozones at Brewster Creek provide an opportunity (1) to determine whether vegetation change in northeastern Illinois correlates with the North Atlantic record, specifically with the $\delta^{18}O$ record from the Greenland ice cores, and (2) to investigate the composition of the late-glacial vegetation. With 12 AMS ^{14}C dates for the late-glacial period, Brewster Creek is one of the best-dated late-glacial records derived from the Midwest.

Local-scale variability of past vegetation is another concern. On a subcontinental scale, relationships clearly exist between vegetation and climate. On a more local scale, climatic control on the vegetation mosaic may not be strong (Grimm 1984). For example, the prairie-forest border in Minnesota is sharply delineated by firebreaks, typically rivers and lakes, with prairie on one side and mesic forest on the other (Grimm 1984). As another example in the Great Lakes region, *Pinus banksiana* (jack pine) forests occur on sandy outwash plains, whereas mesic hardwoods occur on adjacent moraines with loamy soils (Brubaker 1975, Jacobson 1979, Almendinger 1992). These different vegetation types occur under the same regional climate. Numerous paleovegetation studies in the Midwest have focused on local landscape variability during the Holocene (McAndrews 1966, Brubaker 1975, Jacobson 1979, Grimm 1984, Gajewski 1987, Almendinger 1992, Ewing 2002), but not late-glacial time. For most of these studies, modern analogs exist for the Holocene vegetation, and interpretation is fairly straightforward in terms of climate and ecological processes. However, for the late-glacial interval in the Midwest, the vegetation has no modern analog (Overpeck et al. 1992; Williams et al. 2001, 2004; Jackson and Williams 2004). Late-glacial climate also probably had no modern analog, and some ecological processes may not have modern analogs (mastodons and mammoths, for example, still roamed the landscape (Graham and Grimm 1990)). A local vegetation mosaic would be expected to have existed on the landscape, but little information about this mosaic has been found. The contrast in vegetation may be observed by comparing and contrasting the pollen records at Brewster Creek with those at Nelson Lake and Crystal Lake, both located within 20 km of the Brewster Creek site.

Nelson Lake

Curry et al. (2002) reported on the hydrological functioning of Nelson Lake and the paleovegetation and paleoenvironment of the lake based on pollen and ostracode analysis of a 13.79-m core. As with Brewster Creek, Nelson Lake occupies a kettle basin. Ostracode and pollen diagrams of the core were discussed in that report; additional details have been discovered in subsequent studies of the core (Grimm and Maher 2002, Curry et al. 2004, Nelson et al. 2006).

The Nelson Lake investigation showed that vegetation responded to environmental changes brought on by global climate change during the last glacial-to-interglacial transition (Curry et al. 2002, Grimm and Maher 2002). Many deciduous tree elements that constitute the early Holocene forests at 11,000 cal yr BP first began to invade the area much earlier, starting at about 14,700 cal yr BP during the Bølling-Allerød intervals (fig. 10). In pollen zone 7, correlating with the Younger Dryas chronozone (12,890 to 11,650 cal yr BP), black ash pollen decreased as spruce pollen increased. By the onset of the Holocene at about 11,650 cal yr BP, all the elements of the modern forest had become established in Illinois, including oak, hickory, and elm. Spruce had virtually disappeared. The Nelson Lake investigation was the first from the interior of North America to show excellent evidence for environmental response to these relatively short-lived global changes; this discovery was made possible because of a superior sediment accumulation model based on 14 AMS ^{14}C ages (Curry et al. 1999, 2002; Grimm and Maher 2002).

One of the interesting results of the Nelson Lake study is that the Younger Dryas interval is represented in the lake sediment core by a relatively thin layer of sediment. Out of a 15-m-long core representing more than 18,000 cal yr of sedimentation, the 1,240-year Younger Dryas interval (from 12,890 to 11,650 cal yr BP) is represented by only about 30 cm of sediment. The sediment accumulation rate changed from about 0.024 cm/yr during the Younger Dryas to an average of 0.10 cm/yr for the Holocene—an increase of more than four times.

Methods

Coring

Twelve 4.3-cm-diameter sediment cores were sampled at Brewster Creek with a track-mounted GeoProbe Model 6400. The tracks allowed the rig to maneuver easily across the soft peat soils. During sampling, the corer was pushed and hammered from about 1.0 to 1.5 m into the sediment. The sediment cores were recovered in transparent acrylic tubes, labeled, and described. Next, the ends of the acrylic tubes were closed off with duct tape, and the core segments were transported to the ISGS and stored in a cold room prior to detailed study. The location of the borings (fig. 1) was determined using a Garmin GPSmap76S unit.

Monoliths were collected at two test pits (fig. 1a). A monolith is similar to a core, but is physically cut from a vertical section and stored in a long tray. The main monolith was collected in a large pit near the center of the transect of borings. The "beach" monolith was collected in a shallow pit that rapidly deteriorated due to slumping of well-sorted sand. The location of the beach monolith was on the northern margin of the transect of borings.

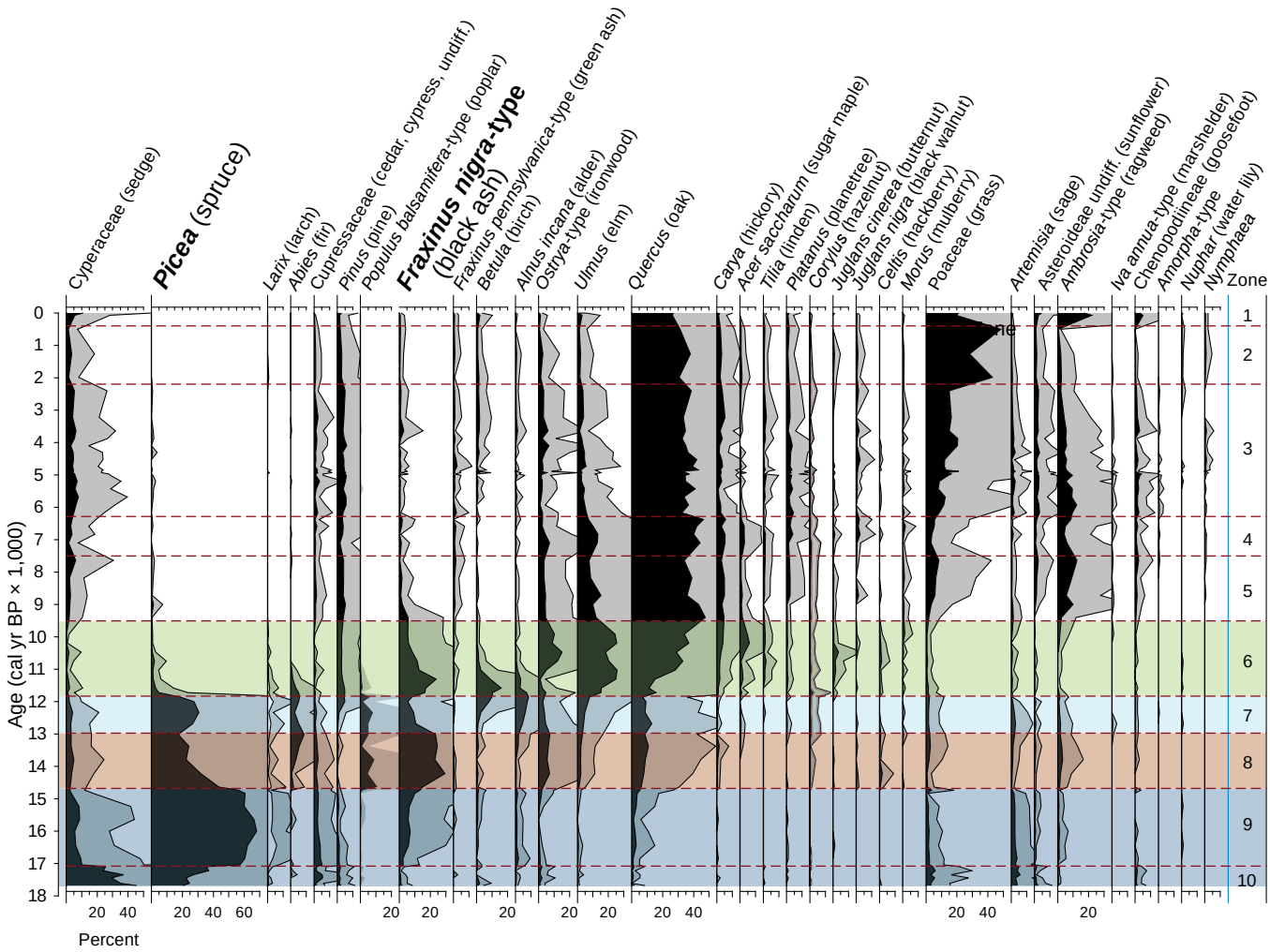

Figure 10 Diagram showing the percentage of pollen from Nelson Lake plotted against age expressed as thousand calibrated years before present (cal yr BP). The gray area shows five times exaggeration of the data from Curry et al. (2002). Pollen Zones 6 through 10 correspond with the following chronozones: early Holocene (Zone 6), Younger Dryas (Zone 7), Bølling-Allerød (Zone 8), and late glacial (Older Dryas; Zones 9 and 10).

Appendix 1 provides descriptions of the sediments recovered from this part of the project. Core loss is reported. Core loss is the difference between the length of the recovered core and the length pushed. The core loss interval is assumed to have come at the end of the run due to sediment jamming in the tube either by swelling sediment or by friction from dragging silt, sand, or gravel along the acrylic liner. Other factors also may have come into play and caused the core loss zone to occur anywhere in the sampled interval, especially in soft sediment. For example, initially core recovery in marl was poor. The marl consists of beds of shell-rich and low-density, shell-poor material. As the corer pushed through this material, resistance to sediment sliding into the sampling tube caused by the shells dragging on the liner surface may have been great enough that the sampler pushed through the shell-poor sediment and missed sampling it. To attempt to overcome this uncertainty, we used shorter runs (1.0-m runs instead of standard 1.5-m runs) or sampled overlapping intervals at adjacent coring sites.

Based on our observations of the GeoProbe cores, master cores BC-1A and BC-1B (collectively referred to later in the report as core BC-1) were sampled by hand at 1-m-long drives on November 10, 2003, with a 5-cm-diameter Wright square-rod piston corer. The cores were offset 50 cm to ensure complete recovery of the sediment succession. Cores were extruded in the field and wrapped in plastic wrap and aluminum foil. The cores were kept in cool storage until February 2004, when they were transported to the Core Characterization Lab at the Limnological Research Center, University of Minnesota, Minneapolis. The cores were sliced in half and scanned at true color and true scale; the resulting digital files allow for true color reproductions of the core with no image distortion (fig. 11). The cores were sliced into 1-cm sections and

stored in airtight sample cups. The volume of each slice is approximately 20 cm^3. The labeled cups were put into cold storage at 39.2°F (4°C) at the ISM. Samples used in our analyses were taken from the material stored in the sample cups.

Pollen identification was done on samples from 748 to 232 cm, dating from approximately 16,000 to 10,500 cal yr BP. The pollen sum included trees, shrubs, and upland herbs. The percentages of pollen for aquatic species are based on the pollen sum plus aquatics. Sedge is included with the aquatics. Spruce was distinguished as white spruce or black spruce (Hansen and Engstrom 1985). Conifer stomata also were identified (Hansen 1995, Hansen et al. 1996, Glaser et al. 2004). Pollen is preserved in the sediment above and below this interval, but pollen concentration is low in the deeper silty sediment, and, in the overlying peaty deposits, pollen is difficult to concentrate from the peat. Pollen from these intervals was not counted because of time constraints.

Pollen samples (0.5 or 1.0 mL) were prepared using standard methods (Fægri et al. 1989), including treatment with potassium hydroxide to remove humics, 10% hydrochloric acid to remove carbonate, 48% hydrofluoric acid to remove silicates, and acetolysis to remove organic matter. Samples were also sieved with a 10-m Nitex screen to remove clay and fine silt particles. When necessary, samples were treated with 10% nitric acid to remove pyrite. The remaining residue contained pollen, charcoal, other resistant organic matter, and some resistant minerals.

To prepare sediment for diatom analysis, 0.5 mL was heated in nitric acid and potassium nitrate to remove most organic matter and carbonate minerals (Patrick and Reimer 1966). The resulting sediment and diatom slurry was mounted onto glass microscope slides with the mounting medium Zrax (MicrAP enterprises, http://www.sas.upenn.edu/~dailey/micrap.htm). Diatom taxa were identified at 1,000× magnification with a Leitz Orthoplan microscope with a NPL Fluotar objective (numerical aperture 1.32), and 150 valves were counted per depth using Krammer and Lange-Bertalot (1991a, 1991b, 1997a, 1997b), Lange-Bertalot (1993), and Patrick and Reimer (1966, 1975) as the primary identification references. Selected diatoms and ostracodes were imaged with a scanning electron microscope at Northern Illinois University. Diatoms were analyzed from a depth of 374 to 684 cm and at 328, 716, 740, and 764 cm. Diatoms were rare or absent above 374 cm (with the exception of 328 cm) and below 684 cm (with the exception of 716, 740, and 764 cm).

Ostracodes were analyzed at 8-cm intervals. To pretreat the 10-cm^3 sample for sieving, about 0.5 teaspoon (2.5 cm^3) of sodium bicarbonate was added to the moist samples, followed by immersion in hyper-boiling tap water. After cooling, the sediment slurry was washed on a Tyler #100-mesh sieve with a shower spray. The residue was air-dried. Ostracodes were identified using a binocular microscope. All adult valves were identified and counted using the descriptions of Hoff (1942) and Delorme (1970a, 1970b, 1970c, 1971). Most species were imaged digitally under reflected light using a MicroPublisher 3.3 RTV mounted to a Nikon SMT-2T trinocular microscope. Ostracodes were identified in the 772- to 238-cm depth interval. Samples prepared from 208 to 234 cm and 776 to 860 cm were barren of ostracodes.

Loss-on-ignition (LOI) analyses were done on 1-cm^3 subsamples from the 4-cm intervals used for the pollen and diatom analysis. Organic matter, carbonate content, and terrigenous sediment were estimated from LOI data (Dean 1974). The percentage of organic matter was determined by weighing the loss of dry mass after the sample was heated for 24 hours at 932°F (500°C); the percentage of carbonate is the proportion of weight loss after the residue was heated from the 932°F (500°C) for 24 hours at 1,652°F (900°C), multiplied by a correction factor of 2.27, compared with the original dry weight. The weight percentage of the 1,652°F (900°C) residue with respect to the original dry mass is attributed to mineral matter other than carbonate, is primarily terrigenous (i.e., not biogenic), and is composed of clay minerals, quartz, feldspar, other silicate minerals (such as mica), and well-crystallized oxides (such as magnetite). Diatom frustules are composed of opal, a hydrated form of silica, and are destroyed during the final heat treatment.

Clay Mineral and Particle-Size Distribution

Sediment samples were analyzed for clay mineral and particle-size distribution at 8-cm intervals. Sample mass ranged from 10 g to about 25 g. Samples were pretreated separately with household bleach and 10% hydrochloric acid to rid them of organic matter and carbonate minerals, respectively. Since the acid treatment removed both biogenic and geogenic carbonate, the results are not representative of the geogenic sediment.

The X-ray diffraction techniques of Hughes et al. (1994) were used for clay mineral analyses of 79 samples. X-ray diffraction peak heights were analyzed from glycolated aggregate slides of the <2-µm clay using a Scintag Model XPH-103 diffractometer and the peak intensity factors in Hughes et al. (1994). Peak heights for common phyllosilicates and silicates in the clay-size fraction were measured at fixed °2θ positions (Curry and Grimley 2006). The relative proportion of two mineral suites was determined: (1) clay minerals (expandable clays, illite, kaolinite, and chlorite) and (2) silicate minerals (quartz, potassium feldspar, and plagioclase). In many previous clay mineral studies of Quaternary sediment in Illinois, the relative percentage of kaolinite and chlorite were combined and based on the relative intensity of the compound first-order kaolinite/second-order chlorite peak at 12.4°2θ (Willman et al. 1963). In this study, the relative percentage of kaolinite and chlorite were determined by calculating the ratio of the intensity (in counts per second) of the second-order kaolinite peak at 24.9°2θ versus the fourth-order chlorite peak at 25.1°2θ and applying that ratio to the compound peak (Curry and Grimley 2006).

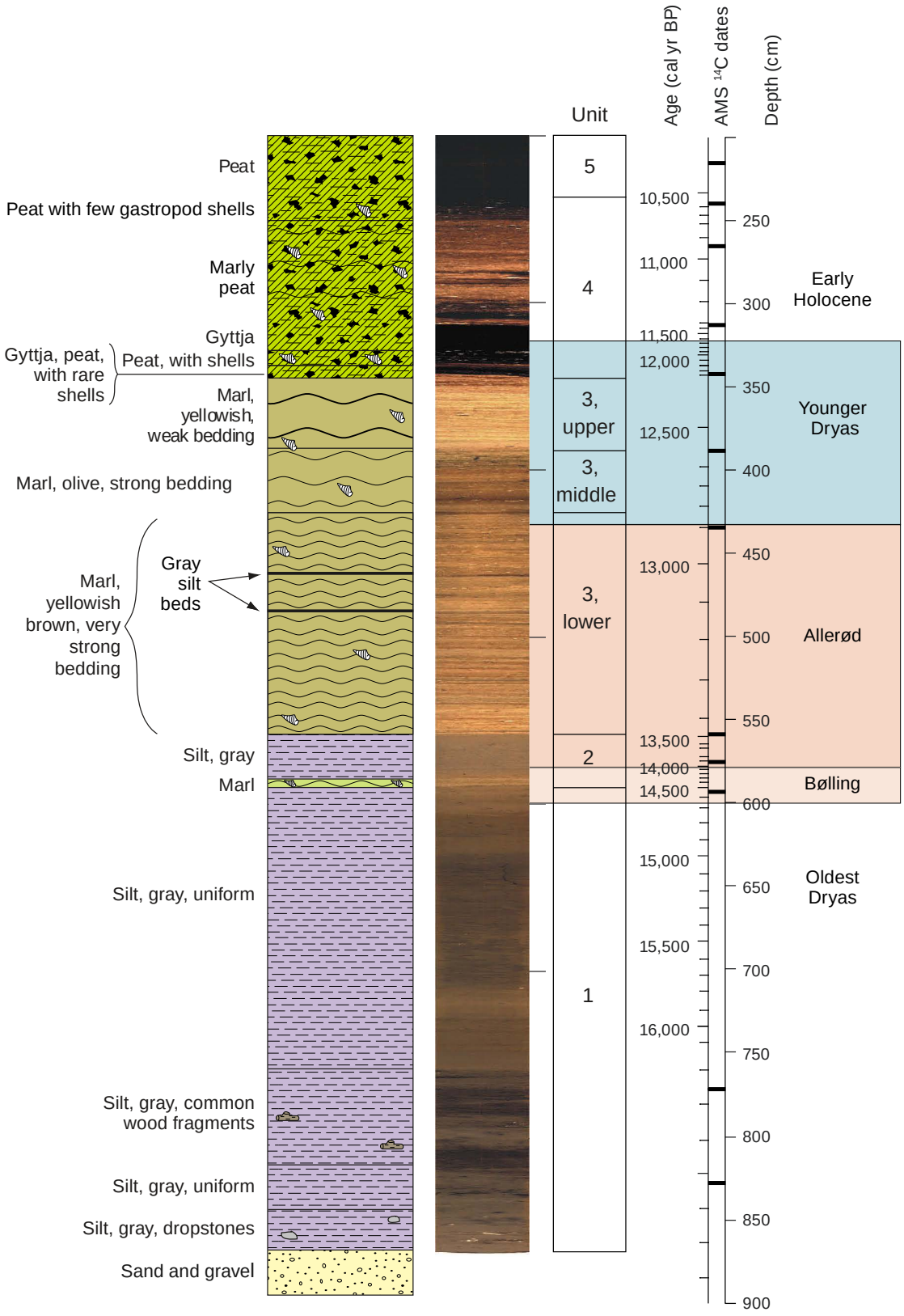

Figure 11 Schematic of stratigraphic lithologic units and compressed scanned image of core BC-1 related to age determinations, depth intervals, and chronozones discussed in the text; AMS, accelerated mass spectrometer.

In northeastern Illinois, the glacial diamicton units are rich in illite, and loess is rich in expandable clay minerals (Willman et al. 1963). Most illite is derived from glacial erosion and comminution (grinding up) of Paleozoic shale. Most expandable clay minerals in Illinois Quaternary sediments are derived ultimately from reworked Tertiary shale in the High Plains (Willman et al. 1966). To make its way to Illinois, the shale was first eroded by glaciers and stored as outwash in the valleys of major rivers, such as the Missouri and Mississippi Rivers. Under very cold and dry conditions, wind later picked this exposed sediment and transported it eastward great distances. Loess is about 1 m thick in the study area. Compared with Illinois glacial tills, midwestern loess also is rich in quartz relative to feldspars (Curry and Grimley 2006).

The mineral in Illinois soil profiles that is most easily weathered is chlorite, which upon oxidation breaks down to vermiculite (a semi-expandable clay mineral) and magnesium and iron oxides. This sensitive measure of weathering is captured in the values of the diffraction intensity ratio, which is the ratio of the compound kaolinite/chlorite peak at 12.4°2θ versus the illite peak at 8.8°2θ (in counts per second). Unweathered glacial till in Illinois generally has diffraction intensity values of about 1.5 or less. Samples of the modern soil developed in glacial till have diffraction intensity values as great as 6 or higher (Willman et al. 1966).

Particle-size analysis was conducted using a modified pipette procedure (Soil Survey Staff 1996). The following particle-size classes were determined: sand (63 to 2,000 µm), silt (2 to 63 µm), and clay (< 2 µm). Subclasses included very coarse sand (1,000 to 2,000 µm), coarse sand (500 to 1,000 µm), medium sand (250 to 500 µm), fine sand (125 to 500 µm), and very fine sand (63 to 125 µm), very coarse silt (32 to 64 µm), coarse silt (16 to 32 µm), medium silt (8 to 16 µm), fine silt (4 to 8 µm), and very fine silt (2 to 4 µm). The geometric mean particle diameter size was calculated using a modified Wentworth size fractionation scheme (Krumbein and Pettijohn 1938, Walter et al. 1978, Konen 1999). The samples of marl and peat contained too little terreginous material for particle-size analysis. In addition to the small sample size, the samples did not redisperse after the bleach and acid pretreatments.

Among the erosive agents on the earth's surface, glaciers are a primary producer of silt-sized particles. Once produced and deposited as a component of till, lake sediment, or alluvium, the subclasses of silt-sized particles are readily sorted into grain-size subclasses. For example, relative to finer silt fractions, the very coarse silt fraction is difficult for wind to entrain and transport far from its alluvial source. Far-traveled loess, therefore, is enriched in coarse silt relative to very coarse silt; glacial deposits, such as till, contain about equal amounts of both silt fractions. The ratio of very coarse silt (32 to 64 µm) to coarse silt (16 to 32 µm) may be used to gauge the input of eolian silt to soil and lake systems (Follmer 1982, Curry 1989, Curry and Follmer 1992).

Statistical Analysis

Principal components analysis (PCA) is a multivariate statistical method used to measure the similarity of variables among numerous samples. For this and other paleoecological studies in which there are downcore data for several variables, PCA is used for two primary purposes. First, PCA determines variables that respond in similar ways, and when used iteratively, PCA can be used to simplify data sets by indicating to the user whether to combine similar variables or use a single representative variable. Second, PCA identifies variables or groups of variables that behave independently. Ecologists often use stratigraphic plots of PCA scores to identify environmental parameters that affect the data structure (Jongman et al. 1987).

Radiocarbon Ages

Two of 14 samples were large enough to date by conventional methods at the ISGS Radiocarbon Laboratory. The remaining 12 radiocarbon ages were determined by AMS on fossil needles and seeds (table 1, figs. 12 and 13). The ages were converted to calibrated calendar years with CALIB 5.02 using the IntCal04 calibration (Reimer et al. 2004). CALIB provides a 1σ or 2σ probability range for each calibrated date. To fit an age model, the 50% median probability was used for each calibrated date, except for the two dates from the upper marl unit, as discussed in the Results section.

Results

Stratigraphy and Radiocarbon Ages

The succession of fossiliferous sediment recovered from the Brewster Creek study fills a depression formed in deposits of oxidized sandy loam diamicton and very poorly sorted, stratified sand and gravel. These materials are interpreted to be debris flows (the diamicton) and outwash (the sand and gravel). Water-well borings indicate that the total drift thickness in this area is about 20 to 37 m and that the surface of the bedrock is at an elevation of about 201 to 210 m above sea level, more than 18 m below what is shown on figure 14.

Fossiliferous kettle-fill sediment overlies glacial sediment. Very poorly sorted sand and gravel outwash was sampled at the base of a few cores (Appendix 1). The sand and gravel unit correlates with the Henry Formation (Willman and Frye 1970). Neither the diamicton nor the sand and gravel units contain fossils. The Henry Formation is as much as about 9 m thick in aggregate pits just east of the wetland site. These exposures reveal planar bedding and shallow cross-bedding in wide, shallow channel fills about 0.6 to 0.9 m deep and 1.5 to 3.3 m wide.

Diamicton (sandy loam matrix) was observed in the base of most cores. The unit is very pebbly, and sample recovery was generally poor. The matrix was oxidized even in areas in which the overlying silt was gray, fossil-bearing, and unoxidized. The thickness of this unit varies from at least 0.24 m to about 0.12 m at the site; exposures at nearby sand and

gravel pits indicate that the unit is not more than about 1.0 m thick. The loose texture of the diamicton, proximity of the West Chicago Moraine, and location on an alluvial fan (outwash plain) surface indicate that this unit was likely deposited by debris flow. The diamicton unit is a facies (variant) of the Henry Formation.

The thickness, distribution, and lithological characteristics of the units that fill the kettle are portrayed in cross section A–A′ (fig. 14) and tabulated in table 2; the line of section is shown on figure 1. The core descriptions are in Appendix 1. The five fossiliferous units that overlie the glacial sediment are listed here:

Unit 1. Basal silt about 2.58 m thick with locally common wood fragments as much as 4 cm across.

Unit 2. A transition zone between silt and marl 0.30 m thick that includes a thin bed of marl 0.05 m, and a thicker bed of gray silt 0.25 m thick.

Unit 3. Bedded marl 2.15 m thick.

Unit 4. A transition zone between marl and peat composed of thin interbeds of marl, peat, and sand about 1.09 m thick.

Unit 5. Peat about 2.35 m thick.

The fossiliferous units pinch out toward the basin margin. In the uplands, the Henry Formation sand and gravel is overlain by a 1-m-thick mantle of silt loam to silty clay loam known as Peoria Silt. This mantle was deposited by the wind and is loess. The loess becomes buried by peat and sand along the basin margins and by marl that thickens basinward. Particle-size analyses and stratigraphic relationships indicate that the loess is laterally equivalent to Units 1 and 2.

Unit 1 Composed chiefly of silt, Unit 1 is as much as 3.6 m thick in boring BC-5. This unit is the basal lacustrine unit at the Brewster Creek site and correlates with the Equality Formation (Willman and Frye 1970). Thirty-four samples of the silt unit analyzed for particle-size distribution contained 24.7 ± 12.4% sand, 70.1 ± 10.9% silt, and 3.7 ± 4.5% clay. The silt

Table 1 Radiocarbon ages[1] for the core, Brewster Creek-1 (BC-1).

Lab number	Sample depth (cm)	Material dated	^{14}C age	1σ	Calibrated age: 2σ lower bound	Calibrated age: 50% median probability	Calibrated age: 2σ upper bound	δ^{13}C
Core BC-1								
CAMS-105794	216	*Larix* needles	9,185	40	10,244	10,342	10,487	ND
CAMS-105795	240	*Larix* needles	9,335	40	10,421	10,549	10,671	ND
CAMS-105796	256	*Larix* needles	9,525	40	10,686	10,860	11,082	ND
CAMS-116405	314	*Larix* needles	9,925	35	11,236	11,312	11,596	ND
CAMS-111247	341.5–345	*Larix* needles	10,555	40	12,395	12,430[2]	12,738	ND
		Picea needle						
		Picea seed						
CAMS-116406	389– 390	*Larix* needles	10,495	35	12,246	12,530[3]	12,678	ND
CAMS-111248	435	*Schoenoplectus* seeds	10,980	35	12,854	12,909	12,974	ND
CAMS-111409	557–559	*Larix* needles	11,605	45	13,319	13,440	13,598	ND
CAMS-111410	575–576	*Larix* needles	12,055	45	13,793	13,907	14,023	ND
CAMS-111411	592–594	charcoal and	12,495	45	14,247	14,614	14,940	ND
		Larix needles						
CAMS-105797	772	*Picea* needles	13,750	40	16,034	16,380	16,761	ND
CAMS-105798	828	*Picea* needles	13,870	60	16,148	16,526	16,909	ND
Main monolith								
ISGS-5223	~300	*Larix* wood	9,150	70	10,205	10,333	10,499	–26.9
ISGS-5225	~300	wood	10,860	70	12,784	12,856	12,938	–26.2
Core BC-6		wood in gleyed						
		sand layer	11,020	80	12,960	12,850	13,090	–26.2
Mastodon site								
ISGS-5858	100–200	wood above rib	12,120	70	13,810	13,970	14,130	–24.1
ISGS-5860	100–200	wood below rib	11,710	70	13,400	13,560	13,730	–25.9
UCIAMS-22177	100–200	collagen/dentine	11,455	35	13,230	13,300	13,390	–14.9

[1]Ages were calibrated using CALIB 5.2 (Reimer et al. 2006) online. Samples ISGS-5225 and ISGS-5223 are shown in figures 2 and 3 (http://calib.quib.qub.ac.uk/calib/calib.html).

[2]The probability distribution of the calibrated date is bimodal. This date is the first mode.

[3]The 1σ probability distribution of the calibrated date is bimodal. This date is the second mode.

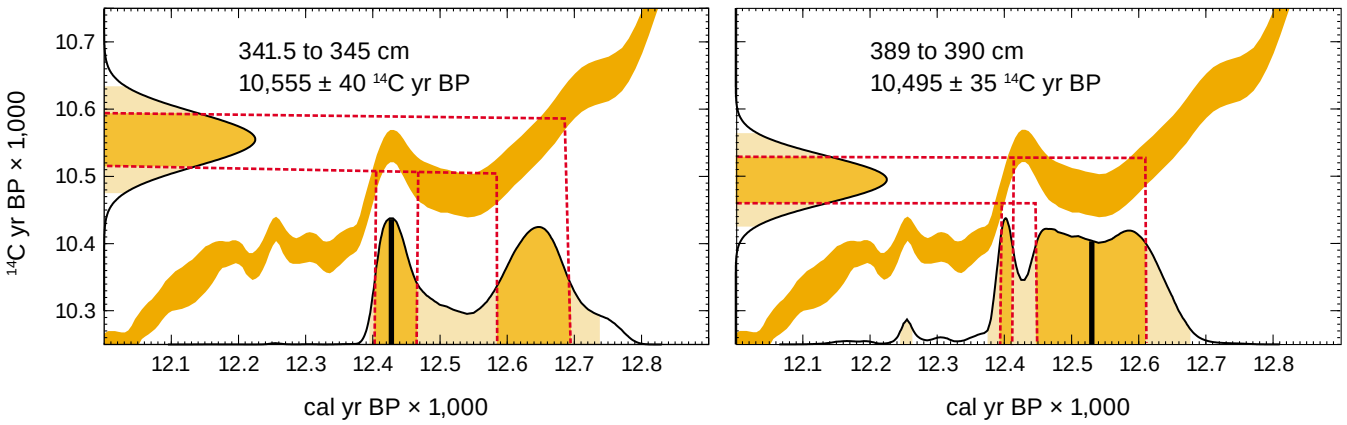

Figure 12 Probability distributions of the two inverted radiocarbon dates. The calibrated probability distributions are bimodal. The thick black lines indicate the modes selected so that the calibrated dates for the age model are not inverted.

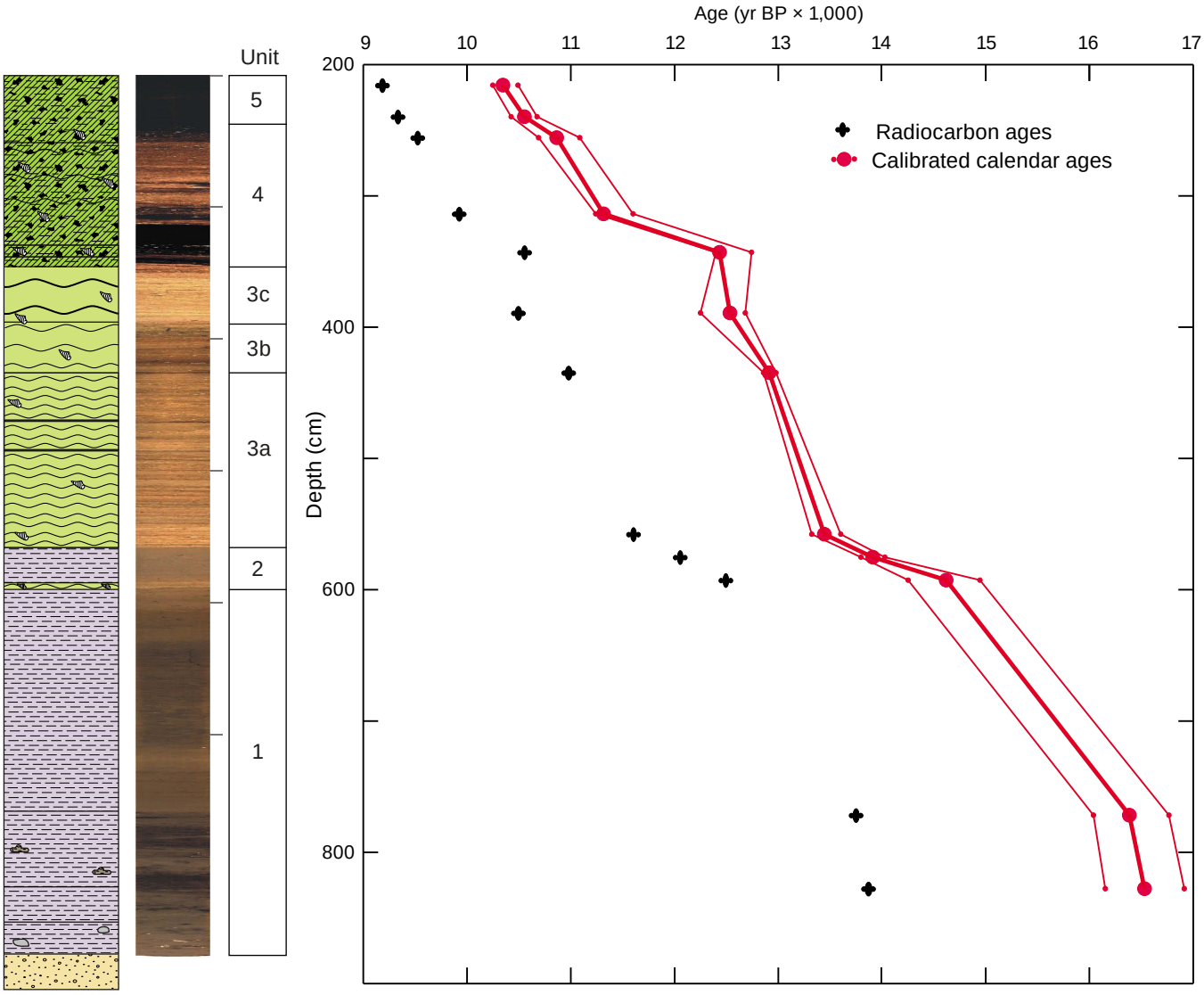

Figure 13 Uncalibrated radiocarbon (black) and calibrated (red) calendar ages from core BC-1 (table 1). The age-depth model used in the report is the thick red line that connects the median ages.

unit comprises three facies, including a basal facies of gleyed silt with abundant stones. The basal silt facies is as much as 0.05 m thick in boring BC-3. Much of the Equality Formation is the uniform to stratified, wood-bearing facies. This unit is as much as 3.17 m thick in boring BC-12. An upper fossil-poor facies 1.69 m thick was identified in the main core BC-1. The LOI analyses showed little difference in organic carbon content among the three facies; the silt unit as a whole contains by weight about 4.7 ± 1.6% organic carbon, 26.7 ± 6.8% carbonate minerals, and 68.6 ± 7.4% terrigenous material (chiefly quartz, feldspar, and clay minerals; fig. 15). The unit contains abundant expandable clay minerals relative to illite, chlorite, and kaolinite, averaging 50.9 ± 7.9% expandable clay minerals, 33.5 ± 6.4% illite, 9.4 ± 1.3% kaolinite, and 6.7 ± 1.0% chlorite (fig. 16). Diffraction intensity values are <1.5, indicating that the chlorite is intact and that the sediment did not undergo any oxidation (weathering). Above a depth of about 7.5 m, the silt unit is enriched in coarse silt relative to very coarse silt, indicating that the silt source was eolian (fig. 16). The lower part of the silt unit has several intervals with relatively abundant, very coarse silt (relative to coarse silt), indicating some contribution from the local glacial sediment. Such horizons are modestly enriched in illite 10 to 20% relative to expandable clay minerals, an expected result since the local glacial sediment is illite-rich. The lower part of the wood-bearing facies yielded radiocarbon ages of

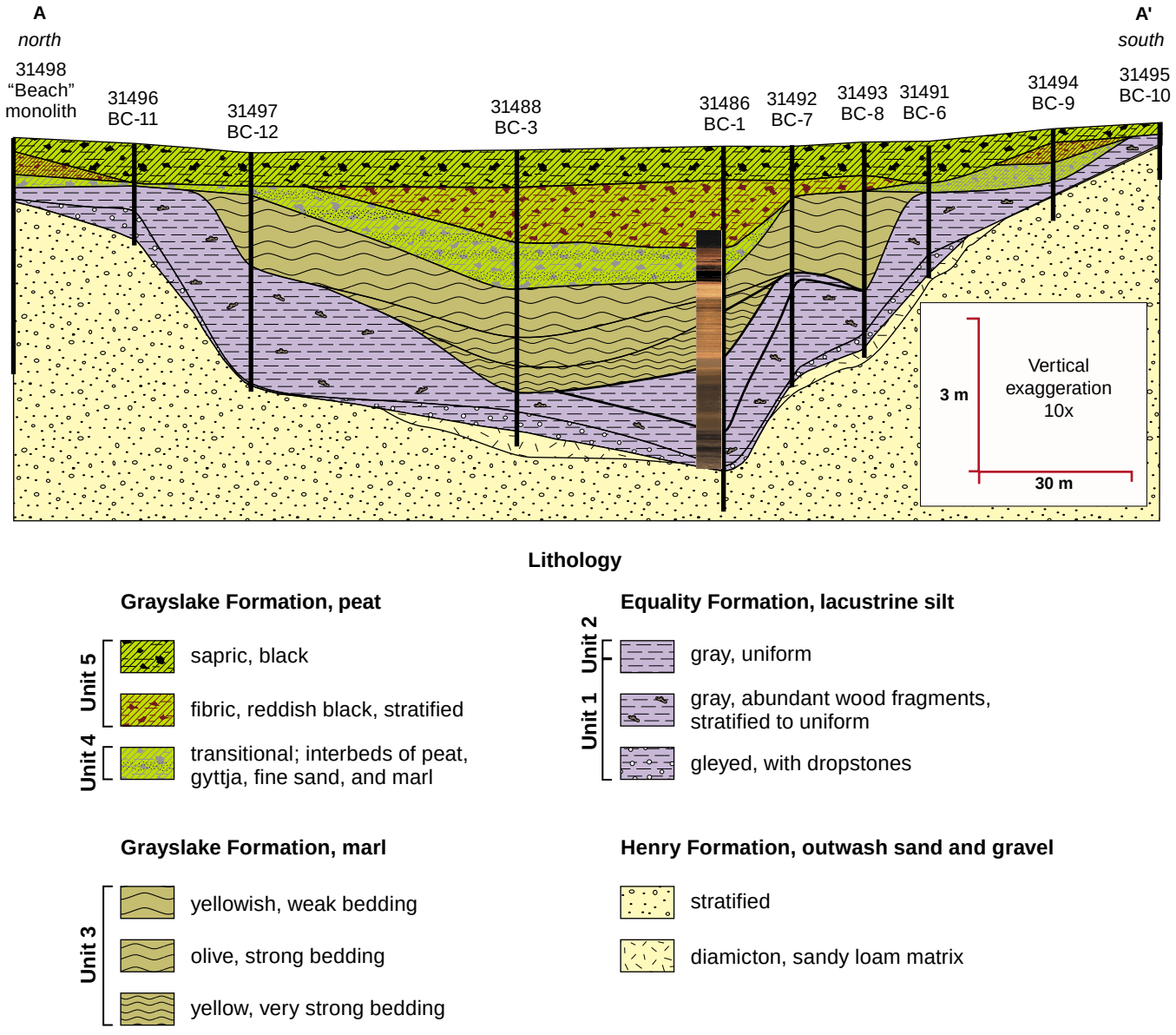

Figure 14 Cross section of lithologic units across the Brewster Creek site. The line of section is shown on figure 1. The numbers that occur with the boring numbers are the API numbers that identify the associated field descriptions and logs on file at the Illinois State Geological Survey.

13,870 ± 60 ^{14}C yr BP and 13,750 ± 40 ^{14}C yr BP. In Brewster Creek core BC-1, the uppermost part of the unit yielded an age of 12,495 ± 45 ^{14}C yr BP (table 1).

Unit 2 The lower transition zone, Unit 2, between the silt and marl units, was identified only in master core BC-1; similar horizons may have been missed in the other cores because of core loss. The unit is composed of a basal layer of marl 5 cm thick and an overlying layer of gray silt 25 cm thick. Based on LOI, the composition of the silt and marl in the transition zone is similar to, but not the same as, as the associated sediments above and below it (fig. 15). In that sense, the unit is truly transitional. The clay mineralogy of the lower transition zone is more like the underlying silt unit than the overlying marl (fig. 16).

Two radiocarbon ages were determined on *Larix* needles and charcoal from the lower transition zone. The oldest age of 12,055 ± 45 ^{14}C yr BP comes from a depth of 575 cm near the middle of the transition zone. The younger age of 11,605 ± 45 ^{14}C yr BP comes from a depth of 557 to 558 cm immediately below the contact with the overlying marl unit, described below. Together with radiocarbon age from the upper part of the silt unit of 12,495 ± 45 ^{14}C yr BP from a depth of 592 to 594 cm, the sediment accumulation rate for this part of the core was about four times slower than the underlying silt unit (0.04 cm/yr compared with 0.18 cm/yr).

Unit 3 The marl, Unit 3, is as much as 2.74 m thick in boring BC-3 and is composed of chiefly biogenic carbonate with little organic matter and terrigenous sediment. The marl is part of the Grayslake Peat (Willman and Frye 1970). The biogenic carbonate includes (by weight) primarily aquatic gastropods with less mass from ostracode valves and encrustations on stems and oogonia of charophytes (fig. 17). Along the margins of the basin, the marl is typically uniform, but toward the center, the marl is bedded. Three facies, separated on the basis of bedding, were identified in the main core BC-1 and correlated with the other core descriptions (fig. 14). The lower facies (574 to 492 cm) has very strong bedding and is chiefly yellowish brown; the middle facies (492 to 402 cm) has strong bedding and is olive; the upper facies (402 to 359 cm) has weak bedding or is uniform and is light yellowish brown. Thin beds of gray silt occur at depths of 462 to 463 cm and 483 to 484 cm. The LOI analyses of 24 samples indicate that, overall, the marl contains 9.6 ± 6.0% organic carbon, 77.7 ± 8.0% inorganic carbon, and 12.7 ± 5.9% terrigenous sediment.

Two clay mineral zones are identified in the marl unit; a lower, illite-rich zone, and an upper zone with variable values that include some with expandable clay mineral proportions similar to that of the silt unit. The lower clay mineral zone occurs from a depth of about 417 to 554 cm and, based on the analysis of 18 samples, contains 20.3 ± 8.8% expandable clay minerals, 57.4 ± 8.3 % illite, 12.0 ± 2.8% kaolinite, and 10.3 ± 1.9% chlorite. The upper clay mineral zone occurs from a depth of 349 to 417 cm and, based on the analysis of 10 samples, contains 35.0 ± 14.7% expandable clay minerals, 47.1 ± 12.4% illite, 10.5 ± 2.0% kaolinite, and 7.4 ± 2.9% chlorite.

Three radiocarbon ages were obtained from the marl unit in core BC-1. *Schoenoplectus* (bulrush) seeds from a depth of 435 cm yielded an age of 10,980 ± 35 ^{14}C yr BP. A mid-depth sample of seeds and needles from a depth of 389 to 390 cm yielded an age of 10,495 ± 35 ^{14}C yr BP. The top of the marl unit (341.5 to 345.0 cm) yielded larch needles with an age of 10,555 ± 40 ^{14}C yr BP. The latter two ages are chronologically inverted, but statistically the same when the error is taken into account. As already discussed, the calibration procedure yielded a bimodal distribution of potential age ranges at the 95% confidence interval. If the first and second modes are chosen for these samples, respectively, the ages are not chronologi-

Table 2 Thickness[1] of stratigraphic units for borings and monoliths collected at Brewster Creek.

	Boring number or monolith name													
	1	2	3	4	5	6	7	8	9	10	11	12	Beach	Main
Unit 5 (peat)	235	122	247	165	238	117	130	124	108	30	107	91	56	166
Unit 4 (transition)	109	30	128	6	119	23	0	7	35	0	6	0	78	24
Unit 3 (marl)	215	152	274	183	146	0	206	268	0	0	0	213	0	166
Unit 2 (transition)	30	0	0	0	0	0	0	0	0	0	0	0	0	
Unit 1 (silt)	258	216	107	20	360	213	271	153	40	61	160	317	4	
Diamicton		12	24	23	0	12	18	24	0	0	0	0		
Sand and gravel		143			155				73	64	5	12		
Unit 5 (peat)	7.7	4.0	8.1	5.4	7.8	3.8	4.3	4.1	3.5	1.0	3.5	3.0	1.8	5.4
Unit 4 (transition)	3.6	1.0	4.2	0.2	3.9	0.8	0.0	0.2	1.1	0.0	0.2	0.0	2.6	0.8
Unit 3 (marl)	7.1	5.0	9.0	6.0	4.8	0.0	6.8	8.8	0.0	0.0	0.0	7.0	0.0	5.4
Unit 2 (transition)	1.0	0.0	0.0	0.0	0.0	0.0	0.0	0.0	0.0	0.0	0.0	0.0	0.0	
Unit 1 (silt)	8.5	7.1	3.5	0.7	11.8	7.0	8.9	5.0	1.3	2.0	5.2	10.4	0.1	
Diamicton		0.4	0.8	0.8	0.0	0.4	0.6	0.8	0.0	0.0	0.0	0.0		
Sand and gravel		4.7			5.1				2.4	2.1	0.2	0.4		

[1]Units in upper half of table are in centimeters and, for the lower half, in feet.

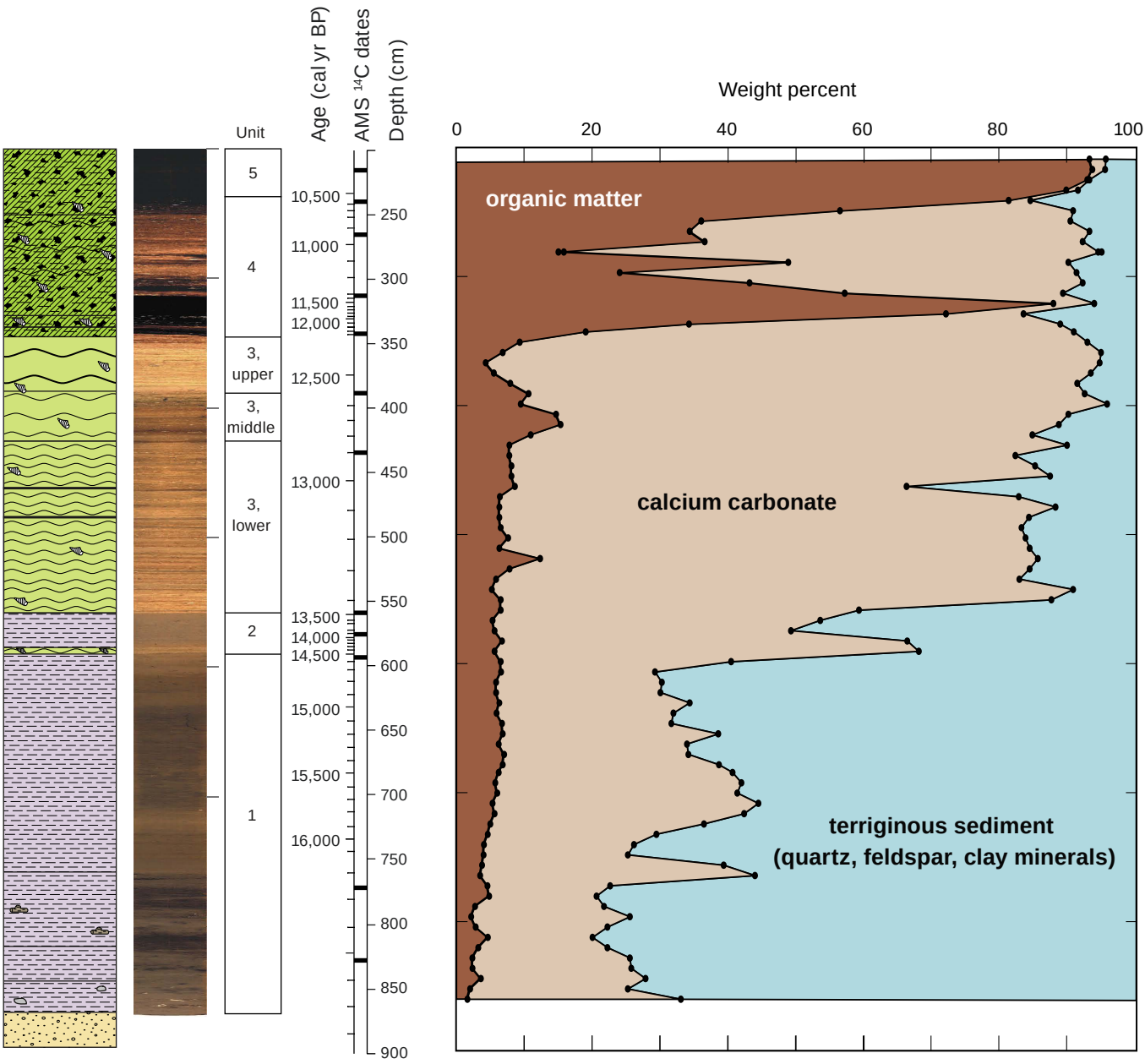

Figure 15 Downcore loss-on-ignition data of core BC-1. AMS, accelerated mass spectrometer.

cally reversed (fig. 12). The sediment accumulation rate of the lower marl facies was about half that of the upper marl facies (0.23 vs. 0.46 cm/yr. The branch pictured in figure 2 occurred in the upper part of the marl unit and yielded an age 10,860 ± 70 ^{14}C yr BP.

Unit 4 The upper transition zone, Unit 4, between the marl and peat units is as much as 1.28 m thick in boring BC-3. The transition zone is composed of thin beds of peat, marl, and hybrids thereof. In core BC-1, the upper part of the transition zone, from a depth of about 235 to 313 cm, contains abundant larch needles ideal for radiocarbon dating. From a depth of about 313 to 344 cm, the peat beds are composed of very fine and spongy material of unknown origin. The most prominent of these beds contains about 89% organic carbon (based on LOI; fig. 15), which is almost as high as the carbon content of the basal stratified peat in the overlying unit.

More samples yielded intermediate values that ranged from about 18 to 50% organic material and 15 to 50% biogenic carbonate.

The basal part of the upper transition zone yielded three analyses that were uniformly rich in illite (fig. 16) and that averaged 3% expandable clay minerals, 78% illite, 10% kaolinite, and 9% chlorite. Standard treatment of other sediment samples from this unit to remove organic matter and

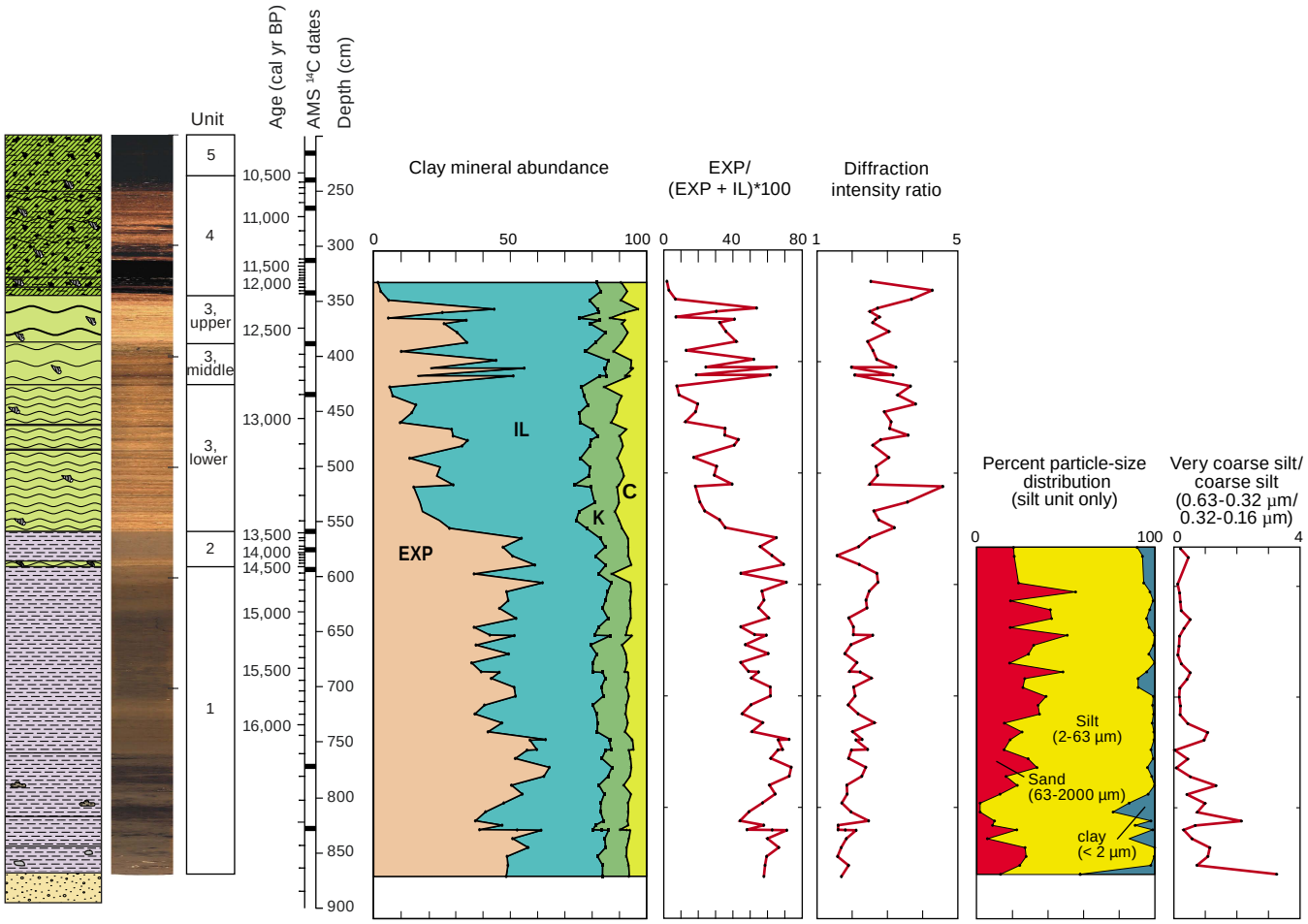

Figure 16 Downcore relative clay mineral abundance, relative abundance of expandable clay minerals (EXP) with respect to illite (IL), and diffraction intensity (DI) ratio, particle size distribution, and the ratio of very coarse silt (63 to 32 µm) to coarse silt (32 to 16 µm). K, kaolinite; C, chlorite.

carbonate (bleach and acid, respectively) yielded virtually no sediment for either clay mineral or particle-size distribution analysis. Larch needles from three levels in the upper transition zone yielded radiocarbon ages from 9,525 ± 40 to 9,185 ± 40 ^{14}C yr BP (table 1). The sediment accumulation rate of the upper transition zone was moderate at about 0.097 cm/yr.

Unit 5 Unit 5, the peat, is as much as 2.47 m thick in boring BC-3. This unit is part of the Grayslake Peat described by Willman and Frye (1970). The lower peat is stratified and dark reddish brown when first exposed to air, but rapidly oxidizes to black. Five LOI analyses of the peat unit yielded 90.1 ± 5.2% organic carbon, 1.9 ± 1.0% carbonate minerals, and 8.0 ± 4.6% terrigenous sediment. In some places, there are large pieces of wood, including rooted larch stumps with bark (fig. 3); in other places, the peat is friable (easily crushed) and composed of decomposed wood fragments with little fibrous material. The upper part of the peat unit had been disturbed and was not examined in detail.

Sand Beds In several borings, beds of well-sorted, very fine- to fine-grained sand were observed. In some places, the sand separated the peat and marl units from the silt unit (e.g., boring BC-9, fig. 18; and the "beach" monolith, fig. 19). In other places, the sand was in the mid-portion of the upper transition zone, and, in some borings, sand layers were noted in the base of the peat unit. The following sand thicknesses were measured at the following borings: BC-11 and the beach monolith, 35 cm; BC-6, 23 cm; BC-8, 7 cm; and, BC-4, 6 cm. Where the sand is thin, it is fine to very fine grained and is gleyed to a greenish hue. A clay mineral analysis of this material yielded high illite values.

Biological Records

We sought evidence for environmental change in three biological records: vegetation (pollen), ostracodes, and diatoms. The latter two groups are aquatic organisms and provide a local record of hydrological change. The pollen record reflects change in vegetation, but the signal is both local and regional in character. The combined responses of the three records, along

Figure 17 Scanning electron micrographs of a charophyte ovum and carapace of the ostrocode *Limnocythere verrucosa*. Charophyte oogonia and ostracodes are especially abundant in the marl unit; *L. verrucosa* is a species found only in the upper, weakly bedded marl subunit and in the upper transition zone from marl to peat.

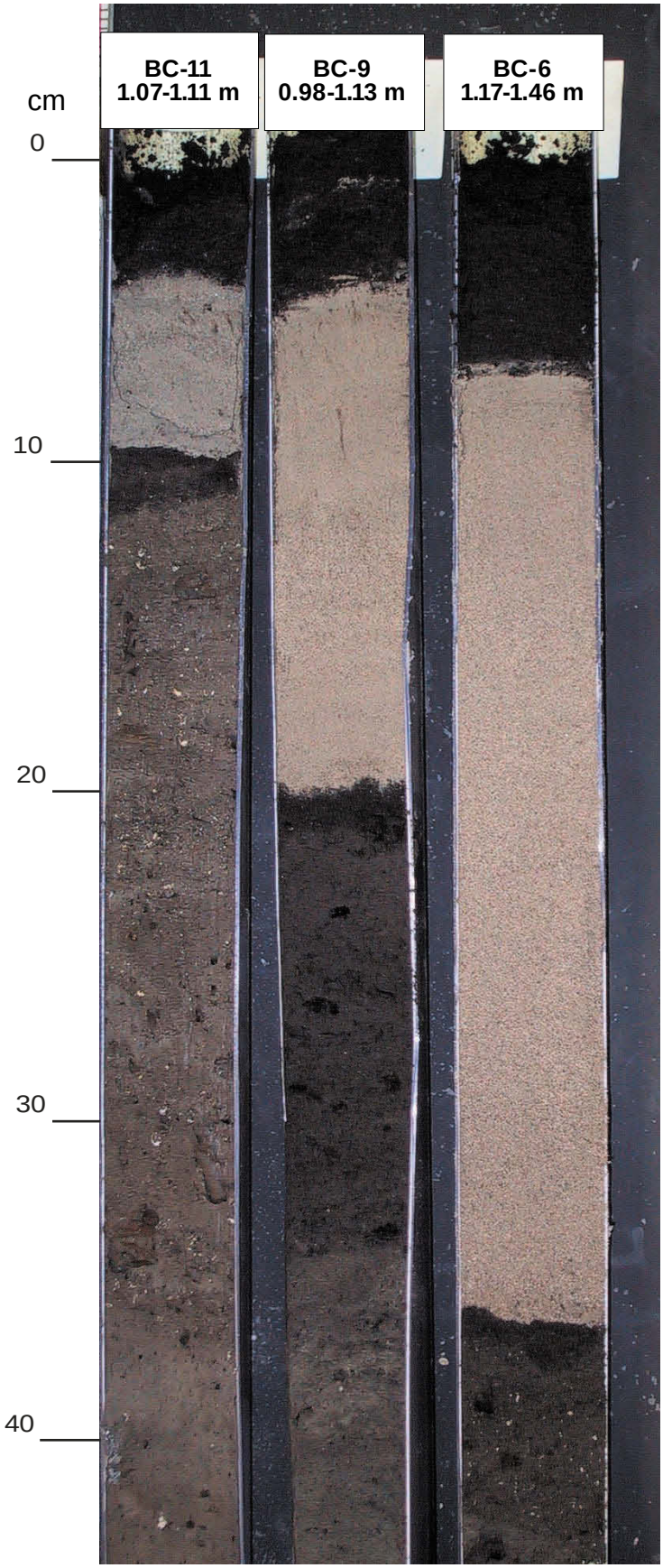

Figure 18 Sand layers in cores BC-11, BC-9, and BC-6 sandwiched by Unit 5 (peat) above and Unit 1 (silt) below.

with the physical parameters just discussed, provide the evidence for our conclusions of paleoenvironmental change at Brewster Creek.

Paleovegetation (Pollen)

Pollen analysis results for Brewster Creek are presented in figure 20. The first vegetation was a spruce forest dominated by white spruce *(Picea glauca)*. Larch *(Larix)* and small numbers of black ash *(Fraxinus nigra)* were present. *Fraxinus nigra*-type includes both *Fraxinus nigra* (black ash) and *Fraxinus quadrangulata* (blue ash). Blue ash occurs in the southern Midwest and mid-South; black ash is a more northern species, and its range overlaps the boreal spruce species. Black ash was almost certainly the source of the late-glacial and early Holocene *Fraxinus nigra*-type pollen in our record. At about 14,900 cal yr BP, white spruce pollen abundance fell, and, by 14,700 cal yr BP, was replaced largely by black spruce *(Picea mariana)* with less black ash and oak *(Quercus)* pollen. A black spruce-larch-*Sphagnum* peatland developed around Brewster Creek at this time and persisted through the Younger Dryas. During the Bølling, spruce declined gradually, and black ash increased to about 20%. Fir *(Abies)* also increased during the Bølling, and a number of deciduous tree taxa appeared, including hackberry *(Celtis)*, hornbeam/ironwood *(Ostrya/Carpinus)*, elm *(Ulmus)*, hickory *(Carya)*, butternut *(Juglans cinerea)*, and sugar maple (*Acer saccharum)*. Although minor components of the vegetation, these species indicate warming conditions. Spruce declined to <20% at the end of the Allerød and then increased sharply at the beginning of the Younger Dryas. This increase is primarily black spruce. Black ash decreased, whereas speckled alder *(Alnus incana)* and larch increased during the Younger Dryas. The latter species persisted into the Holocene, and abundant larch stomata in the peat indicate local pres-

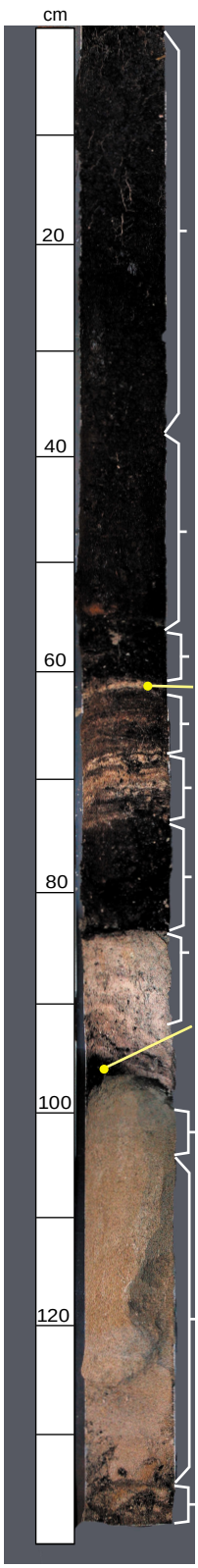

0–38 cm	Peat, sapric, black
38–56 cm	Peat, fibric, wood-bearing, dark reddish brown (10YR 3/1)
62.5–63.0 cm	Marl, gray (5Y 5/1), continuous thin layer
63–69 cm	Marly peat; stratified, fibric, dark reddish brown (5YR 3/2)
69–74 cm	Peaty marl with thin layers of marly peat. Peaty marl is light olive-gray (5Y 6/2); marly peat is black (5Y 2.5/1)
74–84 cm	Peat, wood-rich, abrupt upper contact, irregular lower contact (wood fragment sticks into marl; sampled for ^{14}C)
84–92 cm	Marl, fossiliferous (snails), light olive-brown (5Y 6/2), slanted lower boundary to 95 cm
92–95.5 cm	Peaty marl, as above, but darker (olive-gray, 5Y 4.5/2)
95.5–99.0 cm	Peat, black, varies in thickness from 0.7 to 3.5 cm, few wood fragments
99.0–100.5 cm	Sand, medium, well-sorted, olive-gray (5Y 5/2)
100.5–101.3 cm	Sand, very fine, abrupt upper boundary, fining upward below lower contact
101.3–103.0 cm	Fining-upward zone
103–134 cm	Sand, medium, well-sorted, uniform, light brownish gray (2.5Y 6/2) to olive-yellow (2.5Y 6/6)
134–138 cm	Disturbed, sand and dark gray (5Y 4/1) silt

Figure 19 The "beach" monolith, Brewster Creek (see fig. 1 for location). The monolith was sampled from a short-lived excavation. A thick succession of the silt unit underlies the monolith, including several large, well-preserved logs, probably *Picea glauca* (white spruce).

ence. Spruce declined at the end of the Younger Dryas and completely disappeared over about 700 years. The presence of cattail *(Typha)* suggests that the wetland was a rich fen. A peak of birch *(Betula)* occurred at the Younger Dryas-Holocene transition. Jack pine *(Pinus)* and elm increased in the early Holocene. Oak and a number of other deciduous tree taxa (hornbeam/ironwood, hickory, butternut, sugar maple, and linden *(Tilia)* increased a few hundred years later.

The pollen diagrams from Brewster Creek and Nelson Lake are quite different (compare figs. 10 and 20). An important difference occurs at the beginning of the Bølling chronozone. At Nelson Lake, spruce decreased dramatically as black ash increased. At Brewster Creek, total spruce did not decrease at the beginning of the Bølling as it did at Nelson Lake, but the separation of spruce species reveals a precipitous decline in white spruce and a concomitant increase in black spruce such that total spruce changed little. Clearly, this switchover in the spruce species carries a climatic signal, which is hidden if the spruce species are not separated. This separation will be the focus of a follow-up study of pollen records at Nelson Lake and Crystal Lake within the next three years.

The pollen diagrams from Brewster Creek and Nelson Lake both indicate very wet conditions throught the last glacial-interglacial transition, but different vegetative responses. During the Bølling-Allerød, a conifer peatland developed between the broad, shallow kettle basins on the expansive outwash plain around Brewster Creek. On the outwash plain and moraines at Nelson Lake, black ash and spruce were major components of the local vegetation. At Nelson Lake, black ash pollen increased again in the early Holocene, whereas, at Brewster Creek, black ash pollen abundance was the same during the Younger Dryas and early Holocene. We attribute this lack of change to persistence of the local conifer peatland. Collectively, the pollen suggests cool, moist conditions during the Younger Dryas. Spruce disappeared in the early Holocene at Brewster Creek, but not as pre-

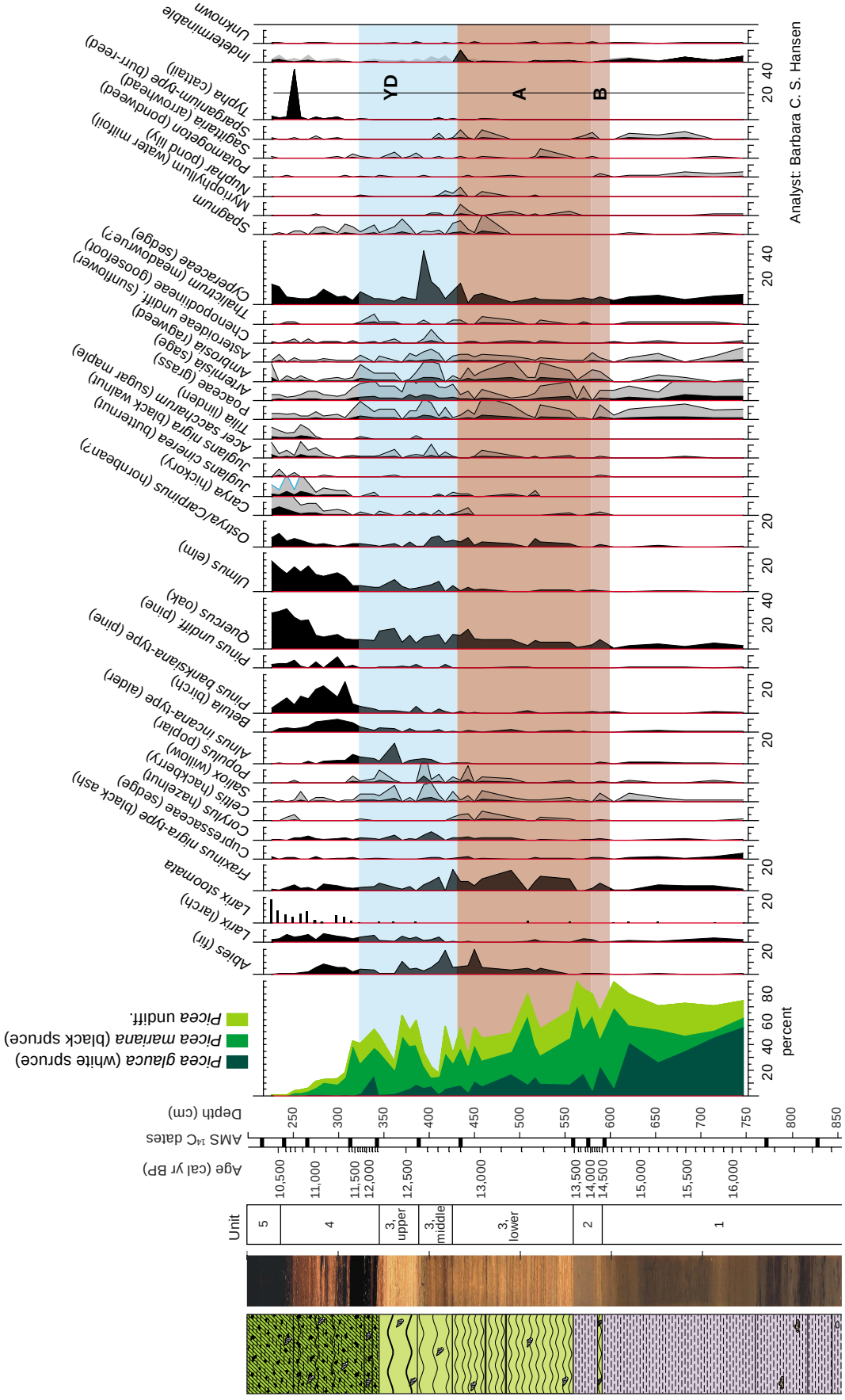

Figure 20 Pollen diagram for Brewster Creek. Gray curves indicate 5× exaggeration. The age axis is scaled to depth. B, Bølling; A, Allerød; YD, Younger Dryas; AMS, accelerated mass spectrometer.

cipitously as at Nelson Lake; larch persisted even longer. Although black spruce does not occur in northern Illinois today, larch and *Sphagnum* do occur in a few wetlands, for example, at Volo Bog (King 1981). The early Holocene increase in pine pollen at Brewster Creek, but not at Nelson Lake, probably indicates the development of jack pine stands on the sandy soils of the outwash plain.

Not only do the pollen diagrams from Brewster Creek and Nelson Lake indicate very wet conditions during the Bølling-Allerød, but the number of deciduous taxa also suggests that temperatures were quite warm. The warmth was not as great as that of northern Illinois today but was warmer than the modern boreal forest. Wet conditions may also have allowed spruce to flourish at warmer temperatures than it does today (Webb et al. 1993). In the modern boreal forest, jack pine and birch are typically postfire successional species. Moist climate and lack of fire may explain the absence of pine and birch from the late-glacial forest. Fir, a poor pollen producer, which is common during the Bølling-Allerød and very early Holocene, is also an indicator of abundant precipitation, especially during winter (Webb et al. 1983, Prentice et al. 1991, Thompson et al. 2000).

In summary, the pollen data from Brewster Creek and Nelson Lake show striking vegetation changes in the northeastern Illinois coeval with major changes in the North Atlantic region. However, as today, significant fine-scale variability existed in the late-glacial vegetation, and different communities in different landscape positions responded differently to these changes. In the case of Brewster Creek, some of the differences are attributed to the relative importance of submergent vegetation that grew in shallow water (cattails, for example), an environment that was present at Nelson Lake, but that was relatively less important than at Brewster Creek. The separation of spruce pollen at Brewster Creek was critical to understanding the apparently different sensitivities of these sites to late-glacial climate change. Otherwise, the persistence of high spruce abundance at Brewster Creek might well be interpreted as evidence of little vegetation and climate change at the beginning of the Bølling and Younger Dryas chronozones.

Ostracodes

Aquatic organisms, such as ostracodes and diatoms, respond to climate insofar as climate impacts the body of water they inhabit. Thus, associating these organisms with climate presents two challenges. First, it must be shown that the occurrence of these organisms is related to limnological parameters and, second, that those limnological parameters are sensitive to climate (Curry 1999, 2003). Some aquatic environments are more climatically sensitive than others. Groundwater-fed ponds, for example, are relatively insensitive to climate because the temperature of groundwater is nearly constant and reflects the mean annual temperature. Unlike thermally insensitive deep lakes, the temperature of shallow ponds often follows trends in diurnal air temperature (Forester 1987); however, the sediment records of shallow ponds are more likely to be fragmented and truncated, reflecting sensitivity to desiccation during droughts and limited sediment storage.

Ostracodes are microcrustaceans that form a protective valve (shell) of low-magnesium calcite (fig. 17). The valves are molted eight times during the life span of an ostracode, and the molted valves are readily preserved in lake sediment and other aquatic habitats. The size of most adult freshwater ostracodes from North America is from about 0.5 to 2.0 mm long. Five main classes of continental (freshwater) ostracodes are known in lakes and ponds: (1) ones that prefer living in or near groundwater discharge (springs), (2) ones that live in and around where rivers and streams debouche into lakes, (3) ones that float (planktonic), (4) ones that swim among aquatic vegetation (nektonic), and (5) ones that crawl in the upper 3 cm or so in the bottom sediment (benthic). Kitchell and Clark (1979) showed that the ratio of benthic to nektonic ostracodes in Lake Mendota, Wisconsin, is indicative of water depth.

Environmental factors such as temperature and the concentration and composition of dissolved solutes (including limiting nutrients such as phosphorus) limit the abundance and distribution of ostracodes and diatoms (Delorme 1969; Forester 1983, 1986; Smith 1993; Curry 1999). The variability of these parameters is also limiting. For example, specialized ostracode assemblages live in freshwater springs because the temperature and chemistry of the water at the spring orifice is, in many cases, invariable (Forester 1991). The relationships between ostracode species and assemblages and environmental factors are determined from analysis of either regional or local modern analog databases. A regional database includes species abundance, water-quality data (e.g., alkalinity, concentrations of major and minor dissolved constituents, and pH), temperature, depth, and the geographic coordinates of the collection sites. Optional information in the database may include climatic data (such as mean maximum July temperature, the number of frost-free days, etc.) and the terrestrial vegetation of the drainage basin. For this study, we have used ostracode, climatic data, and hydrochemistry data from NANODe—the North American Non-Marine Ostracode Database—which comprises about 600 lakes, streams, and wetlands in the contiguous United States (fig. 21) (Forester et al. 2006). A separate database exists for Canada. This data set has not been published, and modern analog reconstructions are only possible through contractual arrangement with its proprietor, Denis Delorme. The latter data set provides ranges of environmental factors associated with ostracodes collected from a regional database of more than 5,500 sites.

The ostracode diagram (fig. 22) shows the relative abundance of species counted at 69 1-cm-thick intervals spaced 8 cm apart in core BC-1. Ostracodes were found in samples ranging

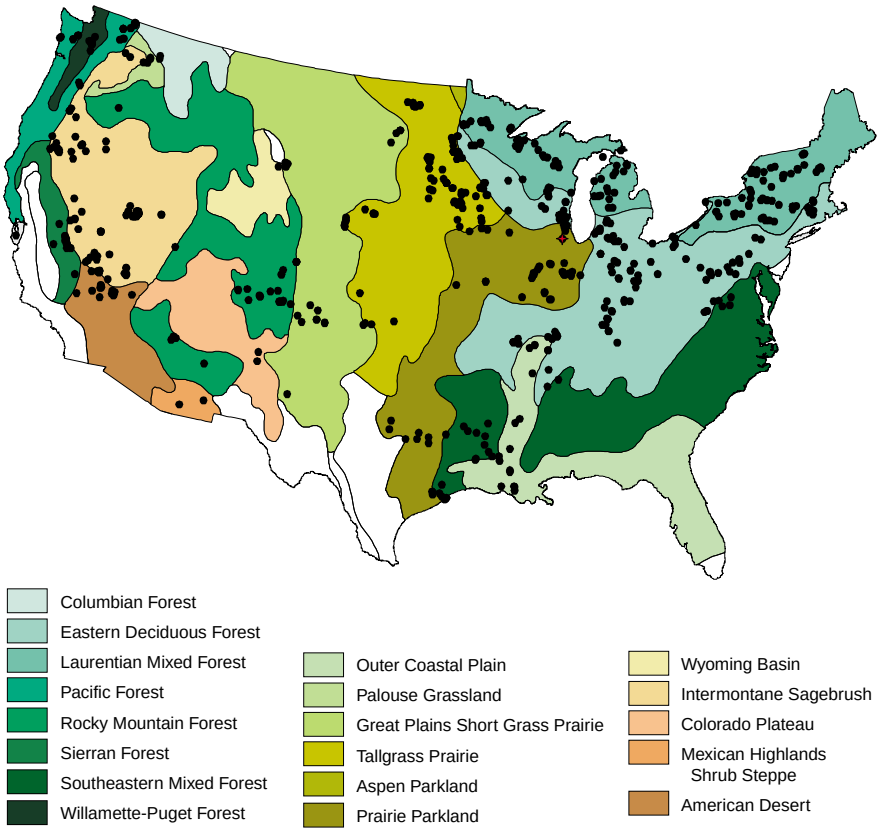

Figure 21 The locations of lakes (black) that are included in NANODe, The North American Non-Marine Ostracode Database (Forester et al. 2006), which includes information about the water quality, climatic conditions, ostracode species, and other information used in the reconstructions discussed in the text.

in depth from 248 to 772 cm. Only two samples within this interval were barren of ostracodes (the samples at 320 and 328 cm). The average abundance of ostracodes was 232 valves per interval, ranging from 2 to 990 valves per interval. In the order of abundance, the species identified (and the number of valves identified) include *Cyclocypris ampla* (3,790), *Cyclocypris laevis* (2,311), *Cypridopsis vidua* (2,083), *Limnocythere verrucosa* (1,729), *Physocypria* sp. (1,564), *Candona inopinata* (1,137), *Cyclocypris sharpei* (951), *Candona punctata* (836), *Candona distincta* (539), *Candona stagnalis* (431), *Fabaeformiscandona rawsoni* (200), *Candona ohioensis* (172), *Candona candida* (98), *Candona elliptica* (87), *Candona paraohioensis* (46), *Candona compressa* (39), *Cypria ophthalmica* (30), *Limnocythere ornata wabashensis* (20), *Fabaeformiscandona caudata* (5), *Cypria obesa* (4), and *Potamocypris smaragdina* (3). The abundance of *Candona compressa, Cypria opthalmica, Fabaeformiscandona caudata, Cypria obesa,* and *Potamocypris smargdina* is low and not shown in figure 22. More than 16,300 adult valves were identified. A stratigraphically constrained cluster analysis (Grimm 1987) and visual inspection reveals five biozones and two subzones.

The five biozones include

1. Biozone A: 720 to 776 cm; *Candona candida* zone. The presence of *C. candida* and absence of *Fabaeformiscandona rawsoni* in this zone suggests this interval was deposited in water with a total dissolved solids content of less than 1,000 mg/L (Forester et al. 2006). *Cyclocypris ampla* is also abundant.

2. Biozone B: 589 to 720 cm; *Fabaeformiscandona rawsoni* zone. The presence of this species implies greater hydrochemical variability and overall higher total dissolved solids (Smith 1993; Curry 1999, 2003; Forester et al. 2006). It is a frequent denizen of "prairie potholes," which are hydrologically variable lakes in kettles that typically have seasonal, if not year-round, internal drainage. In large lakes, such as Lake Michigan, *F. rawsoni* tolerates low salinity (ca. 100 mg/L), but in smaller, shallower lakes and ponds (such as what once occupied the Brewster Creek site), its abundance is much higher in lakes with greater than about 400 mg/L salinity, and its average salinity tolerance is about 3,500 mg/L (Curry 1999, Forester et al. 2006). *Fabaeformiscandona rawsoni* is absent in samples from 674 to 650 cm.

3. Biozone C: 442 to 589 cm; *Candona punctata-C. inopinata* zone. The base of this zone coincides with the first appearance of marl. Above a depth of 494 cm, Subzone C2 is marked by the absence of *C. punctata* and a concomitant rise in the abundance of *C. inopinata*. At this point, the relative abundance of benthic ostracodes decreases, as nektonic species increase, suggesting shallower conditions.

4. Biozone D: 333 to 442 cm; *Limnocythere verrucosa* zone. This biozone coincides with the upper marl unit; it contains most of the species found in Zone C except for the presence of *L. verrucosa,* which increases upcore. The abundance of *Cyclocypris laevis* also increases upcore as *Cyclocypris ampla* abundance decreases. *Limnocythere verrucosa* is an ostracode known to prefer spring-fed wetlands in carbonate terrains (A. Smith, Kent State University, personal communication 2005), so its abundance may reflect shallow water and a greater proportion of groundwater relative to overland flow and precipitation.

   Barren zone: 316 to 333; cm; the lithology at the base of the upper transition zone here is fine, spongy gyttja.

5. Biozone E: 252 to 316 cm; *Cypridopsis vidua-Cyclocypris sharpei* zone. The continued occurrence of

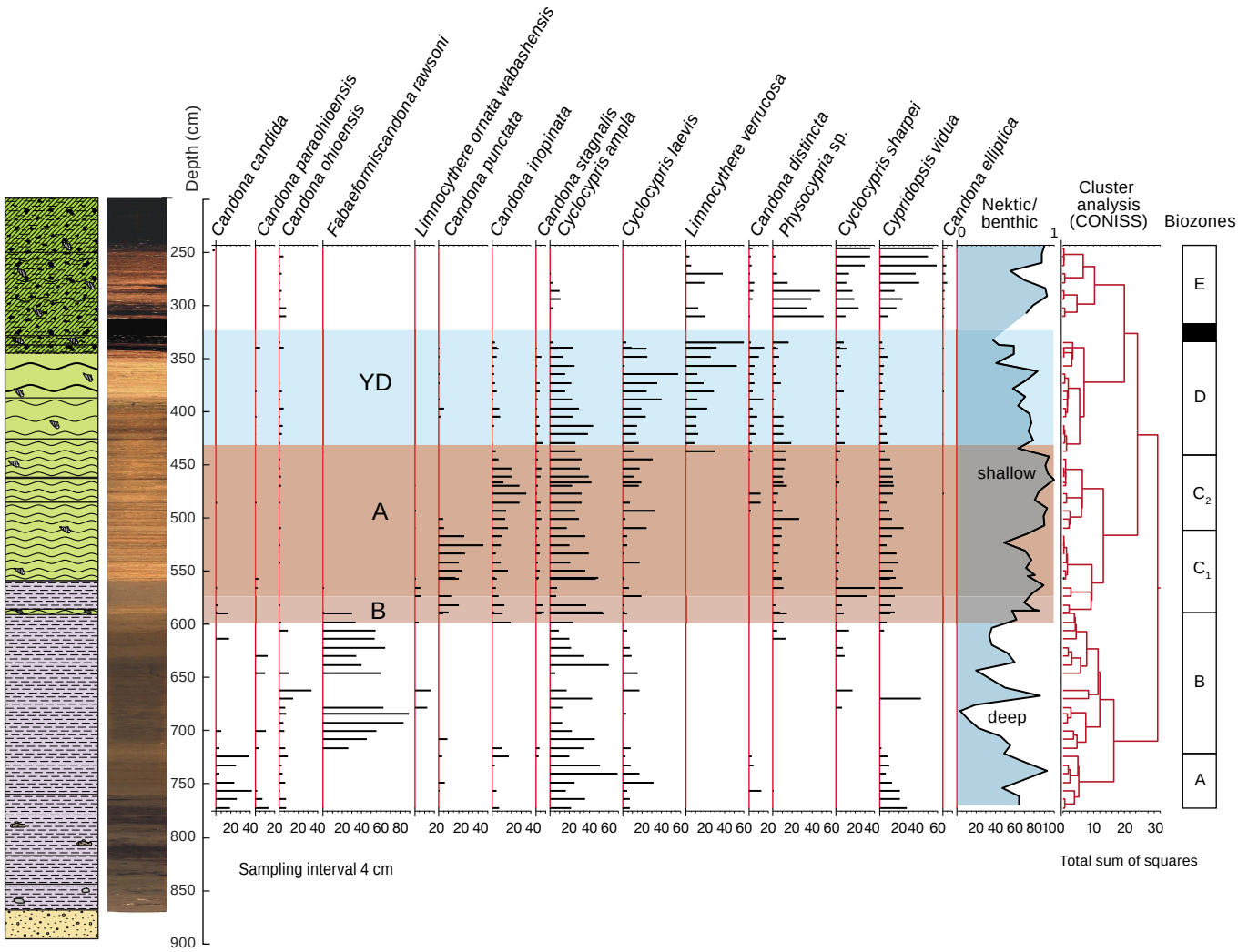

Figure 22 Diagram of the relative abundance of ostracodes, core BC-1, Brewster Creek. YD, Younger Dryas; A, Allerød; B, Bølling.

Limnocythere verrucosa and abundant nektic (swimming) ostracodes (including *C. vidua* and *C. sharpei*) implies continued shallow conditions and groundwater through flow.

Interpretations of the Ostracode Data Our modern analog analyses attempt to find lakes and other aquatic environments on the modern landscape that are most similar to the ancient environments of interest by finding the greatest number of ostracode species in a database of modern aquatic environments in common with assemblages in the fossil record. The relative abundance of key species identified in each zone was used to determine modern analogs using the Range Method (Smith and Forester 1994) on the NANODe data set (Forester et al. 2006; fig. 21). The result of this analysis is skewed toward sites with warmer climates because NANODe includes no sites from Canada. The Delorme data set would be superior to NANODe because it would include lakes that are surrounded by boreal forests, the vegetation that surrounded Brewster Creek during the time of interest. Using the Delorme data set was cost-prohibitive. The mean value and standard deviation of species relative abundance for each biozone and values of key geochemical parameters are given in table 3. The names of the modern analog lakes are given in table 4. The range method uses a presence-absence matrix to determine the modern analogs (table 5). Three species were initially used. For example, the range zone matched 23 lakes from NANODe for subzone C2 based on the presence of *Candona inopinata, Cyclocypris ampla,* and *Physocypria globula*. Sites were eliminated that did not also include *Cypridopsis vidua*, *Cyclocypris ovum* (cf. *sharpei*), and *Candona ohioensis,* or that did include *Limnocythere verrucosa* and *Candona punctata*, key species in biozones above and below subzone C2. After culling unwanted sites, 7 modern analogs were selected (table 5).

The reconstructed water chemistry indicates that the Brewster Creek site was always a "hard water" lake; that is, more than 50% of its ions are derived from dissolved $CaCO_3$ (table 5). Consistent with high alkalinity are the high pH values (mean values from

Table 3 Ostracode abundance (mean ± standard deviation) per biozone; valves per gram dry sediment.

Biozone	CCAN[1]	CPAR	COHI	FRAW	LORN	CPUN	CINO	CSTA	CYCA	CYCL	LVER	CDIS	PHGL	CYCS	CYPV	CELL	Total valves
E																	
Mean	0.0	0.0	0.6	0.0	0.0	0.0	0.0	0.0	0.7	0.0	2.9	0.7	4.3	5.6	9.6	0.8	27.9
SD	0.0	0.0	0.4	0.0	0.0	0.0	0.0	0.0	1.1	0.0	4.6	0.5	4.3	3.8	6.7	0.5	11.4
D																	
Mean	0.0	0.1	0.4	0.0	0.0	0.1	1.4	1.2	9.5	9.8	8.4	2.4	3.5	1.8	2.3	0.1	41.0
SD	0.0	0.2	0.5	0.0	0.0	0.3	1.2	1.1	6.3	8.4	6.1	1.8	2.9	1.1	1.5	0.2	18.1
C2																	
Mean	0.0	0.0	0.1	0.0	0.1	0.0	5.8	0.9	7.3	3.8	0.0	1.0	2.3	0.2	3.0	0.0	24.6
SD	0.1	0.1	0.2	0.0	0.1	0.0	3.3	0.6	2.3	4.1	0.0	1.5	1.6	0.1	1.5	0.1	10.8
C1																	
Mean	0.1	0.0	0.0	0.3	0.1	4.6	2.2	0.8	7.2	1.2	0.0	0.0	1.9	0.8	3.2	0.0	22.6
SD	0.3	0.1	0.1	0.8	0.1	5.7	2.2	0.7	4.3	2.0	0.0	0.0	2.2	0.6	2.1	0.0	13.4
B																	
Mean	0.1	0.0	0.1	0.9	0.0	0.1	0.1	0.1	1.2	0.1	0.0	0.0	0.2	0.1	0.0	0.0	3.3
SD	0.3	0.1	0.1	0.8	0.1	0.4	0.3	0.3	2.3	0.1	0.0	0.0	0.4	0.2	0.1	0.0	4.4
A																	
Mean	0.7	0.1	0.1	0.2	0.0	0.0	0.2	0.0	0.9	0.2	0.0	0.1	0.0	0.0	0.4	0.0	2.9
SD	0.9	0.1	0.1	0.1	0.0	0.0	0.2	0.0	0.5	0.1	0.0	0.3	0.0	0.0	0.5	0.0	2.2

[1]CCAN, *Candona candida;* CPAR, *Candona paraohioensis;* COHI, *Candona ohioensis;* FRAW, *Fabaeformiscandona rawsoni;* LORN, *Limnocythere ornata wabashensis;* CPUN, *Candona puncata;* CINO, *Candona inopinata;* CSTA, *Candona stagnalis;* CYCA, *Cyclocypris ampla;* CYCL, *Cyclocypris laevis;* LVER, *Limnocythere verrucosa*; CDIS, *Candona distincta;* PHGL, *Physocypria* sp.; CYCS, *Cyclocypris sharpei;* CYPV, *Cypridopsis vidua;* CELL, *Candona elliptica.*

8.2 to 8.6). The reconstructed total dissolved solids values (mean values 238 to 490 mg/L) are similar to lakes in the area today (Curry 1995).

The most intriguing changes in the reconstructed water chemistry of the Brewster Creek site are the high total dissolved solids values and other dissolved ions during deposition of Biozone B (table 5), the upper part of the silt unit. Values of the climatic variables of Biozone B are not that much different from the overlying Biozone C1 that is composed largely of marl. An interesting difference between the reconstructed water quality parameters of Biozone B versus the other biozones are the high SO_4^- and Mg^{2+} concentrations (table 3). The high dissolved sulfate content (108 mg/L), especially when considered with the very low concentrations in the other biozones (9.7 to 20.4 mg/L), suggests that sulfate reduction, which occurs during anoxia, did not occur. Mixing the water column with wind-driven currents is one way to limit anoxia and is consistent with the high sediment accumulation rate and redeposition of wind-blown loess.

Table 4 Modern analog lakes from NANODe (Forester et al. 2005).

Biozone	Location
E	Upper Little York Lake, New York; Middle Eau Claire Lake, Wisconsin; Moose Lake, Minnesota; Half Moon Lake, Michigan
D	Moose Lake, Minnesota; Mina Lake, Minnesota; Elk Lake, Grant County, Minnesota
C2	Mina Lake, Minnesota; George Lake, Minnesota; Half Moon Lake, Michigan; Little Itasca Lake, Minnesota; Little Ball Lake, Minnesota; West Lost Lake, Minnesota
C1	Nokay Lake, Minnesota; Maple Lake, Minnesota; Turner Lake, Illinois; Elizabeth Lake, Illinois; Little Itasca Lake, Minnesota; Mina Lake, Minnesota
B	Fish Lake, Michigan; Bassett Lake, Michigan; Barney's Lake, Michigan; Cary Lake, Michigan, Hunter Lake, Wisconsin
A	Loon Lake, Indiana; Upper Little York Lake, New York

Diatoms

Diatoms are tiny algae that form frustules, support structures composed of opal that are preserved in lake sediment (fig. 23). Opal is microcrystalline silica with attached water molecules. Like ostracodes, diatoms have environmental preferences but no structures that allow them to crawl or swim.

The Brewster Creek diatom record indicates that shallow conditions generally prevailed. In contrast, for Nelson Lake, planktonic diatoms, indicative of deep water, were common in the late-glacial sediment. In the lower part (566 to 765 cm) of the Brewster Creek diagram (fig. 24), right side, the small *Fragilariaceae* species *(Fragilaria brevistriata* var. *inflata, F.*

pinnata var. *lancettula, Pseudostaurosira brevistriata, Staurosira construens, S. construens* f. *binodis, S. construens* f. *subsalina, S. construens* f. *ventor, Staurosirella lapponica,* and *S. pinnata)* average 79% of the diatoms (compared with 51% above 566 cm; fig. 24). This result is expected; small Fragilariaceae species dominate the diatom species composition in late-glacial lake sediment in temperate regions of North America (Smol and Boucherle 1985, Brugam et al. 1988, Wilson et al. 1993). Although they are ubiquitous worldwide and can survive in a wide range of environmental conditions, they also thrive in cold, alkaline, ice-covered water (Fallu et al. 2002).

The diatom assemblage in the subzone from 674 to 650 cm in ostracode Zone B indicates a period of low salinity. The assemblage includes *Cymbella diluviana,* a species that has a salinity optimum of 120 mg/L but cannot tolerate salinity in excess of 340 mg/L (Wilson et al. 1996). The subinterval in which *C. diluviana* occurs corresponds to depths in ostracode Biozone B in which *Fabaeformiscandona rawsoni* does not occur. Hence, agreement in the data for ostracodes and diatoms indicate that the lake had relatively low salinity from about 15,700 to 15,200 cal yr BP.

Above 566 cm, the species composition of the diatoms shifts and corresponds to the species shifts in ostracodes and pollen and the sediment change from silt to marl. Small Fragilariaceae species decrease in abundance (to an average of 51% between depths of 550 to 328 cm). They are replaced by pennate diatoms that in most cases (but not always) are epiphytic (e.g., *Cymbella affinis, Encyonema minutum, Encyonema silesiacum, Gomphonema angustum, Mastogloia smithii, M smithii* var. *lacustris, Navicula radiosa,* and *Sellaphora pupula*). Epiphytic diatoms adhere to aquatic vegetation, a lifestyle that is consistent with abundant charophyte encrustations and oogonia and the establishment of aquatic vegetation (Karst and Smol 2000). Silica dissolution compromised the quality of the frustules in the sample at 764 cm. Because frustules of *Mastogloia smithii* and M *smithii* var. *lacustris* are resistant to dissolution, their dominance at 764 cm must be interpreted with caution.

Paleohydrology Based on Diatoms and Ostracodes Although the diatoms indicate consistently shallow conditions, the ratio of benthic-to-nektic ostracodes indicates significant fluctuations in water depth. The physical evidence, as shown in figure 14, indicates that the silt unit was deposited in water that never exceeded a depth of about 7 m. The basin shoaled to a maximum depth of about 4 m when the sediment composition changed over to marl. The lake

Table 5 Environmental data determined by modern analogs using the range method on the NANODe data set (ostracodes).

Biozone[1]	LAT[2]	LONG	ELEVM	MJANT	MJULT	MAT	MJANP	MJULP	MAP	pH	Ca^{2+}	Mg^{2+}	Na^{+}	HCO_3^-	SO_4^-	Cl^-	TDS	$CaCO_3$ (%)	HCO_3^-/Ca^{2+}
E																			
Mean	42.2	–80.6	319.4	–5.6	21.4	8.5	58.0	92.0	949.0	8.4	53.5	14.5	19.0	182.0	12.5	35.0	317.9	62.8	1.1
SD	20.5	42.1	134.1	3.8	10.0	3.6	25.1	40.3	444.9	4.0	19.6	5.5	7.0	69.1	4.3	11.3	107.0	27.8	0.5
D																			
Mean	43.2	–86.0	238.0	–6.3	21.4	8.2	45.4	84.2	838.4	8.2	47.4	21.6	7.9	182.6	20.4	16.4	297.3	65.8	1.3
SD	1.5	1.4	35.9	1.7	1.4	1.4	7.9	9.1	35.1	0.4	14.7	9.0	8.5	52.3	14.6	20.4	103.7	8.7	0.3
C2																			
Mean	45.4	–92.9	360.7	–12.6	21.2	5.9	24.7	95.9	716.0	8.3	33.5	26.1	7.0	218.9	18.5	10.2	317.7	64.8	2.2
SD	2.1	3.2	89.4	4.0	1.1	2.1	8.8	8.5	98.6	0.6	4.9	13.7	4.7	78.3	16.0	15.3	105.9	12.5	0.8
C1																			
Mean	46.2	–93.4	389.4	–13.9	20.8	5.1	22.0	87.8	657.5	8.5	37.5	20.2	6.5	204.2	15.5	7.4	294.6	68.5	1.9
SD	1.6	4.1	68.8	3.9	0.7	1.6	9.9	11.1	69.0	0.2	6.6	9.4	5.1	37.5	24.1	10.3	57.6	10.3	0.5
B																			
Mean	46.4	–95.0	393.3	–14.6	20.9	4.9	19.3	90.3	646.0	8.6	37.7	52.3	10.0	268.7	108.3	8.9	490.1	55.9	2.3
SD	0.9	1.1	24.7	0.9	1.2	1.0	1.2	11.9	23.6	0.1	2.3	5.5	7.9	116.0	134.9	9.1	319.8	22.0	0.9
A																			
Mean	44.9	–86.6	331.9	–10.1	20.3	6.1	39.5	93.3	819.0	8.4	40.3	11.4	9.4	151.0	9.7	14.6	237.5	71.5	1.3
SD	2.3	7.9	58.8	4.9	0.9	2.2	21.1	16.7	144.7	0.3	18.2	5.2	7.2	56.2	8.0	15.4	101.6	8.3	0.2

[1]See Table 3 for key to ostracode acronyms. Biozone E: CYPV, CYCO, LVER (2 analog lakes); Biozone D: LVER, CDIS, CYCA (5 analog lakes); note: CYCL is abundant in this biozone, and only present in one analog lake; Biozone C2: CINO, CYCA, PHGL, CYPV, CYCO, COHI (7 analog lakes); Biozone C1: CPUN, CINO, CYCA (6 analog lakes); Biozone B: FRAW, COHI, CYCA (3 analog lakes); Biozone A: CCAN, CPAR, CYCA (CYPV) (4 analog lakes). Data are expressed as mean ± standard deviation.

[2]LAT, latitude; LONG, longitude; ELEVM, elevation (meters); MJANT, mean January temperature (ºC); MJULT, mean July temperature (ºC); MAT, mean annual temperature (ºC); MJANP, MJULP, and MAP same as above, except for precipitation (millimeters); chemical parameters and TDS (total dissolved solids) are in milligrams per liter.

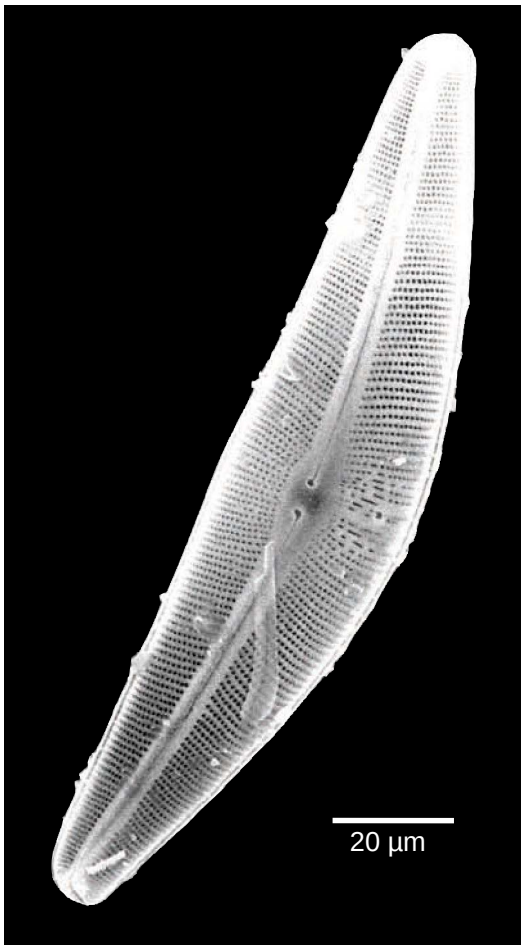

Cymbella aspera (550x)

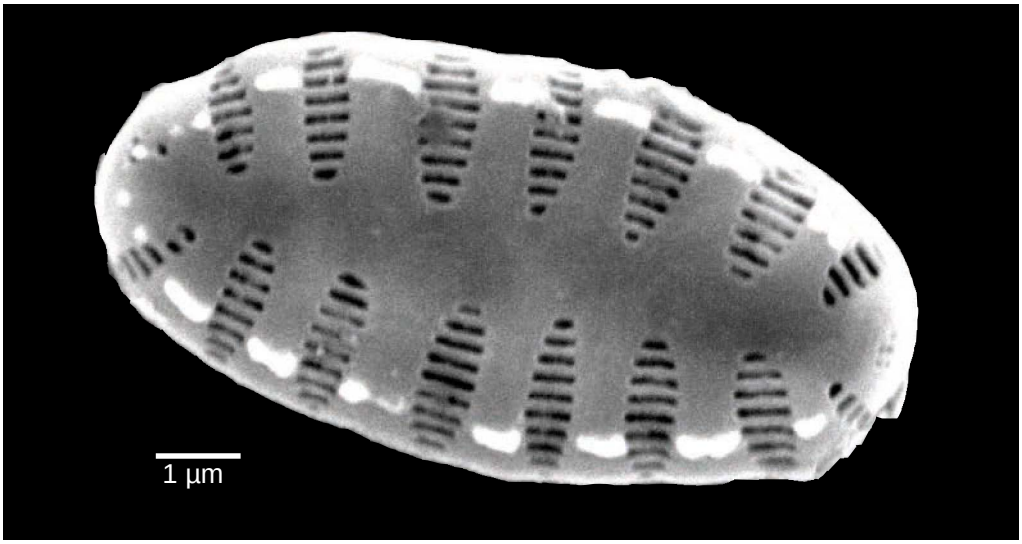

Staurosirella pinnata (12000x)

Figure 23 Scanning electron micrograph images of diatoms. *Cymbella aspera* is representative of the diatoms in the silt unit, and *Staurosirella pinnata* is representative of the Fragilariaceae species in the marl.

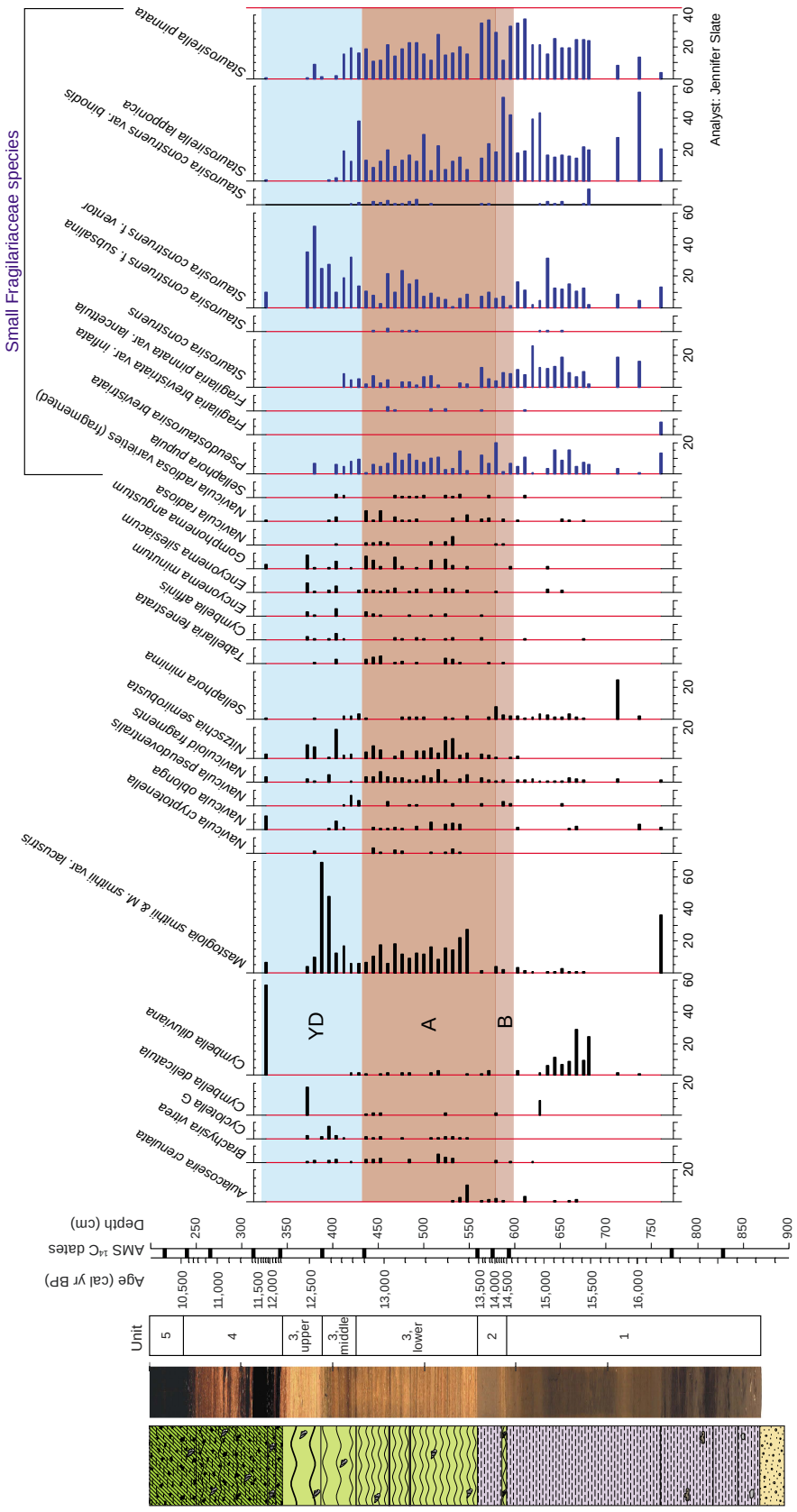

Figure 24 Diagram of the relative abundance of diatoms, core BC-1, Brewster Creek. AMS, accelerated mass spectrometer. YD, Younger Dryas; A, Allerød; B, Bølling.

Table 6 Characteristics and interpretations of environmental proxies associated with Unit 1 (ca. 16,500 to 14,600 cal yr BP; Oldest Dryas); Unit 2 (14,600 to 13,440 cal yr BP; early Bølling chronozone); and lower Unit 3 (13,400 to 12,900 cal yr BP; Bølling chronozone), and their contacts.

	Unit 1 (silt)	Unit 2 (transition)	Unit 3 (marl)	Figure	Transition	Type of Interpretation
Ostracodes	*Fabaeformiscandona rawsoni*	*Candona inopinata, Candona punctata*	no change from Unit 2	22	fairly abrupt	change from sulfate-rich to sulfate-depleted water
Diatoms	small fragilarian species	no remarkable changes	*Mastogolia smithii* et al.	24	abrupt	as above
Pollen	*Picea glauca* dominant	*Picea mariana* dominant	less spruce; *P. mariana* still dominates; *Abies* and *Fraxinus* become important	20	gradual/ variable	relative change from cold/dry to cold/moist to cool/moister
PSD[1]	silt, sand	silt, sand	no silt, sand	16	abrupt	continued reworking of new loess into basin through deposition of Unit 2
Mineralogy, lithology	expandable clays, quartz, feldspars, clay minerals	expandable clays, mostly silt; some biogenic carbonate	illite, biogenic carbonate	16 15	abrupt stepwise	as above stepwise change from geogenic to biogenic dominated sedimentation

[1]PSD, particle-size distribution.

shoaled further to a maximum depth of about 2.4 m when the first peat was deposited. It is therefore not surprising to find in the marl the kinds of ostracodes and diatoms that thrived among aquatic vegetation of the photic zone (the depth of light penetration). The charophyte fossils and modern analog lake chemistry determined by the ostracode assemblages indicate that the water at the Brewster Creek site was "hard"; moreover, the modern analog lakes suggest that Brewster Creek was fed by ground-water-fed artesian springs that upwelled in the lake. The influence of groundwater means that the aquatic environment (and the attendant aquatic fauna) did not respond as readily to diurnal temperature changes as did sites less influenced by groundwater, such as Nelson Lake. The climate reconstructions based on ostracode modern analogs should thus be used to look for relative changes in temperature and precipitation rather than as specific values to compare with modern data or climatic simulations.

Discussion

To what degree do the proxy records of environmental change at Brewster Creek reflect the changes that are evident in Greenland's "global standard" GISP2 $\delta^{18}O$ record (fig. 4)? The collective evidence of pollen, ostracodes, diatoms, clay mineralogy, particle-size distribution, and organic carbon content shows robust changes for the two most significant transitions: (1) the initial change from glacial to interglacial conditions at 14,670 cal yr BP, formally known as the transition from the Oldest Dryas to Bølling chronozones (fig. 4); and (2) the final switch from glacial to interglacial conditions at about 11,650 cal yr BP, the transition from the Younger Dryas to Early Holocene. However, unlike other published records from the North Atlantic coastal region (Yu and Wright 2001) and from Nelson Lake and Crystal Lake in northeastern Illinois (Curry et al. 2002, 2004; Zajac et al. 2006), evidence for changes within the broad transition zone that define, for example, the Allerød and Younger Dryas chronozones, are subtle to ambiguous at Brewster Creek. In particular, the Nelson and Crystal Lake pollen records show increases in the relative percentage of *Picea mariana* (black spruce) relative to *Fraxinus nigra*-type (black ash) during the Younger Dryas. These trends are not evident at Brewster Creek. The other important difference between Brewster Creek and the other Illinois sites is that, during the latter half of the Younger Dryas, the basin was nearly filled with sediment, and there was little room for fluctuating water levels. However, excellent fossil preservation indicates the Brewster Creek site never desiccated. The implied continuous throughflow of water was likely promoted by groundwater input. Because there is little seasonal change in the temperature and chemistry of groundwater, the proxy records of paleohydrology (ostracodes and diatoms) were less responsive to seasonal environmental variability (especially winter cold) than were Nelson Lake and Crystal Lake.

Figure 25 A groundwater-fed pond in north-central Ohio with charophytes mounded over spring vents (photograph courtesy of A. Smith, Department of Geology, Kent State University).

The environmental proxies at Brewster Creek reacted at different rates during the initial change from glacial to interglacial conditions. In general, the responses of endogenic paleohydrological proxies were abrupt and occurred in the sediment between lithologic units. Conversely, responses of exogenic proxies of sediment and pollen occurred during deposition of transition zones. The styles of transition range from gradual to stepwise and span a period of about 900 years (table 6). The chronologically ordered radiocarbon ages in this transition interval are a strong indication that reworking was minimal.

The pollen diagram indicates that a black spruce-larch-*Sphagnum* peatland developed around Brewster Creek during the Bølling and Allerød chronozones. The pollen record further indicates that conditions during the Bølling-Allerød were warmer than during the Oldest Dryas, judging from the increase in the pollen of deciduous trees (as well as in the pollen of aquatic species, macrofossils of charophytes, and the abundant nektic ostracodes and epiphytic diatoms). The gain in black ash pollen, however, is not as dramatic as it is in the Nelson Lake record, suggesting significant local variation in vegetation growing under the same climatic regime. Upward increases in fir pollen indicate a growing importance of winter precipitation. Several peaks and valleys suggest that the vegetation may have responded to the short-term anomalies of the Bølling and Allerød chronozones (such as the Inter-Allerød Cold Period; could this be represented by the peak of black spruce pollen at about 510 cm?). The pollen and ostracode records are monotonic during the Bølling and Allerød chronozones and likely reflect shallow, groundwater-influenced conditions.

The transition from the Allerød to the Younger Dryas chronozone is marked by a subtle change in organic matter content in the marl, in addition to the appearance of *Limnocythere verrucosa,* an ostracode that favors living in water charged with dissolved bicarbonate adjacent to wetlands. Another interesting characteristic is the gain in illite content in the clay minerals. Illite is a clay mineral that is most abundant in the glacial drift, and it is not as abundant in the loess. An increase in this mineral indicates reworking of glacial drift, probably as lake levels subsided and shoreline sediment was exposed and eroded. As the water levels dropped, the fringing wetlands encroached upon the site, judging from the increase in *Sphagnum* pollen and the wetland/groundwater-loving ostracode *Limnocythere verrucosa*. Based on the pollen record from Nelson Lake, an increase in spruce pollen abundance was expected, but this response is not obviously seen in the Brewster Creek pollen record. Concentrations of black spruce pollen increase somewhat during the Younger Dryas with

respect to the Allerød, but the spectra are very similar to the Bølling.

And finally, what is seen in the records during the Younger Dryas to early Holocene transition? Spruce pollen, especially black spruce pollen, tapers off but does not go away completely until about 9,300 ^{14}C yr BP During this transition, there is a concomitant increase in the pollen of deciduous trees such as oak, elm, and hickory. This kind of response is seen in virtually every pollen record in the region. The changeover takes place as the lithology changes from interbeds of marl and peat to pure peat. Larch needles and stomata are abundant in the organic-rich sediment. The ostracode analogs indicate warming and wetter terrestrial conditions, although there is no indication that the paleohydrology responded significantly. The likely reason for this hydrological inertia was the continued abundance of groundwater, which muted changes in the short-term maximum and minimum temperature and moisture balance.

In summary, the data collected thus far from the Brewster Creek site offer insight into environmental change during the dramatic changes in global climate during the last glacial to interglacial transition. The response of aquatic organisms was subtle, probably due to the mitigating effects of abundant groundwater on temperature and chemistry. Ostracode analog reconstructions of paleohydrology and paleoclimate are encouraging, but the optimum data set was not available. The paleochemical reconstructions presented here are adequate since temperature (in the range indicated by the paleovegetation) played a relatively small role in affecting gross lake water chemistry, such as total dissolved solids. The modern analog lakes are distributed throughout the northern part of the United States where the vegetation suggests precipitation exceeds or equals evaporation. Most of the analog lakes have in common abundant charophytes that mound over shallow springs, such as the lake shown in figure 25 (Alison Smith, Kent University, personal communication 2005).

One of the more useful conclusions of this investigation is that lithology changed during the major climatic changes of the last glacial to interglacial transition. With some complications, the tripartite succession of (1) smectite-rich silt, (2) illite-rich marl, and (3) peat corresponds to (1) the final stages of the last glaciation (the Oldest Dryas), (2) the Bølling, Allerød, and Younger Dryas chronozones, and (3) the early Holocene. The sediment accumulation rate slowed at the base of each of the transition zones between the silt-marl contact and the marl-peat contact (fig. 13). For example, the sediment accumulation rate of the lower transition zone (Unit 2) was 3.6 times slower than during deposition of the lower silt layer (0.039 vs. 0.14 cm/yr, respectively). The implication of this observation is that, as the succession is traced shoreward, the zones of slow sediment accumulation likely become unconformities above which thin lag deposits of fine sand were deposited. Such unconformities are intervals along which fossils may concentrate, such as snail shells or the remains of large vertebrates such as mastodons.

Acknowledgments

The authors are grateful for the support of the Forest Preserve District of DuPage County Board of Commissioners and particularly to following staff members: Maggie Zoellner (retired), John Oldenburg, Leslie Berns, and Tom Pray. Additional field support from the Illinois State Museum was provided by Pietra Mueller, Jeffrey Saunders, Bonnie Styles, Bruce McMillan, and Jim Oliver. Thanks are expressed to James Miller, ISGS, and David Nelson, University of Illinois, for their peer reviews of this publication. This work was funded in part by the National Science Foundation under Grant DEB-0613952 to B.B. Curry and E.C. Grimm.

References

Alley, R.B., 2000, The two-mile time machine: Ice cores, abrupt climate change, and our future: Princeton, New Jersey, Princeton University Press, 229 p.

Alley, R.B., P.A. Mayewski, T. Sowers, M. Stuiver, K.C. Taylor, and P.U. Clark, 1997, Holocene climate instability: A prominent widespread event at 8200 yr ago: Geology, v. 25, p. 483–486.

Alley, R.B., D.A. Meese, C.A. Shuman, A.J. Gow, K.C. Taylor, P.M. Grootes, J.W.C. White, M. Ram, E.D. Waddington, P.A. Mayewski, and G.A. Zielinski, 1993, Abrupt increase in Greenland snow accumulation at the end of the Younger Dryas event: Nature, v. 362, p. 527–529.

Almendinger, J.C., 1992, The late Holocene history of prairie, brush-prairie, and jack pine *(Pinus banksiana)* forest on outwash plains, north-central Minnesota, USA: The Holocene, no. 2, p. 37–50.

Amundson, D.C., and H.E. Wright, Jr., 1979, Forest changes in Minnesota at the end of the Pleistocene: Ecological Monographs, v. 49, p. 1–16.

An Inconvenient Truth, 2007, D. Guggenheim, dir.: Los Angeles, California, Paramount Classics and Participant Productions.

Baker, R.G., L.J. Maher, C.A. Chumbley, and K.L. Van Zant, 1992, Patterns of Holocene environmental change in the midwestern United States: Quaternary Research, v. 37, p. 379–389.

Björck, J., T. Andrén, S. Wastegård, G. Possnert, and K. Schoning, 2002, An event stratigraphy for the last glacial-Holocene transition in eastern middle Sweden: Results from investigations of varved clay and terrestrial sequences: Quaternary Science Reviews, v. 21, p. 1489–1501.

Björck, S., M.J.C. Walker, L.C. Cwynar, S. Johnsen, K.-L. Knudsen, J.J. Lowe, B. Wohlfarth, and I. Members, 1998, An event stratigraphy for the last termination in the North Atlantic region based on the Greenland ice-core record: A proposal by the INTIMATE group: Journal of Quaternary Science, v. 13, p. 283–292.

Borns, H.W., Jr., C.C. Dorion, G.L. Jacobson, Jr., K.J. Kreutz, W.B. Thompson, T.K. Weddle, L.A. Doner, M.R. Kaplan, and T.V. Lowell, 2003, The deglaciation of Maine, *in* J. Ehlers and P.L. Gibbard, eds., Quaternary glaciations—Extent and chronology, Part II: North America: Amsterdam, Elsevier.

Broecker, W.S., J.P. Kennett, B.P. Flower, J.T. Teller, S. Trumbore, G. Bonani, and W. Wolfli, 1989, Routing of meltwater from the Laurentide ice sheet during the Younger Dryas: Nature, v. 341, p. 318–321.

Brubaker, L.B., 1975, Postglacial forest patterns associated with till and outwash in north-central Upper Michigan: Quaternary Research, v. 5, p. 499–527.

Brugam, R.B., E.C. Grimm, and N.M. Eyster-Smith, 1988, Holocene environmental changes in Lily Lake, Minnesota inferred from fossil diatom and pollen assemblages: Quaternary Research, v. 30, p. 53–66.

Cronin, T.M., 1999, Principles of paleoclimatology: New York, Columbia University Press, 560 p.

Curry, B.B., 1989, Absence of Altonian glaciation in Illinois: Quaternary Research, v. 31, p. 1–13.

Curry, B.B., 1995, Late Pleistocene lithofacies, paleolimnology and ostracode fauna of kettles on the Illinoian till plain, Illinois, U.S.A : University of Illinois at Urbana-Champaign, Ph.D. dissertation, 511 p.

Curry, B.B., 1999, An environmental tolerance index for ostracodes and its paleohydrological applications: Palaeogeography, Palaeoclimatology, and Palaeoecology, v. 148, p. 51–63.

Curry, B.B., 2003, Linking ostracodes to climate and landscape, *in* L.E. Park, and A.J. Smith, eds., Bridging the gap: Trends in the ostracode biological and geological sciences: New Haven, Connecticut, The Paleontological Society Papers, The Paleontological Society, p. 223–246.

Curry, B.B., 2005, Surficial geology of Crystal Lake Quadrangle, McHenry and Kane Counties, Illinois: Illinois Geologic Quadrangle Map, IGQ Crystal Lake-SG, Illinois State Geological Survey, 1:24,000.

Curry, B.B., 2007, Surficial geology of Elgin Quadrangle, Cook and Kane Counties, Illinois: Illinois State Geological Survey, Illinois Geologic Quadrangle Map, IGQ Elgin, 1:24,000.

Curry, B.B., 2008, Surficial geology of the Hampshire Quadrangle, Kane County: Illinois State Geological Survey, Illinois Quadrangle Map, IGQ Hampshire, 1:24,000.

Curry, B.B., W.S. Dey, E.C. Grimm, S.L. Sargent, and S.A. Kuzin, 2002, Investigation of the geology, hydrology, water balance, paleovegetation, and paleohydrology of Nelson Lake Marsh: Illinois State Geological Survey, contract report to Kane County Forest Preserve, Geneva, IL.

Curry, B.B., and L.R. Follmer, 1992, The last interglacial-glacial transition in Illinois: 123–25 ka, *in* P.U. Clark, and P.D. Lea, eds., Geologic Society of America Special Paper: Boulder, Colorado, Geological Society of America, p. 71–88.

Curry, B.B., and D.A. Grimley, 2006, Provenance, age, and environment of mid-Wisconsin Episode slackwater lake sediment in the St. Louis Metro East area: Quaternary Research, v. 65, p. 108–122.

Curry, B.B., D.A. Grimley, and J.A. Stravers, 1999, Quaternary geology, geomorphology, and climatic history of Kane County, Illinois: Guidebook 28, Illinois State Geological Survey, 40 p.

Curry, B.B., E.C. Grimm, D. Nelson, J. Slate, S.E. Greenberg, and J.W. Scott, 2004, Contrasting hydrological responses to Holocene climate at Nelson Lake and Crystal Lake, northeastern Illinois, *in* American Quaternary Association Program and Abstracts of the 18th Biennial Meeting: Lawrence, Kansas, American Quaternary Association, p. 110–112.

Curry, B.B., and M.J. Pavich, 1996, Absence of glaciation in Illinois during marine isotope stages 3 through 5: Quaternary Research, v. 31, p. 19–26.

Curry, B.B., and C.H. Yansa, 2004, Evidence of stagnation of the Harvard sublobe (Lake Michigan lobe) in northeastern Illinois, USA, from 24 000 to 17 600 BP and subsequent tundra-like ice-marginal paleoenvironments from 17 600 to 15 700 BP: Géographie physique et Quaternaire, v. 58, p. 305–321.

Cushing, E.J., 1965, Problems in the Quaternary phytogeography of the Great Lakes region, *in* H.E. Wright, Jr., and D.G. Frey, eds., The Quaternary of the United States: Princeton, New Jersey, Princeton University Press, p. 403–416.

Cwynar, L.C., and A.J. Levesque, 1995, Chironomid evidence for late-glacial climatic reversals in Maine: Quaternary Research, v. 43, p. 405–413.

Dean, W.E., Jr., 1974, Determination of carbonate and organic matter in calcareous sediments and sedimentary rocks by loss on ignition: Comparison with other methods: Journal of Sedimentary Petrology, v. 44, p. 242–248.

Deevey, E.S., Jr. , 1951, Late-glacial and post-glacial pollen diagrams from Maine: American Journal of Science, v. 249, p. 177–207.

Delorme, L.D., 1969, Ostracodes as Quaternary paleoecological indicators: Canadian Journal of Earth Sciences, v. 6, p. 1471–1476.

Delorme, L.D., 1970a, Freshwater ostracodes of Canada, Part II, Subfamily Cypridopsinae and Herpetocypridinae, and family Cyclocyprididae: Canadian Journal of Zoology, v. 48, p. 253–266.

Delorme, L.D., 1970b, Freshwater ostracodes of Canada, Part III, Subfamily Candonidae: Canadian Journal of Zoology, v. 48, p. 1099–1127.

Delorme, L.D., 1970c, Freshwater ostracodes of Canada, Part IV, Families Ilyocyprididae, Notodromadidae, Darwinulidae, Cytherideidae, and Entocytheridae: Canadian Journal of Zoology, v. 48, p. 1251–1259.

Delorme, L.D., 1971, Freshwater ostracodes of Canada, Part V, Families Limnocytherdae, Loxoconchidae: Canadian Journal of Zoology, v. 49, p. 43–64.

Doner, L.A., 1996, Late-Pleistocene environments in Maine and the Younger Dryas dilemma: Orono, Maine, University of Maine, M.S. thesis, 68 p.

Dorale, J.A., L. Edwards, E. Ito, and L. Gonzalez, 1998, Climate and vegetation history of the midcontinent from 75 to 25 ka: A speleothem record from Crevice Cave, Missouri, USA: Science, v. 282, p. 1871–1874.

Dorion, C.C., 1997, An updated high resolution chronology of deglaciation and accompanying marine transgression in Maine: Orono, Maine, University of Maine, M.S. thesis, 147 p.

Drexler, C.W., W.R. Farrand, and J.D. Hughes, 1983, Correlation of glacial lakes in the Superior Basin with eastward discharge events from Lake Agassiz, *in* J.T. Teller and L. Clayton, ed., Glacial Lake Agassiz: Ottawa, Ontario, Canada, Geological Association of Canada, p. 309–329.

Ewing, H.A., 2002, The influence of substrate on vegetation history and ecosystem development: Ecology, v. 83, p. 2766–2781.

Fægri, K.I., P.E. Kaland, and K. Krzywinski, 1989, Textbook of pollen analysis, 4th ed.: Chichester, England, John Wiley & Sons, 328 p.

Fallu, M.A., N. Allaire, and R. Pienitz, 2002, Distribution of freshwater diatoms in 64 Labrador (Canada) lakes: Species-environment relationships along latitudinal gradients and reconstruction models for water colour and alkalinity: Canadian Journal of Fisheries and Aquatic Sciences, v. 59, p. 329–349.

Farrand, W.R., and C.W. Drexler, 1985, Late Wisconsinan and Holocene history of the Lake Superior Basin, *in* P.F. Karrow, and P.E. Calkin, eds., Quaternary evolution of the Great Lakes: Ottawa, Ontario, Canada, Geological Association of Canada, p. 17–32

Fay, H., 2002, Formation of ice-block obstacle marks during the November 1996 glacier-outburst flood (jökulhlaup), Skeiðarársandur, southern Iceland: Special Publication of the International Association of Sedimentologists, v. 32, p. 85–97.

Follmer, L.R., 1982, The geomorphology of the Sangamon surface: Its spatial and temporal attributes, *in* Thorn, C., ed., Space and time in geomorphology: London, Allen & Unwin, Binghampton Symposia in Geomorphology, p. 117–146.

Forester, R.M., 1983, Relationship of two lacustrine ostracode species to solute composition and salinity: Implications for paleohydrochemistry: Geology, v. 11, p. 435–438.

Forester, R.M., 1986, Determination of the dissolved anion composition of ancient lakes from fossil ostracodes: Geology, v. 14, p. 796–798.

Forester, R.M., 1987, Late Quaternary paleoclimate records from lacustrine ostracodes, *in* W.F. Ruddiman, and H.E. Wright, Jr. , eds., North America and adjacent oceans during the last deglaciation: Boulder, Colorado, Geological Society of America, p. 261–276.

Forester , R.M., A.J. Smith, D. Palmer, and B.B. Curry, 2006, NANODe —North American Non-Marine Ostracode Database Project, Version 1. (http://www.kent.edu/NANODe).

Gajewski, K., 1987, Climatic impacts on the vegetation of eastern North America during the past 2000 years: Vegetatio, v. 68, p. 179–190.

Glaser, P.H., B.C.S. Hansen, D.I. Siegel, A.S Reeve, and P.J. Morin, 2004, Rates, pathways and drivers for peatland development in the Hudson Bay Lowlands, northern Ontario: Canada Journal of Ecology, v. 92, p. 1036–1053.

Graham, R.W., and E.C. Grimm, 1990, Effects of global climate change on the patterns of terrestrial biological communities: Trends in Ecology and Evolution, v. 5, p. 289–292.

Grimm, E.C., 1984, Fire and other factors controlling the Big Woods vegetation of Minnesota in the mid-nineteenth century: Ecological Monographs, v. 54, p. 291–311.

Grimm, E.C., 1987, CONISS: A FORTRAN 77 program for stratigraphically constrained cluster analysis by the method of increment sum of squares: Computers and Geosciences, v. 13, p. 13–35.

Grimm, E.C., and G.L. Jacobson, Jr., 2004, Late-Quaternary vegetation history of the eastern United States, *in* A.R. Gillespie, S.C. Porter, and B.F. Atwater, eds., The Quaternary Period in the United States: The Netherlands, Elsevier, p. 381–402.

Grimm, E.C., and L.J. Maher, Jr. , 2002, AMS radiocarbon dating documents climate events in the upper Midwest coeval with the Bølling/Allerød and Younger Dryas episodes: Boulder, Colorado, Geological Society of America Abstracts with Programs, v. 34, no. 6, p. 352.

Hansel, A.K., and W.H. Johnson, 1996, Wedron and Mason Groups: Lithostratigraphic reclassification of deposits of the Wisconsin Episode, Lake Michigan Lobe area: Illinois State Geological Survey, Bulletin 104, 116 p.

Hansel, A.K., J.M. Masters, and B.J. Socha, 1985, The Beverly Section *in* Depositional environments and correlation problems of the Wedron Formation (Wisconsinan) in northeastern Illinois: Illinois State Geological Survey, Guidebook 16, p. 53–70.

Hansen, B.C.S., 1995, Conifer stomate analysis as a paleoecological tool: An example from the Hudson Bay

Lowlands: Canadian Journal of Botany, v. 73, p. 244–252.

Hansen, B.C.S., and D.R. Engstrom, 1985, A comparison of numerical and qualitative methods of separating pollen of black and white spruce: Canadian Journal of Botany, v. 63, p. 2159–2163.

Hansen, B.C.S., G.M. MacDonald, and K.A. Moser, 1996, Identifying the tundra-forest border in the stomate record: an analysis of lake surface samples from the Yellowknife area, Northwest Territories, Canada: Canadian Journal of Botany, v. 74, p. 796–800.

Hoff, C.C., 1942, The ostracods of Illinois, their biology and taxonomy: Illinois Biological Monographs, v. 1–2, 196 p.

Hughes, R.E., D.M. Moore, and H.D. Glass, 1994, Qualitative and quantitative analysis of clay minerals in soils, *in* L.E. Amonette and L.W. Zelazny, eds., Quantitative methods in soil mineralogy: Madison, Wisconsin, Soil Science Society of America, p. 330–359.

Jackson, S.T., and J.W. Williams, 2004, Modern analogs in Quaternary paleoecology: Here today, gone yesterday, gone tomorrow?: Annual Review of Earth and Planetary Sciences, v. 32, p. 495–537.

Jacobson, G.L., Jr., 1979, The palaeoecology of white pine *(Pinus strobus)* in Minnesota: Journal of Ecology, v. 67, p. 697–726.

Johnson, W.H., and A.K. Hansel, 1989, Age, stratigraphic position, and significance of the Lemont drift, northeastern Illinois: Journal of Geology, v. 97, p. 301–318.

Jongman, R.H., C.J.F. ter Braak, and O.F.R. van Tongeren, 1987, Data analysis in community and landscape ecology: Wageningen, The Netherlands, Pudoc, 299 p.

Karst, T.L., and J.P. Smol, 2000, Paleolimnological evidence of limnetic nutrient concentration equilibrium in a shallow, macrophyte-dominated lake: Aquatic Sciences, v. 62, p. 20–38.

Killey, M.M., 2007, Illinois' ice age legacy: Illinois State Geological Survey, Geoscience Education Series 14, 74 p.

King, J.E., 1981, Late Quaternary vegetational history of Illinois: Ecological Monographs, v. 51, p. 43–62.

Kitchell, J.A., and D.L. Clark, 1979, Distribution, ecology and taxonomy of recent freshwater ostracoda of Lake Mendota: Madison, Wisconsin, Natural History Council, University of Wisconsin, 24 p.

Konen, M.E., 1999, Human impacts on soils and geomorphic processes on the Des Moines Lobe: Ames, Iowa, Iowa State University, 259 p.

Krammer, K., and H. Lange-Bertalot, 1997a, Bacillariophyceae, 1 Teil: Naviculaceae, *in* H. Ettl, J. Gerloff, H. Heynig, and D. Mollenhauer, eds., Sübwasserflora von Mitteleuropa: Stuttgart, Germany, G. Fisher Verlag, 876 p.

Krammer, K., and H. Lange-Bertalot, 1997b, Bacillariophyceae, 2 Teil: Bacillariaceae, Epithemiaceae, Surirellaceae, *in* H. Ettl, J. Gerloff, H. Heynig, and D. Mollenhauer, eds., Sübwasserflora von Mitteleuropa: Stuttgart, Germany, G. Fisher Verlag, 611 p.

Krammer, K., and H. Lange-Bertalot, 1991a, Bacillariophyceae, 3 Teil: Centrales, Fragilariaceae, Eunotiaceae, *in* H. Ettl, J. Gerloff, H. Heynig, and D. Mollenhauer, eds., Sübwasserflora von Mitteleuropa: Stuttgart, Germany, G. Fisher Verlag, 599 p.

Krammer, K., and H. Lange-Bertalot, 1991b, Bacillariophyceae, 4 Teil: Achnanthaceae, Kritische Ergänzungen zu Navicula (Lineolatae) und Gomphonema, *in* H. Ettl, G. Gärtnet, J. Gerloff, H. Heynig, and D. Mollenhauer, eds., Sübwasserflora von Mitteleuropa: Stuttgart, Germany, G. Fisher Verlag, 437 p.

Krumbein, W.C., and F.J. Pettijohn, 1938, Sedimentary petrography: New York, D. Appleton-Century, 549 p.

Lange-Bertalot, H., 1993, Eighty-five new taxa and much more than 100 taxonomic clarifications supplementary to Sübwasserflora von Mitteleuropa, v. 2/1–4, *in* Lange-Bertalot, H., ed., Bibliotheca diatomologica, Band 27: Berlin, Germany, J. Cramer.

Larson, G., and R. Schaetzl, 2001, Origin and evolution of the Great Lakes: Journal of Great Lakes Research, v. 27, p. 518–546.

Levesque, A.J., L.C. Cwynar, and I.R. Walker, 1994, A multiproxy investigation of late-glacial climate and vegetation change at Pine Ridge Pond, southwest New Brunswick, Canada: Quaternary Research, v. 42, p. 316–327.

Levesque, A.J., L.C. Cwynar, and I.R. Walker, 1996, Richness, diversity and succession of late-glacial chironomid assemblages in New Brunswick, Canada: Journal of Paleolimnology, v. 16, p. 257–274.

Lowell, T.V., G.J. Larson, J.D. Hughes, and G.H. Denton, 1999, Age verification of the Lake Gribben forest bed and the Younger Dryas advance of the Laurentide Ice Sheet: Canadian Journal of Earth Sciences, v. 36, p. 383–393.

Maher, L.J., 1982, The palynology of Devil's Lake, Sauk County, Wisconsin, *in* J.C. Knox, L. Clayton, and D.M. Mickelson, eds., Quaternary history of the driftless area: Madison, Wisconsin, University of Wisconsin-Extension, Geological and Natural History Survey, p. 119–135

Mangerud, J., S.T. Anderson, B.E. Berglund, and J.J. Donner, 1974, Quaternary stratigraphy of Norden, A proposal for terminology and classification: Boreas, v. 3, p. 109–128.

Mayle, F.E., and L.C. Cwynar, 1995a, Impact of the Younger Dryas cooling event upon lowland vegetation of Maritime Canada: Ecological Monographs, v. 65, p. 129–154.

Mayle, F.E., and L.C. Cwynar, 1995b, A review of multi-proxy data for the Younger Dryas in Atlantic Canada: Quaternary Science Reviews, v. 14, p. 813–821.

Mayle, F.E., A.J. Levesque, and L.C. Cwynar, 1993, Accelerator-mass-spectrometer ages for the Younger Dryas event in Atlantic Canada: Quaternary Research, v. 39, p. 355–360.

McAndrews, J.H., 1966, Postglacial history of prairie, savanna, and forest in northwestern Minnesota: Torrey Botanical Club Memoir, v. 22, no. 2, p. 1–72.

Nelson, D.M., F.S. Hu, E.C. Grimm, B.B. Curry, and J.E. Slate, 2006, The influence of aridity and fire on Holocene prairie communities in the eastern Prairie Penninsula, Ecology 87: p. 2523–2536.

Overpeck, J.T., R.S. Webb, and T.I. Webb, 1992, Mapping eastern North American vegetation change of the past 18 ka: No-analogs and the future: Geology, v. 20, p. 1071–1074.

Patrick, R., and C.W. Reimer, 1966, The diatoms of the United States, volume 1: Philadelphia, Pennsylvania, Monographs of the Academy of Natural Sciences of Philadelphia, no. 13, 688 p.

Patrick, R., and C.W. Reimer, 1975, The diatoms of the United States, volume 2, part 1: Philadelphia, Pennsylvania, Monographs of the Academy of Natural Sciences of Philadelphia, no. 13, 213 p.

Prentice, I.C., P.J. Bartlein, and T.I. Webb, 1991, Vegetation and climate change in eastern North America since the last glacial maximum: Ecology, v. 72, p. 2038–2056.

Reimer, P.J., M.G.L. Baillie, E. Bard, A. Bayliss, J.W. Beck, C.J.H. Bertrand, P.G. Blackwell, C.E. Buck, G.S. Burr, K.B. Cutler, P.E. Damon, R.L. Edwards, R.G. Fairbanks, M. Friedrich, T.P. Guilderson, A.G. Hogg, K.A. Hughen, B. Kromer, G. McCormac, S. Manning, C.B. Ramsey, R.W. Reimer, S. Remmele, J.R. Southon, M. Stuiver, S. Talamo, F.W. Taylor, J. van der Plicht, and C.E. Weyhenmeyer, 2004, INTCAL04 terrestrial radiocarbon age calibration, 0–26 cal kyr BP: Radiocarbon, v. 46, p. 1029–1058.

Rind, D., D. Peteet, W. Broecker, A. McIntyre, and W. Ruddiman, 1986, The impact of cold North Atlantic sea surface temperatures on climate: Implications for the Younger Dryas cooling (11–10 k): Climate Dynamics, v. 1, p. 3–33.

Roy, M., P.U. Clark, R.W. Barendregt, J.R. Glasmann, and R.J. Enkin, 2004, Glacial stratigraphy and paleomagnetism of late Cenozoic deposits of the north-central United States: Geological Society of America Bulletin, v. 116, p. 30–41.

Shane, L.C.K., 1987, Late-glacial vegetational and climatic history of the Allegheny Plateau and the till plains of Ohio and Indiana, U.S.A.: Boreas, v. 16, p. 1–20.

Shane, L.C.K., and K.H. Anderson, 1993, Intensity, gradients and reversals in late glacial environmental change in east-central North America: Quaternary Science Reviews, v. 12, p. 307–320.

Shuman, B., T.I. Webb, P. Bartlein, and J.W. Williams, 2002, The anatomy of a climatic oscillation: Vegetation change in eastern North America during the Younger Dryas chronozone: Quaternary Science Reviews, v. 21, p. 1777–1791.

Smith, A.J., 1993, Lacustrine ostracodes as hydrochemical indicators in lakes of the north-central United States: Journal of Paleolimnology, v. 8, p. 121–134.

Smith, A.J., and R.M. Forester, 1994, Estimating past precipitation and temperature from fossil ostracodes, *in* The 5th Annual International High-Level Radioactive Waste Management Conference and Exposition Proceedings, Las Vegas, NV, p. 2545–2552.

Smol, J.P., and M.M. Boucherle, 1985, Postglacial changes in algal and cladoceran assemblages in Little Round Lake, Ontario: Archiv fuer Hydrobiology, v. 103, p. 25–49.

Soil Survey Staff, 1996, Soil survey laboratory methods manual, Soil Survey Investigations, Rep. No. 42, version 3.0: Washington, DC, U.S. Government Printing Office, 693 p.

Southon, J.R., 2002, A first step to reconciling the GRIP and GISP2 ice-core chronologies, 0–14,500 yr B.P.: Quaternary Research, v. 57, p. 32–37.

Stea, R.R., and R.J. Mott, 1998, Deglaciation of Nova Scotia: Stratigraphy and chronology of lake sediment cores and buried organic sections: Géographie physique et Quaternaire, v. 52, p. 3–21.

Stuiver, M., P.M. Grootes, and T.F. Braziunas, 1995, The GISP2 $\delta^{18}O$ climate record of the past 16,500 years and the role of the sun, ocean, and volcanoes: Quaternary Research, v. 44, p. 341–354.

Taylor, K. C., G.W. Lamorey, G.A. Doyle, R.B. Alley, P.M. Grootes, P.A. Mayewski, J.W.C. White, and L.K. Barlow, 1993, The "flickering switch" of late Pleistocene climate variability: Nature, v. 361, p. 432–436.

Taylor, K.C., P.A. Mayewski, R.B. Alley, E.J. Brook, A.J. Gow, P.M. Grootes, D.A. Meese, E.S. Saltzman, J.P. Severinghaus, M.S. Twickler, J.W.C. White, S. Whitlow, and G.A. Zielinski, 1997, The Holocene-Younger Dryas transition recorded at Summit, Greenland: Science, v. 278, p. 825–827.

Thompson, R.S., K.H. Anderson, and P.J. Bartlein, 2000, Atlas of relations between climatic parameters and distributions of important trees and shrubs in North America: Reston, Virginia, U.S. Geological Survey, Professional Paper 1650 A-B (http://pubs.usgs.gov/pp/1650-a).

Walter, N.F., G.R. Hallberg, and T.E. Fenton, 1978, Particle-size analysis by the Iowa State University Soil Survey Laboratory, Standard procedures for evaluation of Quaternary materials in Iowa: Iowa City, Iowa, p. 61–74.

Webb, R.S., K.H. Anderson, and T.I. Webb, 1993, Pollen response-surface estimates of late-Quaternary changes in the moisture balance of the northeastern United States: Quaternary Research, v. 40, p. 213–227.

Webb, T., III, E.J. Cushing, and H.E. Wright, Jr., 1983, Holocene changes in the vegetation of the Midwest, *in* H.E. Wright, Jr., and D.G. Frey, eds., The Holocene: Late-Quaternary environments of the United States 2: Minneapolis, Minneapolis, University of Minnesota Press, p. 142–165.

Wickham, S.S., W.H. Johnson, and H.D. Glass, 1988, Regional geology of the Tiskilwa Till Member, Wedron Formation, Northeastern Illinois: Illinois State Geological Survey, Circular 543, p. 35 p.

Williams, J.W., B.N. Shuman, and T.I. Webb, 2001, Dissimilarity analyses of late-Quaternary vegetation and climate in eastern North America: Ecology, v. 82, p. 3346–3362.

Williams, J.W., B.B. Shuman, T.I. Webb, P.J. Bartlein, and P.L. Luduc, 2004, Late-Quaternary vegetation dynamics in North America: Scaling from taxa to biomes: Ecological Monographs, v. 74, p. 309–334.

Willman, H.B., and J.C. Frye, 1970, Pleistocene stratigraphy of Illinois: Illinois State Geological Survey, Bulletin 94, 204 p.

Willman, H.B., J.C. Frye, and H.D. Glass, 1966, Mineralogy of glacial tills and their weathering profiles, Part II, Weathering profiles: Illinois State Geological Survey, Circular 400, 76 p.

Willman, H.B., H.D. Glass, and J.C. Frye, 1963, Mineralogy of glacial tills and their weathering profiles, Part I, Glacial tills: Illinois State Geological Survey, Circular 347, 55 p.

Wilson, S.E., B.F. Cumming, and J.P. Smol, 1996, Assessing the reliability of salinity inference models from diatom assemblages: An examination of a 219-lake data set from western North America: Canadian Journal of Fisheries and Aquatic Sciences, v. 53, p. 1580–1594.

Wilson, S.E., I.R. Walker, R.J. Mott, and J.P. Smol, 1993, Climatic and limnological changes associated with the Younger Dryas in Atlantic Canada: Climate Dynamics, v. 8, p. 177–187.

Wright, H.E., Jr., T.C. Winter, and H.L. Patten, 1963, Two pollen diagrams from southeastern Minnesota: problems in the regional late-glacial and postglacial vegetational history: Geological Society of America Bulletin, v. 74, p. 1371–1396.

Wright, J. W., and H.M. Rauscher,1990, *Fraxinus nigra* Marsh. black ash, *in* R.M. Burns and B.H. Honkala, eds., Silvics of North America, volume 2, Hardwoods: Washington, DC, U.S. Department of Agriculture, p. 344–347.

Yu, Z., 2000, Ecosystem response to late glacial and early Holocene climate oscillations in the Great Lakes region of North America: Quaternary Science Reviews, v. 19, p. 1723–1747.

Yu, Z., and U. Eicher, 1998, Abrupt climate oscillations during the last deglaciation in central North America: Science, v. 282, p. 2235–2238.

Yu, Z., and U. Eicher, 2001, Three amphi-Atlantic century-scale cold events during the Bølling-Allerød warm period: Géographie physique et Quaternaire, v. 55, p. 175–183.

Yu, Z., and H.E. Wright, Jr., 2001, Response of interior North America to abrupt climate oscillations in the North Atlantic region during the last deglaciation: Earth-Science Reviews, v. 52, p. 333–369.

Zajac, L.M., E.C. Grimm, B.B.Curry, and B.C.S. Hansen, 2006, Reconstruction of late glacial vegetation response to climate shifts in northeastern Illinois: American Quaternary Association Program and Abstracts of the 19th Biennial Meeting, Montana State University, Bozeman, August 17–20, p. 175–176.

Epilogue

On May 22, 2007, a fortunate rain fell on the recently overturned peaty soils at Pratt's Wayne Woods. The rain was opportune because it washed the dirt and grime off three mastodon teeth. A DuPage County Forest Preserve contractual employee, Daniel Terpstra, whose primary job was to reseed overturned soil as part of a wetland restoration program, noticed the teeth gleaming in the sun the following day (fig. 26). Dr. Jeffrey Saunders of the Illinois State Museum was contacted to verify the discovery, and soon there was a backhoe opening a 30 × 30-m area for examination (fig. 27). Brandon Curry and Eric Grimm, coauthors of this report, were on hand and soon figured out that the bone material was coming from the base of Unit 5, the surficial peat overlying the fossiliferous gray silt of Unit 1. All other units, the transitional units and marl unit, were missing in this part of the basin. The stratigraphy was similar to that of boring BC-11 (see fig. 14).

The peat was disturbed and from 1 to 1.5 m thick; it was difficult ascertaining true depth because the surface of the entire site had been disturbed by plowing, drainage tile installations, and, finally, by drainage tile removal. Much tusk material was recovered; the largest fragments were somewhat square and about 14 cm across (fig. 28). Near the end of the day, a rib was found in situ. Although not visible in figure 29, the rib was sandwiched by branches of boreal wood. Wood below the rib was resting directly on the fossiliferous gray silt (Unit 5) and yielded a radiocarbon age of 11,710 ± 70 yr BP; wood above the rib dated at 12,120 ± 70 yr BP (table 1). The ages are out of order chronologically at the 2σ level (95% confidence) but only by about 100 years. A sample of purified collagen extracted from one of the teeth yielded a radiocarbon age of 11,455 ± 35 yr BP (table 1). The range of wood and tooth ages indicates that the wood and perhaps the tooth were reworked, which would be expected, considering that the fossiliferous

Figure 26 Daniel Terpstra, discoverer of the mastodon teeth (photograph by Jeffrey Saunders, Illinois State Museum).

Figure 27 Employees of the Forest Preserve District of DuPage County, Illinois State Museum, and Illinois State Geological Survey investigate the discovery site (photograph by Eric Grimm, Illinois State Museum).

Figure 28 (a) Tusk fragment of *Mammut americanum* recovered from the discovery site (photograph courtesy of the Forest Preserve District of DuPage County), and (b) the same tusk fragment, after cleaning (photograph by Tim Cashatt).

Figure 29 In situ rib found at the discovery site (photograph by Eric Grimm, Illinois State Museum).

peat (the base of Unit 1) occurs above an unconformity below which is the gray, fossiliferous silt (Unit 5). With such shallow burial (<2 m) and recent intensive agricultural land use, it is not surprising that the tusk(s) were fragmented. Larger elements, such as the skull, have yet to be found.

In August 2007, the Forest Preserve District of DuPage County and The Field Museum joined to host a pilot education dig, the Mastodon Camp. Twenty-four high school students and 12 teachers learned about the prehistory of northeastern Illinois as they participated in the excavation of additional bones. Over 500 fragments of bone and tusk were discovered during this two-week project. During summer 2008, the site will once again be opened, and an expanded education program will be launched to complete the excavation of the mastodon.

Appendix

Brewster Creek Borings
Drilled by MidAmerica Drilling
Driller: Jeremy
Geologist: B. Brandon Curry
Date: September 23, 2003

BC-1 (API: 31486)
Primary core used in investigation; sampled near BC-5 (see below)
62’ EL, 2,280’ NL, Sec. 6, T40N, R9E
Elevation: 750.2 ft

0.0–7.81 ft (0–235 cm)	Peat, black (5Y 2.5/1), sapric; platy structure (stratified)
7.81–8.69 ft (235–265 cm)	Peat, as above, with uncommon snail shells
8.69–8.92 ft (265–272 cm)	Peaty marl, olive-brown; stratification (imparted by snail shells)
8.92–10.27 ft (272–313 cm)	Marly peat, dark reddish brown (5YR 3/3); stratified as above
10.27–10.76 ft (313–328 cm)	Gyttja, very dark gray (2.5Y 3/1), spongy; made up of particulate organic matter
10.76–11.02 ft (328–336 cm)	Peat, dark reddish brown (5YR 3/3) with few snail shells; stratified as above
11.02–11.29 ft (336–344 cm)	Peat/gyttja hybrid; mostly spongy, particulate organic matter, with some fibric peat and rare snail shells
11.29–12.70 ft (344–387 cm)	Marl, varicolored, weak bedding, pale olive (5Y 6/3) to yellowish brown (10YR 5/2) with very dark gray (2.5Y 3/1) partings and laminae; common snail shells
12.70–15.65 ft (387–477 cm)	Marl, varicolored, strong bedding, primarily olive-gray (5Y 4/3) to pale olive (5Y 6/3); common snail shells; gray silt layer at 15.16–15.19 ft (462–463 cm)
15.65–18.33 ft (477–559 cm)	Marl, varicolored, very strong bedding, pale olive (5Y 6/3) to yellowish brown (10YR 5/2) with very dark gray (2.5Y 3/1) partings and laminae; gray silt layer from 15.85–15.88 ft (483–484 cm); common snail shells; layers do not match up well between duplicate cores, suggesting discontinuous bedding
18.33–19.16 ft (559–584 cm)	Silt, dark gray (5Y 4/1); uniform; no snail shells
19.16–19.32 ft (584–589 cm)	Marl, as above, with less light-colored material; very strongly bedded
19.32–24.87 ft (589–758 cm)	Silt, olive-gray (5Y 4/2), uniform to vaguely mottled; no snail shells
24.87–26.80 ft (758–817 cm)	Silt, as above, with abundant small fragments of black material, including degraded to well-preserved wood; black material imparts weak to moderate bedding; no snail shells
26.80–27.79 ft (817–847 cm)	Silt, as above, but fewer fragments of black material; uniform

End of boring. (Note: Using the succession described in BC-5 for comparison, this boring probably bottomed out on a large dropstone. Dropstones were encountered at a depth of 27.65 ft (843 cm) in BC-5; glacial sand and gravel was encountered at 28.3 ft (863 cm). These materials from BC-5 were used in some analyses (particle-size distribution and clay mineralogy.)

Stratigraphic summary (BC-1)

0–19.32 ft	Grayslake Peat (0–8.69 ft is peat; 8.69–11.29 ft is interbeds of peat, marl, and some gyttja)
19.32–27.79 ft	Equality Formation

BC-2 (API: 31487)
820’ EL, 2140’ NL, Sec. 6, T40N, R 9E
Elevation: 749.8 ft
Recovery: Run 1, 2.1/3.0 ft; Run 2, 3.7/4.0 ft; Run 3, 1.8/4.0 ft; Run 4, 1.8/4.0 ft; Run 5, 2.5/4.0 ft; Run 6, 3.2/4.0 ft
End of boring at 22.2 ft

0.0–4.0 ft	Peat, black (5Y 2.5/1), fibric, leached of carbonate minerals
4.0–5.0 ft	Interbedded peat (as above) and marl, yellowish brown (10YR 5/4); peat layers occur at 4.25 to 4.30 ft and 4.95 to 5.0 ft; core loss in Run 2 is almost certainly due to compaction of the marl and peat
5.0– ~10 ft	Marl, varicolored; 5–6 ft is yellowish brown as above; 6–8 ft is very pale brown (10YR 7/3) with small snail shells; 8.0–8.8 ft is light olive-brown (5Y 5/1/5) with few large snail shells; depth of contact is between 8.8 and 11 ft
~10 ft–12.4 ft	Silt; dark gray (5Y 3.5/1); abundant wood fragments and fibers
12.4–14 ft	Silt, dark greenish gray (10Y 4/1); uniform; calcareous
~14–16.0 ft	Silt; dark gray (5Y 4/1); very fossiliferous; large wood fragments
16.0–16.1 ft	Stone, 0.15 ft × 0.10 ft at 16.0 ft
16.1–17.1 ft	Silt to very fine-grained sand, oxidized brown (7.5YR 5/3) to strong brown (7.5YR 5/6); a layer material oxidized by dewatering via the layer of sand and gravel below
17.1–17.5 ft	Diamicton, silty sandy loam matrix, light yellowish brown (2.5Y 6/4)
17.5–20.6 ft	Sand, coarse, well sorted
20.6–21.7 ft	Sand and gravel, maximum clast diameter 0.08 ft across
21.7–22.2 ft	Sand, fine, olive-yellow (2.5Y 6/6)
End of boring	

Stratigraphic summary (BC-2)

0–10 ft	Grayslake Peat (0–4 ft is peat; 4–5 ft is interbeds of marl and peat; 5–10 ft is marl)
10–17.1 ft	Equality Formation
17.1–22.2 ft	Henry Formation

BC-3 (API: 31488)
670’ EL, 2,095’ NL, Sec. 6, T40N, R9E
Elevation: 750.0 ft
Recovery: Run 1, 1.9/3.0 ft; Run 2, 2.8/4.0 ft ; Run 3, 2.6/4.0 ft; Run 4, 3.8/4.0 ft; Run 5, 3.1/4.0 ft; Run 6, 3.2/4.0 ft; Run 7, 1.6/4.0 ft
End of boring at 25.6 ft

0.0–3.4 ft	Peat, black (5Y 2.5/1); fibric; leached of carbonate minerals
3.4–8.1 ft	Peat, dark reddish brown (5YR 3/3); leached
8.1–˜10 ft	Marl, pale olive (5Y 6/3); few snail shells
˜10–12.3 ft	Peat, as above
12.3–21.3 ft	Marl, varicolored, including pale olive (5Y 6/3) from 12.3–16.4 ft, light olive-brown (2.5Y 5/3) from 16.4–17.6 ft, olive-gray (5Y 5/2) from 17.6–19.0 ft, light yellowish brown (2.5Y 6/4) from 19.0–19.7 ft, light olive-brown (2.5Y 5/3) from 19.7–20.6 ft, and dark gray (2.5Y 4/1) from 20.6–21.3 ft
21.3–˜23 ft	Silt, dark gray (5Y 4/1), with wood fragments
~23–24,8 ft	Silt, with dropstones
24.8–25.6 ft	Diamicton, pebbly, loamy sand matrix, yellowish brown (10YR 5/6); calcareous
End of boring	

Stratigraphic summary (BC-3)

0.0–21.3 ft	Grayslake Peat (0.0–12.3 ft is peat; 12.3–21.3 ft is marl)
21.3–24.8 ft	Equality Formation
24.8–25.6 ft	Henry Formation, diamicton facies

BC-4 (API: 31489)
485’ EL, 2,375’ NL, Sec. 6, T40N, R9E
Elevation: 751.5 ft
Recovery: Run 1, 2.0/3.0 ft; Run 2, 2.8/4.0 ft; Run 3, 2.6/4.0 ft; Run 4, 2.0/4.0 ft
End of boring at 13.0 ft

0.0–4.1 ft	Peat, sapric, black (5Y 2.5/1); leached of carbonate minerals
4.1–5.4 ft	Peat, reddish brown (5YR 3/3), rapidly oxidizing black; leached
5.4–5.6 ft	Sand, very fine, compact, gray (5Y 5.5/1)
5.6–11.6 ft	Marl, very pale brown (10YR 7/3); uncommon snail shells from 5.6–8.3 ft; gray (5Y 5/1) with more abundant snail shells from 8.3–11.6 ft
11.6–12.25 ft	Silt with abundant flecks of organic matter and small wood fragments
12.25–13.0 ft	Diamicton; sandy loam matrix, oxidized, calcareous
End of boring	

Stratigraphic summary (BC-4)

0.0–11.6 ft	Grayslake Peat (0.0–5.6 is peat; 5.6–5.7 ft is very fine sand; 5.7–11.6 ft is marl)
11.6–12.3 ft	Equality Formation
12.3–13.0 ft	Henry Formation

BC-5 (API: 31490)
670’ EL, 2,275’ NL, Sec. 6, T40N, R9E
Elevation: 750.2 ft
Recovery: Run 1, 2.4/3.0 ft; Run 2, 3.7/4.0 ft; Run 3, 2.8/4.0 ft; Run 4, 2.4/4.0 ft, Run 5, 2.2/4.0 ft; Run 6, 2.0/4.0 ft; Run 7, 1.4/4.0 ft; Run 8, 1.7/4.0 ft
End of boring at 33.4 ft

0.0–3.7 ft	Peat, black (5Y 2.5/1), fibric; leached of carbonate minerals
3.7–7.8 ft	Peat, dark reddish brown (5YR 3/3), rapidly oxidizing black; leached, except for snail shells at base
7.8–8.0 ft	Peat, black, sapric; leached
8.0–9.5 ft	Marl, pink (7.5YR 7/3) matrix with flecks of reddish brown plant fragments (5YR 4/3); reddish-pinkish intensity varies with plant fragment concentration; abundant snail shells
9.5–11.2 ft	Marl, reddish brown (5YR 4/4); abundant snail shells
11.2–11.7 ft	Gyttja(?), dark reddish brown (5YR 3/4), somewhat thixothropic and spongy; according to site manager, material behaves Jello-like in excavations; leached carbonate minerals
11.7–16.5 ft	Marl, varicolored, including pale olive (5Y 6/3) from 11.7–12.4 ft; yellowish brown (10YR 5/2) from 12.4–13.4 ft; core loss from 13.4 to 15.0 ft; light yellowish brown from 15.0–16.5 ft; not as many snails as above
16.5–24.4 ft	Silt, varicolored, including gray (5Y 5/1) from 16.5–19.2 ft, light yellowish brown from 19.2–19.4 ft, dark greenish gray (10Y 4/1) from 19.4–23.4 ft, greenish gray (10Y 5/1) from 23.9–24.4 ft
24.4–˜26 ft	Silt, greenish gray (10Y 5/1) as above, but also containing abundant wood fragments and other bits of organic debris

~26–27.3 ft	Silt, greenish gray (10Y 5/1); no fossils observed
27.3–27.65 ft	As above, but containing abundant wood fragments that rapidly oxidize black
27.65–28.3 ft	As above, but no fossils; abundant dropstones
28.3–33.4 ft	Sand and gravel, oxidized
End of boring	

Stratigraphic summary (BC-5):

0–16.5 ft	Grayslake Peat (0–8 ft is peat; 8–16.5 is marl)
16.5–28.3 ft	Equality Formation
28.3–33.4 ft	Henry Formation

BC-6 (API: 31491) (see fig. 18)
715’ EL, 2,445’ NL, Sec. 6, T40N, R9E
Elevation: 750.8 ft
Recovery: Run 1, 2.1/3.0 ft; Run 2, 2.6/4.0 ft; Run 3, 2.0/4.0 ft; Run 4, 1.0/4.0 ft
End of boring at 12.0 ft

0.0–3.85 ft	Peat, sapric, except for wood fragments at 1.6 and 1.9 ft
3.85–4.8 ft	Sand, fine, very-well sorted, white (2.5Y8/1); leached of carbonate minerals
4.8–~10 ft	Silt, dark olive-gray (5Y 3/2); fossiliferous (wood fragments)
~10–11.3 ft	Silt, same color as above; no fossils
11.3–11.6 ft	Silt, oxidized
11.6–12.0 ft	Diamicton, pebbly, loamy sand matrix, yellow (10YR 7/6), calcareous
End of boring	

Stratigraphic summary (BC-6)

0–3.85 ft	Grayslake Peat (all peat)
3.85–4.6 ft	Equality Formation, sand facies
4.6–11.6 ft	Equality Formation
11.6–12.0 ft	Henry Formation, diamicton facies
End of boring	

BC-7 (API: 31492)
675’ EL, 2,350’ NL, Sec. 6, T40N, R9E
Elevation: 750.2 ft
Recovery: Run 1, 1.8/3.0 ft; Run 2, 3.0/4.0 ft; Run 3, 2.4/4.0 ft; Run 4, 2.4/4.0 ft; Run 5, 1.7/4.0 ft; Run 6, 1.5/4.0 ft.
End of boring at 20.5 ft

0.0–3.0 ft	Peat, black (5Y 2.5/1), sapric; leached of carbonates
3.0–4.25 ft	Peat, dark reddish brown (5YR 3/3); leached
4.25–~11 ft	Marl, light yellowish brown (2.5Y 6/3)
~11–11.6 ft	Silt, grayish brown (2.5Y 5.2)
11.6–12.5 ft	Silt, as above, but with shells
12.5–19.3 ft	Silt, as above, but darker (7.5Y 3/2) with shells and wood fragments
19.3–19.9 ft	Silty clay loam, uniform, very dark greenish gray (5GY 3/1)
19.9–20.5 ft	Diamicton, pebbly, sandy loam matrix, yellow (10YR 7/6), calcareous
End of boring	

Stratigraphic summary (BC-7)

0.0–11 ft	Grayslake Peat (0.0–4.3 ft is peat; 4.3–11 ft is marl)
11–19.9 ft	Equality Formation
19.9–20.5 ft	Henry Formation, diamicton facies

BC-8 (API: 31493)
655’ EL, 2,405’ NL, Sec. 6, T40N, R9E
Elevation: 750.6 ft

NOTE: This site was cored twice with offsetting cores to ensure a more complete recovery of the sediment succession; 0–3 ft was not sampled

B-8, Run 1. 3–7 ft	2.05 ft recovered
B-8a, Run 1, 5–9 ft	1.84 ft recovered
BC-8, Run 2, 7–11 ft	1.74 ft recovered
BC-8a, Run 2 , 9–13 ft)	2.07 ft recovered
BC-8, Run 3, 11–15 ft)	2.78 ft recovered
BC-8b, Run 3, 13–17 ft)	2.60 ft recovered
BC-8, Run 4, 15–19 ft	1.98 ft recovery
BC-8a, Run 4, 17–21 ft	1.90 ft recovery

3.00–4.08 ft	Peat, fibric; wood fragments suitable for dating at 3.15 and 3.58 ft (96 and 109 cm); no shells
4.08–4.17 ft	Sand, very fine, light gray (5Y 7/1), uniform
4.17–4.31 ft	Peat; with plentiful gastropod shells
4.31–5.05 ft	Marl, olive (5 Y 5.5/3); abundant gastropod shells, layered
5.05–6.07 ft	Marl, olive (5Y 5/3); wood at 5.74 and 6.07 ft (175 and 185 cm)
6.07–6.50 ft	Marl, coarsely mottled olive as above and pinkish gray (7.5YR 7/2)
6.50–6.84 ft	Marl, pinkish gray as above; abundant wood fragments, largest pieces at 6.53 and 6.77 ft (199 and 206.5 cm)
7.00–7.63 ft	Marl, from olive (5Y 5.5/3) to olive-gray (5Y 4.5/2)
7.63–8.23 ft	Marl, banded; very fossiliferous, 1.5-cm-thick horizons at 7.78, 7.91, and 8.04 ft (237, 241, and 245 cm) with abundant wood fragments
8.23–8.74 ft	Marl, uniform, gray (5Y 4/1)
8.74–9.94 ft	Marl, gray (5Y 4/1); gastropod shells abundant at base, large wood fragment (1.8 cm across) at 9.51 ft (290 cm)
9.94–11.06 ft	Marl, dark gray (5Y4/1); wood-rich at base; not many shells
11.06–11.46 ft	Marl, dark gray (5Y 4/1) as above
11.46–12.07 ft	Marl, gray (5Y 5/1)
12.07–12.47 ft	Marl, dark gray (5Y 4/1)
12.47–13.09 ft	Marl, olive-gray (5Y 5.5/2)
13.09–14.01 ft	Silt, grading from olive-gray (5Y 5.5/2) to dark gray (5Y 4/1); few gastropod shells
14.01–14.24 ft	Wood; thick rings; core is completely wood
14.24–14.63 ft	Silt, dark gray (5Y 4/1); not much wood
14.63–14.73 ft	Wood; smaller piece than above; some silt also in interval
14.73–15.60 ft	Silt, dark gray as above; many small wood fragments

15.00–15.16 ft	Wood; washed and dried; too fragmented for tree-ring work
15.16–16.73 ft	Silt, gray, coarsely mottled; gastropod shells, dark gray (5Y 4/1) to gray (5Y 5/1).
16.73–16.98 ft	Diamicton; silt loam, oxidized strong brown (7.5YR 4/6) to less strongly reddish hues (10YR)
17.00–8.02 ft	Silt, vaguely banded, gray (5Y 4/1)
18.02–18.11 ft	Silt, laminated, oxidized
18.11–18.90 ft	Diamicton, loamy sand matrix, clast-supported, dolomite-rich, brownish yellow (10YR 5/6)

The materials recovered in BC-8a, Run 4, suggest that this run was disturbed, probably by the wood fragment at the top of the run that got partly stuck and pushed some sediment out of the way during the drive. The depth to glacial sediment, as indicated in the very last run (18.11 ft), is probably correct compared against the 16.73 ft depth indicated in the next-to-last run. Hence, the material between the wood and the diamicton in BC-8, Run 4, from 462 to 510 cm is disturbed (shortened).

Stratigraphic summary (BC-8)

0.0–13.09 ft	Grayslake Peat (0.0–4.31 ft is peat with a layer of very fine sand from 4.08–4.17 ft; 4.31 to 13.09 ft is marl)
13.09–18.11 ft	Equality Formation
18.11–18.90 ft	Henry Formation, diamicton facies

BC-9 (API: 31494) (see fig. 18)
695’ EL, 2,545’ NL, Sec. 6, T40N, R9E
Elevation: 751.8 ft
Recovery: Run 1, 1.9/3.0 ft; Run 2, 2.8/4.0 ft; Run 3, 1.4/4.0 ft
End of boring at 8.4 ft

0.0–1.3 ft	Peat, black, sapric
1.3–~3 ft	Peat, reddish brown
~3–3.2 ft	Peat, as above, with very thin beds of very fine sand
3.2–3.7 ft	Sand, very fine, with abundant wood fragments
3.7–4.7 ft	Peat, reddish brown, fibric
4.7–~6 ft	Silt, with wood and rock fragments, dense, sand and gravelly at base
~6–8.4 ft	Gravelly sand, pale yellow (2.5Y 7/4)
End of boring	

Stratigraphic summary (BC-9)

0.0–4.7 ft	Grayslake Peat, all peat
4.7–6.0 ft	Equality Formation
6.0–8.4 ft	Henry Formation

BC-10 (shoreline) (API: 31495)
685’ EL, 2,650’ NL, Sec. 6, T40N, R9E
Elevation: 752.3 ft
Recovery: Run 1, 2.2/3.0 ft; Run 2, 2.1/4.0 ft
End of boring at 5.1 ft

0.0–1.0 ft	Peat, fibric
1.0–2.0 ft	Silt, gray
2.0–~3 ft	Diamicton, gray, silty, no fossils
~3– 5.1 ft	Sand, gravelly, pale yellow (2.5Y 7/4), calcareous

Stratigraphic summary (BC-10)

0.0–1.0 ft	Grayslake Peat
1.0–3.0 ft	Equality Formation
3.0–5.1 ft	Henry Formation

BC-11 (API: 31496) (see fig. 18)
800’ EL, 1,780’ NL, Sec. 6, T40N, R9E
Elevation: 750.5 ft
Recovery: Run 1, 2.2/3.0 ft; Run 2, 2.3/4.0 ft; Run 3, 2.1/4.0 ft
End of boring at 9.1 ft

0.0–3.5 ft	Peat
3.5–3.65 ft	Sand
3.65–3.7 ft	Peat
3.7–~6 ft	Silt; wood-bearing
~6–8.3 ft	Silt; barren of fossils
8.3–8.6 ft	Diamicton, silt loam matrix, soft, gray
8.6–8.95 ft	As above, but oxidized
8.95–9.1 ft	Gravelly sand

Stratigraphic summary (BC-11)

0.0–3.7 ft	Grayslake Peat (all peat)
3.7–9.0 ft	Equality Formation
9.0–9.1 ft	Henry Formation

BC-12 (API: 31497)
745’ EL, 1,865’ NL, Sec. 6, T40N, R9E
Elevation: 749.7 ft
Recovery: Run 1, 2.1/3.0 ft; Run 2, 3.0/4.0 ft; Run 3, 2.0/4.0 ft; Run 4, 2.4/4.0 ft; Run 5, 1.8/4.0 ft; Run 6, 1.8/4.0 ft
End of boring at 20.8 ft

0.0–~3 ft	Peat
~3–3.7 ft	Marl, pinkish gray (7.5YR 7/2)
3.7–~10 ft	Marl, light yellowish brown (2.5Y6/3)
~10–12.0 ft	Silt, gray; wood-bearing
12.0–12.1 ft	Wood (one solid chunk)
12.1–12.4 ft	Silt, as above

12.4–20.2 ft	Silt, dark greenish gray (10Y 4/1); laminated; wood-bearing
20.2–20.4 ft	Silt, laminated, oxidized, varicolored, as bright as yellowish red (5YR 4/6)
20.4–20.8 ft	Sand and gravel, yellowish brown (10YR 5/6)
End of boring	

Stratigraphic summary (BC-12)

0.0–10.0 ft	Grayslake Peat (0–3 ft is peat; 3–10 ft is marl)
10.0–20.4 ft	Equality Formation
20.4–20.8 ft	Henry Formation

"Beach" Monolith (API: 31498) (see fig. 19)
690' EL, 1,760' NL, Sec. 6, T40N, R9E
Elevation: 751.0 ft

0.0–1.2 ft (0–38 cm)	Peat, sapric, black
1.2–1.8 ft (38–56 cm)	Peat, fibric, wood-bearing, dark reddish brown (10YR 3/1)
1.8–1.81 ft (56–56.1 cm)	Silt, gray, (5Y 5/1), discontinuous lamina
1.81–2.05 (56.1–62.5 cm)	Peat, hemic; few/rare wood fragments, few gastropods, modern rootlets
2.05–2.07 ft (62.5–63.0 cm)	Marl, gray (5Y 5/1), continuous thin layer
2.07–2.26 ft (63–69 cm)	Marly peat; stratified, fibric, dark reddish brown (5YR 3/2)
2.26–2.43 ft (69–74 cm)	Peaty marl with thin layers of marly peat; peaty marl is light olive (5Y 6/2); marly peat is black (5Y 2.5/1)
2.43–2.76 ft (74–84 cm)	Peat, wood-rich, abrupt upper contact, irregular lower contact (wood) fragment sticks into marl; sampled for ^{14}C
2.76–3.01 ft (84–92 cm)	Marl; fossiliferous (snails), light olive-brown (5Y 6/2), slanted lower boundary to 95 cm
3.01–3.13 ft (92–95.5 cm)	Peaty marl, as above, but darker (olive-gray, 5Y 4.5/2)
3.13–3.25 ft (95.5–99.0 cm)	Peat, black, varies in thickness from 0.7 to 3.5 cm; few wood fragments
3.25–3.30 ft (99.0–100.5 cm)	Sand, medium, well-sorted, olive-gray (5Y 5/2)
3.30–3.32 ft (100.5–101.3 cm)	Sand, very fine, abrupt upper boundary, fining upward below lower contact
3.32–3.38 ft (101.3–103 cm)	Sand; fining upward zone
3.38–4.40 ft (103–134 cm)	Sand, medium, well-sorted, uniform, light brownish gray (2.5Y 6/2) to olive-yellow (2.5Y 6/6)
4.40–4.52 ft (134–138 cm)	Disturbed; sand and dark gray (5Y 4/1) silt

Stratigraphic summary ("Beach" Monolith)

0.0–3.25 ft	Grayslake Peat, mostly peat with some thin beds of marl and silt
3.25–4.40 ft	Equality Formation (sand facies)
4.40–4.52 ft	Equality Formation